ABSTRACT

Title of Dissertation: SEASONAL NITROGEN CYCLING AND HOMEOSTASIS IN *POPULUS*: SOURCE-SINK COMMUNICATION

Gen Li, Doctor of Philosophy, 2018

Dissertation directed by: Professor Gary D. Coleman
Department of Plant Science and Landscape Architecture

Nitrogen (N) is an essential nutrient for plant growth, development and reproduction. Seasonal N cycling is an adaption to nutrient limitation and a feature of the perennial lifestyle of trees. Poplar (*Populus*) is a model system used to study forest tree genetics and molecular biology, including seasonal N cycling. The accumulation of Bark storage proteins (BSP) is a central feature of seasonal N cycling in poplar, yet our understanding of the contribution of the BSP storage pool to N remobilization during growth and mechanisms that regulate BSP accumulation, catabolism and N remobilization is limited. The research presented in this dissertation is directed towards advancing knowledge of the regulation of seasonal N cycling in poplar using a combination of experimental approaches. The role of the N storage pool to N remobilization was examined through N sink manipulations and the specific role of BSP storage was investigated by N source reduction via RNAi mediated knockdown of BSP accumulation. From this it was found that N remobilization from BSP

significantly contributes to shoot growth following dormancy and initial shoot growth is source limited. Poplar bark transcriptome analyses during regrowth following dormancy revealed an enrichment for up-regulated genes associated with auxin transport and signaling. Based on the transcriptome analysis experiments that manipulate auxin production or polar auxin transport were performed and the results indicate that BSP catabolism and N remobilization likely involves polar auxin transport from expanding buds and shoots and auxin-mediated regulation of protease gene expression. Analysis of DNA microarrays of bark RNA during short-day (SD) induction of *BSP* gene expression was used to identify putative regulatory factors that may play a role of BSP accumulation. The transcriptome analyses indicated that SD represses the expression of genes involved in ethylene production as well as a reduction in bark ethylene biosynthesis. Additionally, treatment of excised stems with ACC or ethephon repressed *BSP* gene expression while AVG induced *BSP* gene expression. This repression was reduced in ethylene-insensitive poplars expressing *Arabidopsis* dominant gain-of-function allele *etr1-1*. Furthermore, transient expression of ERF12 and ERF41, two transcription factors with the greatest induction in SD treatment, in transgenic tobacco stably transformed with *BSPA* promoter fused with GUS resulted in enhanced GUS activity suggesting ERF12 and ERF41 may act as positive regulators of *BSP* gene expression. Since glutamine plays a pivotal role in N partitioning during N storage and remobilization, the possible role of the PII glutamine sensor was studied and it was found that the transcript levels of *PII* increased in bark during SD-induced leaf senescence and BSP accumulation. PII knockdown poplars using RNAi showed reduced glutamine-induced *BSP* gene

expression. Moreover, glutamine-induced *BSP* gene expression was also inhibited by 2-OG, a PII-NAGK interaction antagonist, suggesting a possible role of PII-glutamine sensing in BSP accumulation. Taken together, this study provides important insights into the mechanism of seasonal N accumulation and remobilization in poplar.

SEASONAL NITROGEN CYCLING AND HOMEOSTASIS IN *POPULUS*: SOURCE-SINK COMMUNICATION

by

Gen Li

Dissertation submitted to the Faculty of the Graduate School of the
University of Maryland, College Park, in partial fulfillment
of the requirements for the degree of
Doctor of Philosophy
2018

Advisory Committee:
Professor Gary D. Coleman, Chair
Professor Angus Murphy
Professor Wendy Peer
Professor Jianhua Zhu
Professor Caren Chang, Dean's Representative

Preface

This dissertation is composed of four chapters, summary, three appendices and bibliography. Each chapter is organized in a manuscript format (Abstract, Introduction, materials and methods, results, discussion, conclusion). In this way, descriptions of some material and methods are repeated and some introduction content is presented in a similar manner. The supplementary materials are included in appendices, and each chapter corresponds with each appendix in the order appendices A for chapter 2, appendices B for chapter 3 and appendices C for chapter 3.

As each chapter is organized essentially as a manuscript, two chapters (chapter 2 and 3) involve work of other colleagues. The chapter 1 is a literature review that is under review as a book chapter. In chapter 2, Rongshuang Lin performed the microarray analysis; Emily Pettengill generated BSP RNAi transgenic poplars; Chioma Ebiringa did experiments of competition between proleptic and sylleptic and some protein analyses; Joshua Blakeslee helped with auxin measurement; Benjamin A. Babst compared N partitioning in BSP RNAi poplars with wild type by using ^{13}N labeling. In chapter 3, Rongshuang Lin performed the microarray analysis. The transgenic poplar 1E and wild type T89 is provided by Björn Sundberg (Swedish University of Agricultural Sciences, Sweden).

Dedication

I dedicate this dissertation to my father and mother who eventually grow me as who I am and support me financially and spiritually from elementary school till now even in the most difficult time of my family. For my wife Xingping Chai, without her I would not come here to pursue a doctoral degree and have my lovely son Timothy (Zimu) Li in 2017. Both of them support me with love, happiness, understanding and encouragement.

Acknowledgements

First and foremost, I would like to express my sincere gratitude to my adviser Dr. Gary D. Coleman for his great support, advices and ideas through my pursuit for PhD. He always talks to me with great trust and understanding and expresses special care of my life and family. Thanks for his contribution to my professional development. I would also thank Dr. Angus Murphy who together with Dr. Gary Coleman offered me the opportunity to study in Plant Science program and pursue my PhD degree at University of Maryland and provided valuable ideas for my research. I would also thank Dr. Wendy Peer for teaching me microscope skills and offering great ideas. By the way, thank her for taking and introducing me to Dr. Gary Coleman for the first time in 2013. I want to thank Dr. Caren Chang who offered great inspiration for my research and help for the ethylene experiments. I also thank Dr. Jianhua Zhu for his effective ideas and suggestions on my research and career. I also want to thank Dr. Shunyuan Xiao for the development of my TAing and research skills and attitude. Last but not least, this research could not be finished without the help and work from Rongshuang Lin, Chioma Ebiringa, Emily Pettengill, David Dossick, Nazrul Islam, Joshua Blakeslee, Benjamin A. Babst, John Clay, Jiayang Li, Sydney Wallace, Shaun Faulkner and Meghan Holbert. I would like to also thanks for help from the PSLA business office.

Table of Contents

List of Abbreviations

2-OG, 2-oxoglutarate

AA, amino acid

AAP, amino acid permease

ABA, abscisic acid

ACC, 1-aminocyclopropane- 1-carboxylic acid

ACO, ACC oxidase

ACS, ACC synthase

AL, Argininosuccinate lyase

AMT, ammonium transporter

APC, amino acid, polyamine and choline transporters superfamily

ARF, auxin response factor

Arg, arginine

ASN, asparagine

ASP, aspartate

ATF, amino acid transporter family

AVG, aminoethoxyvinylglycine

bHLH, basic helix-loop-helix

BSP, bark storage protein

CAT, cationic amino acid transporter

DW, dry weight

ERF, ethylene response factor

ET, ethephon

FW, fresh weight

GDH, glutamate dehydrogenase

Gln, glutamine

Glu, glutamate

GO, gene ontology

GOGAT, glutamine-2-oxoglutarate aminotransferase

GS, glutamine synthetase

IAA, indole-3-acetic acid

LD, long day

LT, low temperature

MudPIT, multidimensional protein identification technology

NAGK, N-acetylglutamate kinase

NiR, nitrite reductase

N, nitrogen

NAOD, N-acetylornithine deacetylase

NO, nitric oxide

NPA, 1-N-naphthylphthalamic acid

NPF, nitrate transporter1/peptide transporter family

NR, nitrate reductase

NRT, nitrate transporter

NUE, nitrogen use efficiency

OPT, oligopeptide transporter

OTC, Ornithine transcarbamylase

PCR, Polymerase Chain Reaction

PET, positron emission tomography

PIF, phytochrome interacting factor

PTR, peptide transporter

RUBISCO, ribulose-1, 5-bisphosphate carboxylase/oxygenase

SAG, senescence-associated gene

SD, short day

SDS-PAGE, sodium dodecyl sulfate-polyacrylamide gel electrophoresis

SNP, sodium nitroprusside

TOR, target of rapamycin

VSP, vegetative storage protein

WIN, wound-induced

Chapter 1: Literature review- Nitrogen storage and cycling in trees

Abstract

Seasonal nitrogen cycling is an important trait and adaptive strategy for trees to conserve and reuse nitrogen. This review examines the current progress towards understanding the molecular and physiological basis of seasonal nitrogen cycling in trees. Since most of what is known about nitrogen cycling in trees comes from research in *Populus*, this review relies heavily on research in this genus. We also highlight major knowledge gaps in understanding the regulatory pathways and transport mechanism that govern seasonal N cycling.

Introduction

Trees have existed on earth for over 370 million years. Estimates place the number of trees on earth at approximately 3.04 trillion; 1.30 trillion in tropical and subtropical forests, 0.74 trillion in boreal regions and 0.66 trillion in temperate regions (Crowther et al., 2015). Trees are also long-lived organism and the ring-width chronologies of a bristlecone pine tree (*Pinus longaeva*) in California indicates that this tree has lived for over 5,000 years (Ferguson, 1968; Salzer et al., 2009). One of physiological mechanisms that contribute to the longevity of trees is internal seasonal nutrient cycling including the internal recycling of nitrogen (N) (Eckstein et al., 1999; Fife and Nambiar, 1982; Nambiar and Fife, 1991; Rennenberg and Schmidt, 2010).

Nitrogen (N) is an essential nutrient for plant growth, development and reproduction as it is a basic constitute of amino acids, the building blocks of proteins. N is also found in other important compounds such as amides, nucleic acids, nucleotides, alkaloids, vitamins, chlorophyll and phytohormones. Plant productivity is impacted by N deficiency which can impact photosynthesis by reducing chlorophyll production and enzyme activity and can further affect sugar metabolism and/or carbohydrate partitioning between source and sink tissues as well as root morphology (Hermans et al., 2006).

N is one of the major limiting nutrients for worldwide agricultural production. Since the global population is predicted to approach 9 billion by 2050, expanding food demands will require an annual increase in food production of nearly 44 million metric tons (Godfray et al., 2010). Accordingly, N fertilizer application is predicted to increase by threefold over the next 40 years unless nitrogen use efficiency (NUE) is greatly improved (Xu et al., 2012). Like herbaceous annual plants trees must acquire N from the soil but because trees are perennials a significant portion of N demand is met by seasonal internal cycling. Because the adaptive strategy of seasonal N cycling occurs annually, this recursive process increasingly contributes to the overall N budget as trees age (Millard and Grelet, 2010; Millard et al., 2006). Thus, internal N cycling is a major factor that contributes to the N economy of trees and provides a competitive advantage in N limited environments (Chapin et al., 1990; Millard and Grelet, 2010; Rennenberg and Schmidt, 2010; Vitousek, 1982). Consequently, seasonal N cycling is important to the ecology of N use in trees and makes a major

contribution to NUE (Aerts, 1990; Boerner, 1984; Chapin and Kedrowski, 1983; Ryan and Bormann, 1982; Vitousek, 1982).

In temperate trees seasonal N cycling involves a number of processes including: 1) uptake and assimilation of N from the soil, 2) transport and partitioning associated with N sink demands during growth, 3) autumn redistribution of N from leaves during senescence and storage in perennial tissues and, 4) remobilization and transport of stored nitrogen during renewed growth in the spring. Thus, different spatial and temporal scales of N transport and N fluxes are important in controlling N cycling and partitioning in trees (Figure 1-1). A hallmark of seasonal N cycling in temperate trees are the changes in N source-sink relations that occur between leaves and storage tissues during this process (Figure 1-1). During spring growth leaves and expanding shoots are N sinks while storage tissues are N sources but in autumn the source-sink status of these tissues change with leaves serving as N sources and storage tissues as N sinks. In this review we focus on our current understanding of the physiological and molecular aspects of seasonal N storage and cycling in trees. Although we touch on aspects that regulate N transport and storage, this is not the focus of this review since this topic has been recently reviewed (Babst and Coleman, 2018). We also focus primarily on temperate tree species since these are the species that the majority of studies are focused. Further, since the majority of research related to seasonal N cycling in trees has been conducted in *Populus* (poplars) much of what we present relies on research in this genus.

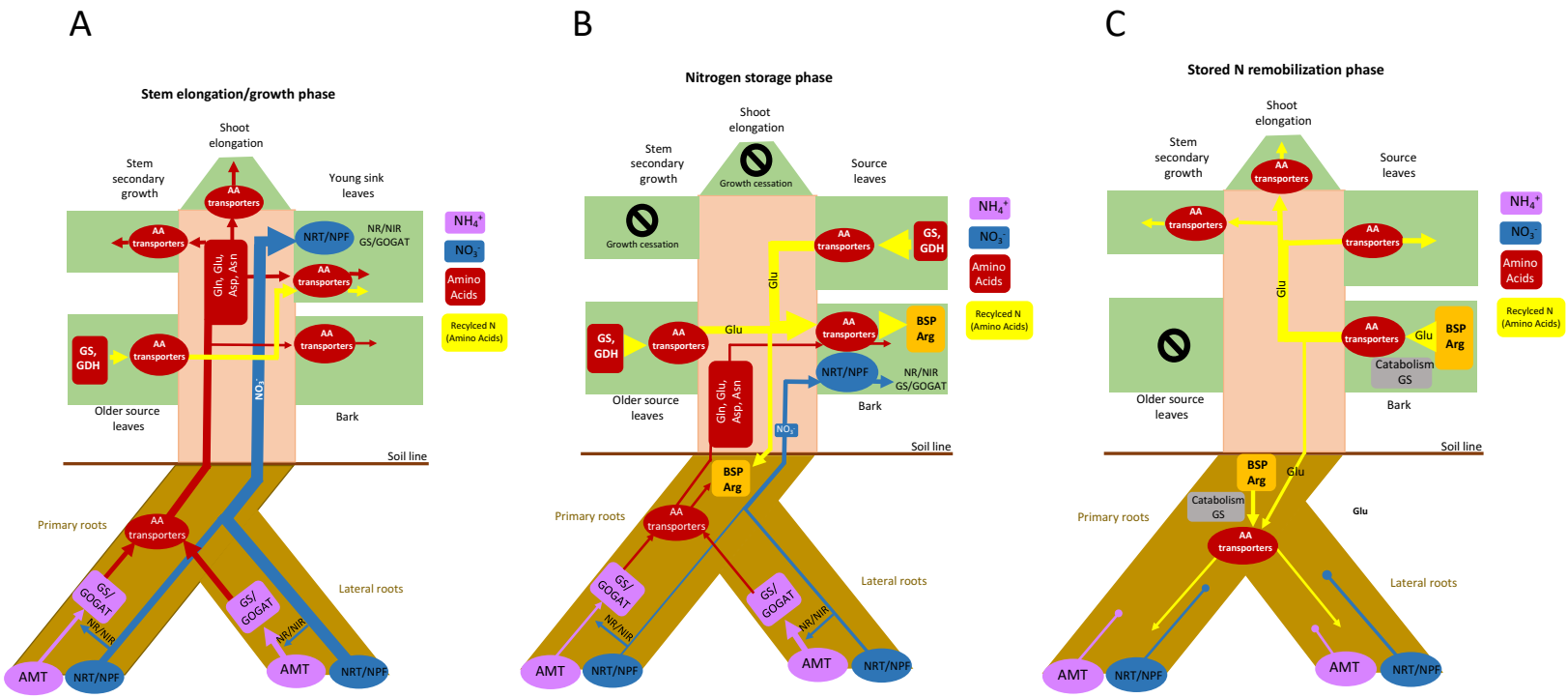

Figure 1-1. Schematic routes and fluxes of N during stages of seasonal N cycling in trees. A) N transport routes and fluxes during growth following N remobilization. During this stage N is acquired from the soil and transported to N sinks associated with growth. B) N transport routes and fluxes during autumn N remobilization and storage. N from senescing leaves (source) is transported to storage tissues (sinks) in the stem and root. C) Transport routes and fluxes during N remobilization in the spring. N from storage tissues (source) is remobilized to expanding buds and shoots (sinks). Possible factors involved (transporters and enzymes) and the chemical nature of N is indicated in the figures. Abbreviations: AA, amino acid; Gln, glutamine; Glu, glutamate; Asp, aspartate; Asn, asparagine; NRT, nitrate transporter; NPF, NITRATE TRANSPORTER1/PEPTIDE TRANSPORTER family; NR, nitrate reductase; NiR, nitrite reductase; GS, glutamine synthetase; GDH, glutamate dehydrogenase; GOGAT, glutamine-2-oxoglutarate aminotransferase; AMT, ammonium transporter; BSP, bark storage protein; Arg, arginine;

Physiology of N storage and cycling

Fruit trees

Since the 1920s, the importance of nitrogen reserves to spring growth has been recognized in fruit trees (Roberts, 1921; Thomas, 1927). In deciduous fruit trees, N cycling involves translocation of leaf N to woody tissues that serves as an N reservoir in autumn and winter. These N reserves are then remobilized and used during growth in the following spring. Apple (*Malus domestica*) is one of the earliest and most extensively studied fruit tree species with respect to seasonal N cycling (Roberts, 1921; Thomas, 1927; Titus and Kang, 1982). N released from senescing apple leaves is translocated to spurs and twigs, bark, and roots (Mason and Whttfield, 1960; Murneek and Logan, 1932) resulting in increased N content of these tissues in autumn. Although N content increased in these various tissues during autumn, a greater proportion of N was stored in bark compared to other perennial tissues (i.e. wood and roots) (Mason and Whttfield, 1960; O'Kennedy et al., 1975). During apple leaf senescence leaf protein contents declined by about one-half while at the same time the total protein content in bark increased by 240% (Kang and Titus, 1980). The majority of the decline in leaf protein content during senescence was attributed to an 80% decline in the leaf content of ribulose 1,5-bisphosphate carboxylase/oxygenase (RUBISCO) (Millard and Thomson, 1989). Therefore, besides its role in photosynthesis and carbon fixation, RUBISCO also serves as a major leaf storage pool of N which is a N source during autumn N remobilization from source (leaf) to sink (bark).

Some controversy still seems to exist as to the chemical nature of N storage in apple (Cheng et al., 2004; Titus and Kang, 1982). Early studies in apple (Oland, 1959), peach (Muñoz et al., 1993; Taylor and May, 1967, 1967; Taylor and Van, 1969, 1970) and pear (Taylor et al., 1975) indicated that N was stored as a soluble form mainly as free amino acids. In contrast, (Kang and Titus, 1980) reported that nearly 90% of N stored in apple bark during that late stage of leaf senescence was in protein. In addition, protein was also found to be the major form of N storage and N reservoir in citrus trees (Kato et al., 1984). The form of N storage in apple may also be related to N status or availability since proteins were observed to be a main form of N storage and independent of N supply while the proportion of stored free amino acids increased as external N supply increased (Cheng et al., 2004). Storing free amino acids may be more metabolically efficient compared to protein and storage of high N containing amino acids (i.e. arginine) when N supplies are abundant suggests flexibility of the N storage pool relative to N supply (Cheng et al., 2004). To the best of our knowledge, how N fluxes between amino acid and protein storage pools are regulated in apple is not known but raises some intriguing questions. Since proteins are stored in protein storage vacuoles (Herman and Larkins, 1999; Müntz, 1998, 2007) it might be possible that under abundant N conditions that protein storage sites or systems become "saturated" which could feedback and alter N fluxes to amino acid storage. Since amino acid storage would need also need to be in the vacuole in order to maintain cellular homeostasis, the regulation of a shift from protein to amino acid storage in relation to N supply could be an important regulatory step in N storage and partitioning.

In fruit trees the timing of fertilization impacts fruit production with late summer and autumn N fertilization commonly used to improve productivity. Fertilization in late summer and autumn appears to increase N storage over winter resulting in increased productivity when N is remobilized during flowering and regrowth the following spring (Bravo et al., 2017; Quartieri et al., 2002). Further, autumn foliar N fertilization results in greater N storage in apple bark compared to soil N fertilization, supporting that autumn N redistribution from senescing leaves contributes to a greater proportion of N storage than N uptake from soil (O'Kennedy et al., 1975). This has important implications in the management of N nutrition and fruit tree productivity and it is possible that crop management strategies or genetic alterations that enhance seasonal N storage could be effective in enhancing fruit tree NUE.

Forest trees

Similar to fruit trees, a leaf N level decline throughout the fall in temperate forest trees and is accompanied by increased bark N content (Côté et al., 1989; Côtté and Dawson, 1986). For many deciduous temperate tree species the autumn increase in bark N levels is closely associated with the accumulation of specific proteins termed bark storage proteins (BSP and BSPs). Over the past 30 years significant progress has been made in identification of storage proteins in many temperate tree species for both angiosperms and gymnosperms. BSPs are characterized by increased abundance during autumn and their disappearance in spring when growth resumes. For example, specific BSPs whose abundance fluctuates seasonally have be reported for *Acer saccharum, Salix* × *smithiana*, *Populus deltoides* (Wetzel et al., 1989), *Larix decidua,*

Pinus sylvestris, Pinus strobus (Wetzel and Greenwood, 1989), *Taxodium distichum* (Harms and Sauter, 1991)*, Alnus glutinosa, Betula papyrifera, Quercus rubra, Fagus sylvatica, Fraxinus americana, Tilia americana and Fagus glutinosa* (Wetzel and Greenwood, 1991a). The wide diversity of tree species from which seasonally fluctuating bark proteins have been observed indicates that seasonal storage of N as protein is extensively used as an adaptive mechanism for the reuse of assimilated N in trees. However, in temperate tree species the location or tissue that serves as an N storage site appears to be associated with leaf habit (Millard and Grelet, 2010). While stems and roots are the major N storage tissues in deciduous trees, evergreen trees appear to store N in leaves and needles that are retained over the winter (for review see Millard & Grelet, 2010). Although most of the research associated with seasonal N storage has been performed in temperate trees species, evidence indicates that tropical and subtropical forest trees also store N and internal cycling is related to phenological changes that occur from the dry season to the rainy season and vice versa (Gérant et al., 2017; Schmidt and Stewart, 1998).

Biochemical and molecular aspects of N storage and cycling

Bark Storage Proteins (BSP)

Bark storage proteins (BSPs) are a class of vegetative storage proteins (VSPs) and are a central component of seasonal N storage and cycling in a wide range of temperate tree species (Millard and Grelet, 2010). For temperate deciduous trees BSPs accumulate in bark and root tissues during autumn and winter and accumulated BSP then disappears from storage tissues once growth resumes in the spring. Presumably, the disappearance of BSP in the spring involves protein catabolism and amino

biosynthesis although little is known about these metabolic processes during spring N remobilization. Because of the importance of BSPs to seasonal N cycling in temperate trees, we present a review of BSPs and aspects that regulate their accumulation and catabolism. Most of this information comes from studies with poplar (*Populus*) since seasonal N cycling has been studied in this genus more than other species.

A number of VSPs and BSPs have been identified in plants and there does not seem to be any consistency in plants as to the class or type of proteins that serve as storage proteins. The majority of VSPs and BSPs have been identified by SDS-PAGE based on the characteristics of their accumulation and disappearance. As a consequence, little information exists about protein sequence and biochemistry. One of the earliest VSPs to be studied is in soybean where two glycosylated proteins called VSPα and VSPβ. Both VSPα and VSPβ were found to be abundant in young sink leaves but disappeared during seed fill (Wittenbach, 1982) and were shown to have acid phosphatase activity (DeWald et al., 1992). Other VSPs have also been shown to have biological properties other than their role in storage. For example, the potato storage protein patatin has lipid acyl hydrolase activity (Andrews et al., 1988) and the storage protein in alfalfa taproots has β-amylase activity (Gana et al., 1998). Examples also exist for storage proteins that have sequence homology to active proteins but appear to have lost their activity including RNAse-like proteins in *Calystegia sepium* (Damme et al., 2000) and lectin-like proteins that appear to lack sugar-binding properties in *Cladastris lutea* (Van Damme et al., 1995), and *Sambucus nigra* (Chen et al., 2002).

In the case of Populus, BSPs are members of a gene family that have homology to nucleoside phosphorylase-like (NP-like) proteins (Pettengill et al., 2013). Bacterial and mammalian nucleoside phosphorylases are involved in nucleoside catabolism through cleavage of the glycosidic bond of (deoxy-) ribonucleosides in the presence of inorganic phosphate (Pi) to produce (deoxy-) ribose-1-phosphate and a nucleobase (Lewkowicz and Iribarren, 2006; Pugmire and Ealick, 2002). The released nucleobase can be either used for synthesis of other metabolites or degraded while the (deoxy-) ribose-1-phosphate can be used by the Pentose Phosphate Pathway and glycolysis (Pugmire and Ealick, 2002). Purine salvaging and degradation in plants could contribute to NUE through the retention and remobilization of N (Smith and Atkins, 2002; Werner and Witte, 2011). However, there is no evidence that nucleoside phosphorylases are involved in purine nucleoside salvage in plants but instead hydrolysis of plant nucleosides seems to involve nucleosidases (EC 3.2.2x) (Guranowski, 1982; Jung et al., 2011; Katahira and Ashihara, 2006a). Since genes in the purine salvage and degradation pathways in plants are induced by abscisic acid, drought, wounding and dark induced senescence suggests a role for purine salvage in N remobilization and NUE ((Brychkova et al., 2008; Hesberg et al., 2004; Katahira and Ashihara, 2006b) yet a role for nucleoside phosphorylase-like proteins in plant nucleoside salvaging and NUE are not known. Moreover, attempts in our lab to show nucleoside catabolism related activity of the nucleoside phosphorylase-like proteins of *Populus* have not been successful, so the question still remains if members of this gene family either retain or possess catalytic activity.

Thus, it appears that a number of proteins have been recruited to serve as storage proteins and there does not seem to be any consistency as to the type of proteins used for vegetative N storage. This presents an intriguing question about the evolution of N storage and the proteins used for storage. Although storage of N involving VSP seems widespread yet the proteins used for storage appears to be diverse. In poplar VSPs including BSPs are highly homologous to seed storage proteins (Beardmore et al., 1996) suggesting that VSPs and BSPs may have been recruited from seed storage proteins but it is still unclear why nucleoside phosphorylase-like proteins would have been used for N storage. It would be interesting to know if this relationship or relatedness between seed storage proteins and VSPs holds for other species that utilize VSPs for vegetative N storage.

Populus BSP and seasonal N cycling

In *Populus*, BSPs comprises the major VSPs that are involved in seasonal N cycling. During autumn and winter BSPs accumulate in *Populus* bark accounting for approximately 62% of total soluble bark protein during dormancy. Over the past twenty years, BSPs and the genes that encode them been described for a number of tree species (Table 1-1). Among these the BSPs of Populus are the most extensively studied in trees. Early studies using SDS-PAGE and immunological analyses of *Populus* BSP revealed multiple isoeletric isoforms with molecular masses between 32 and 38 kDa and a 32 kDa BSP was also observed in closely related Salix (Coleman et al., 1991; Langheinrich and Tischner, 1991; Sauter et al., 1988; Wetzel et al., 1989). Further biochemical analyses also demonstrated that both the *Populus* and *Salix* BSPs are glycosylated and this posttranslational modification appears to be the basis for the

isoelectric isoforms that have been detected (Wetzel and Greenwood, 1991a; Wetzel et al., 1989).

Table. 1-1 Bark storage proteins in trees and their corresponding gene names.

Name	Organisms	Tissue localization	References
BSP	*Acer*, *Salix* and *Populus* spp.	Bark	(Wetzel et al., 1989)
BSP	*Populus deltoides*	Bark	(Coleman et al., 1991)
BSP	*Betula papyrifera*, *Salix microstachya*	Bark	(Wetzel and Greenwood, 1991b)
WIN4	*Populus trichocarpa* × *P. deltoides*	Leaf and bark	(Lawrence et al., 1997)
PNI288	*Populus trichocarpa* × *P. deltoides*	Leaf and bark	(Lawrence et al., 2001; Pettengill et al., 2013)
CiVSP	*Cichorium intybus*	Taproot and leaf	(Richard-Molard et al., 2004)
VSP	*Populus canadensis*	New shoot	(Tian et al., 2005)
VSP	*Litchi chinensis*	Leaf , bark and root	(Tian et al., 2007)
CCA	*Castanea crenata*	Leaf and stem	(Nomura et al., 2008)
BSP A	*Populus trichocarpa*	Shoot tip and bark	(Pettengill et al., 2013)
BSP B	*Populus trichocarpa*	Shoot tip and bark	(Pettengill et al., 2013)
BSP C	*Populus trichocarpa*	Shoot tip, young leaf and bark	(Pettengill et al., 2013)

The availability of the poplar genome (Tuskan and et al., 2006) greatly facilited our understanding of the structure and organization of the poplar VSP gene family which consists of 13 members with homology to NP-like proteins (Pettengill et al., 2013). Phylogenetic analysis of NP-like genes in plants revealed two major clusters. One cluster is characterized by proteins encoded by genes found in a wide range of plant taxa and includes 4 genes in *Populus*, while the second cluster consists primarily of proteins encoded by species of the order *Malpighiales*, including 9 genes encoding *Populus* BSP and WIN4-like proteins. Expression analysis showed that all 13 members of *Populus* NP-like gene family are expressed in various tissues in both long-day (LD) and short-day (SD) conditions (Pettengill et al., 2013). The evolution

of the *Populus* gene family involved duplication events and divergence in expression may have recently occurred (Pettengill et al., 2013).

Populus BSP accumulates in protein storage vacuoles of inner bark parenchyma and xylem ray cells during fall (van Cleve et al., 1988; Sauter et al., 1989; Wetzel et al., 1989). Three genes (*BSPA*, *BSPB*, *BSPC*) encode poplar BSPs and their expression is regulated by environmental factors such as SD photoperiods, N availability and low temperature (Coleman et al., 1991, 1994; Pettengill et al., 2013; Zhu and Coleman, 2001a). Of these factors, SD photoperiod is the main environmental cue that induces BSP gene expression and N storage. Photoperiod perception is mediated by the phytochrome photoreceptors and play an essential role in *Populus* growth cessation and bud set (Howe et al., 1996; Olsen et al., 1997). Like other dormancy-associated processes, phytochrome-mediated perception of SD is also involved in the induction of BSP gene expression and involves both low fluence and very low fluence pathways (Zhu and Coleman, 2001a). It has yet to be determined if phytochrome mediates BSP gene expression directly or indirectly through altered growth resulting in altered C and N partitioning. Using tobacco transformed with the *Populus BSPA* promoter fused to GUS it was found that the transcriptional activation from the *BSPA* promoter occurred in developing floral tissues and in seeds during early stages of embryogenesis and seed germination (Zhu and Coleman, 2001b). These results are consistent with the concept of BSP gene expression being associated with N sink status of tissues and is consistent with a role for N partitioning in regulating BSP gene expression.

A lingering question concerning seasonal N cycling and storage in *Populus* is centered around the mechanism(s) that regulate BSP expression. This is fundamental to N sink establishment in bark which is an essential process for seasonal N storage. The red and far-red light photoreceptor phytochrome mediates diverse developmental and photomorphogenic responses in plants, including SD-induced BSP gene expression, through the action of the reversible inactive Pr and active Pfr forms (Quail, 2002). Phytochrome interacting factors (PIFs) are basic helix-loop-helix (bHLH) transcription factors that play roles in the early phases of phytochrome signaling (Leivar and Quail, 2011). Activated phytochrome translocates to the nucleus and directly interact with PIFs (Quail, 2002) resulting in phosphorylation and degradation of the targeted PIFs, and transcriptional changes in target genes (Al-Sady et al., 2006; Shen et al., 2007). PIFs are also involved in hormonal control of light signaling (Chaiwanon et al., 2016; de Lucas and Prat, 2014) including ethylene production and signaling (Finlayson et al., 1998, 1999; Shi et al., 2016; Zdarska et al., 2015). A family of endoplasmic reticulum-located receptors perceive ethylene that is then transduced through a multi-step signal cascade to the Ethylene-Insensitive 3 (EIN3) and EIN3-Like1 (EIL1) transcription factors (Alonso et al., 1999; Chang and Shockey, 1999). The F box proteins, EBF1 and EBF2, target EIN3/EIL1 for proteasome-mediated degradation through the SCR E3 ligase complex (Binder et al., 2007; Gagne et al., 2004; Guo and Ecker, 2003; Potuschak et al., 2003). Ethylene stabilizes EIN3/EIL1 by inhibition of EBF1/EBF2 through regulation of transcription and protein stability (An et al., 2010; Merchante et al., 2015; Qiao et al., 2012). PhyB has also been shown to directly interact with EIN3 and enhance interactions between

PhyB, EIN3 and EBF1/EBF2 which modulates EIN3 degradation via the SCR E3 ligase complex (Shi et al., 2016). Ongoing research in our lab is directed at determining if an interaction between phytochrome and ethylene mediate SD-induced BSP gene expression in *Populus*.

Nitrogen remobilization from senescing leaves to storage tissues during growth cessation and the onset of dormancy is an essential process in seasonal N cycling and is the overriding factor that contributes to NUE. During the N storage phase of seasonal N cycling, senescing leaves transition to sources of N that are translocated to bark prior to leaf abscission. Consequently, both leaves and bark function as either an N sink or an N source depending on the season and so the nature of the interactions between these organs shifts seasonally. Leaf senescence is a complex developmental process utilized to remobilize nutrients and contributes to NUE (Avila-Ospina et al., 2014; Kim et al., 2016; Schippers, 2015). Autumn leaf senescence in *Populus* is triggered by shortening photoperiod (SD) and once initiated is accelerated by low temperature (Fracheboud et al., 2009). Growth cessation and bud set is also triggered by shortening photoperiods, but the critical photoperiods for bud set and leaf senescence appear to differ (Fracheboud et al., 2009). At a cellular level, autumn senescence of *Populus* leaves occurs in an ordered fashion involving chlorophyll degradation, chloroplast conversion to gerontoplasts, carotenoid degradation and anthocyanin accumulation, and protein degradation (Keskitalo et al., 2005). Autumn leaf senescence also involves extensive changes in gene expression of which cysteine proteases and metallothioneins are highly enriched (Andersson et al., 2004; Bhalerao, 2003).

Glutamine (Gln) is the major amino acid that accumulates in senescing *Populus* leaves and is also the major amino acid transported from senescing leaves to bark via the phloem during N remobilization and storage. The cationic amino acid transporter CAT11 is one of the few amino acid transporters characterized in *Populus* and it appears to play a role in Gln transport from leaf to bark (Couturier et al., 2010). Little is known about other amino acid transporters or facilitators that might be involved in the unloading of amino acids from phloem to bark. Based on data from DNA microarrays it was recently reported that a large number of amino acid transporters are expressed in poplar bark during SD-induced N storage (Babst and Coleman, 2018). This includes genes belonging to the ATF-AAT and NPF families and it was suggested that some of transporters encoded by these genes might be involved in phloem unloading and influx of amino acids into parenchyma storage tissues (Babst and Coleman, 2018) In *Arabidopsis* an amino acid transporter was recently identified that is responsible for loading Gln into phloem (Santiago and Tegeder, 2016) which provides some insight into this important transport step. However, the mechanism for loading and unloading Gln from xylem and phloem are not known in *Populus*. While passive symplastic phloem loading of carbohydrates via plasmodesmata is common and has been demonstrated in *Populus* (Zhang et al., 2014) metabolite un/loading has not been studied in senescing leaves. Although some modest progress has been made in deciphering the transporters involved in amino acid transport during seasonal N storage we only have a rudimentary understanding of this critical process that is likely to govern N partitioning between N source and sink tissues.

The majority of the N released during autumn leaf senescence is translocated to bark and used in the biosynthesis of BSP. Transient increases in stem Gln levels peak during autumn leaf senescence and then again during spring N remobilization, correlating with major developmental processes during the annual growth cycle of *Populus* (Sauter and Cleve, 1992; Wildhagen et al., 2010). The first peak of bark Gln levels coincides with fall leaf senescence, whereas the second peak coincides with spring bud expansion and growth (Wildhagen et al., 2010). Bark Arg levels also increase during autumn leaf senescence and correlate with increased BSP gene expression (Couturier et al., 2010; Wildhagen et al., 2010). However, unlike Gln, increased bark Arg levels have one seasonal peak. Arginine levels begin to accumulate during leaf senescence, remain elevated during dormancy, and then decline when spring bud expansion and growth begins (Wildhagen et al., 2010). BSP gene expression can also be rapidly induced in poplar bark by feeding Gln to *Populus* stems (Zhu and Coleman, 2001a). Thus, in addition to its role as a transport amino acid and as a source of N for incorporation into BSP, Gln also appears to serve as a signal molecule that regulates BSP gene expression. Thus, Gln transport from senescing leaves (source) to bark (sink) would have dual roles in *Populus* N metabolism: (1) as a N source for BSP biosynthesis and (2) a signal for metabolic regulation of seasonal N cycling. These roles suggest a link between bark BSP accumulation and bark sink development with leaf source status.

Since induction of BSP expression and N storage appears to be coupled to changes in the N status of bark mediated by Gln transport and/or accumulation this metabolic change or increased N influx must somehow be sensed. Nutrient sensing is

an important component of how organisms coordinate growth and development and multiple nutrient sensing mechanisms have evolved in both prokaryotes and eukaryotes (Chantranupong et al., 2015). Plants have components of the (1) P_{II}, (2) GCN2 (general amino acid control non-derepressible 2) and (3) TOR (target of rapamycin) kinase nitrogen and amino acid sensing systems, but the role of these systems in plants is not well understood compared to yeast and mammals. Both GCN2 and TOR kinases are involved in sensing intracellular amino acid levels particularly under limiting or starvation conditions (Chantranupong et al., 2015). In plants, GCN2 has been shown to interact with uncharged tRNA and have a role in eIF2a phosphorylation that may play a role in stress and herbicide responses (Faus et al., 2015; Lageix et al., 2008; Zhang et al., 2008). GCN2 is unlikely to be important in seasonal N cycling since N becomes abundant in sink tissues as opposed to N-starvation conditions.

TOR consists of two distinct complexes; TORC1 being sensitive to rapamycin and TORC2 which is insensitive (Wullschleger et al., 2006). Plants possess all of the TORC1 components and this pathway has been shown to play roles in protein synthesis and metabolism, cell proliferation, cell size, autophagy and the auxin signaling pathway (Bögre et al., 2013; Caldana et al., 2013; Dobrenel et al., 2011; Henriques et al., 2014; Leiber et al., 2010; Mahfouz et al., 2006; Menand et al., 2002; Ren et al., 2012; Robaglia et al., 2012), but it is unknown if this pathway has any role in sensing changes in Gln levels during seasonal N storage.

The PII family of conserved nutritional signaling proteins occurs in bacteria, archaea and plants (Chellamuthu et al., 2013; Leigh and Dodsworth, 2007; Sant'Anna

et al., 2009; Uhrig et al., 2009). PII signaling proteins play roles in sensing cellular carbon and N balance and are involved in protein interactions with metabolic enzymes, signal transduction proteins, transcription factors and metabolite transporters (Leigh and Dodsworth, 2007; Osanai and Tanaka, 2007; Uhrig et al., 2009). Plant PII are conserved ~15 kDa proteins that form a ~45 kDa homotrimeric complex (Mizuno et al., 2007a). A hallmark of this sensing mechanism is ATP and 2-oxoglutarate binding to PII homotrimers to produce distinct PII conformations (Fokina et al., 2010; Forchhammer, 2008; Huergo et al., 2013; Zeth et al., 2014). Ligand binding and receptor interaction involve a protruding T loop for each subunit (Forchhammer, 2008; Huergo et al., 2013). High-resolution structural analysis on PII proteins from a variety of species have revealed that trimeric P_{II} sensors interact with hexameric NAGK to alleviate feedback inhibition by Arg (Chellamuthu et al., 2014; Llácer et al., 2007, 2008; Mizuno et al., 2007a, 2007b; Ramón-Maiques et al., 2006). Interestingly, (most) plant PII proteins possess a C-terminal extension that is absent in archaea, bacteria and red algae (Uhrig et al., 2009), but which is required for Gln binding. This so-called Q-loop facilitates the interaction of trimeric P_{II} with hexameric NAGK to alleviate feedback inhibition by Arg (Chellamuthu et al., 2014). On the other hand, it is intriguing that the *Brassicaceae* PII sensors, including that from *Arabidopsis*, lack part of the plant-specific C-terminal extension that comprises the Gln binding loop found in plants (including poplar) (Chellamuthu et al., 2014), yet the *A. thaliana* PII retains the ability to bind NAGK and regulate enzyme activity.

Gln may serve multiple roles in *Populus* seasonal N cycling including N transport from leaves to bark during SD-mediated N storage, an N source for BSP

biosynthesis, and as a metabolic signal of bark N influx. The increased influx of Gln to bark may alter C/N ratios and then be sensed through PII-Gln binding which facilitates PII-NAGK interactions that up-regulate the Arg pathway and Arg accumulation. Increases in bark Arg may function in N storage but may also regulate the expression and accumulation of BSP through unknown mechanisms. On the other hand, if the Arg pathway beyond the PII-NADK step is unaffected, then it is possible that the PII-Gln interaction regulates *BSP* expression independent of Arg. Since PII has been shown to interact with other proteins in *Arabidopsis* (biotin carboxyl carrier protein) (Bourrellier et al., 2010) as well as transporters and transcriptional regulators in bacteria and archaea (Amon et al., 2010; Herrero et al., 2001; Huergo et al., 2013; Leigh and Dodsworth, 2007; Merrick and Edwards, 1995; Sonenshein, 2007) it may be premature to conclude that other PII interactions are not involved in the regulation of *BSP* expression.

Other VSP in *Populus*: WIN4

Besides BSP the *Populus* genome also contains a BSP-like subfamily consisting of 5 genes that have been termed the WIN4-subfamy and consists of WIN4, VSP 425, VSP XIII, VSP 87A and VSP 840 (Pettengill et al., 2013). WIN4, first identified as a wound-inducible gene in *Populus*, shares 75% cDNA sequence identity to BSP and WIN4 also shares common expression patterns, e.g. nitrogen- and wound-induction (Coleman et al., 1994; Davis et al., 1993; Lawrence et al., 1997). WIN4 transcripts accumulate in leaves and stems, while BSP accumulates in stem phloem parenchyma and xylem ray cells. In contrast to BSP, WIN4 is not induced in bark under either SD and low temperature (Davis et al., 1993; Lawrence et al., 2001; Rennenberg et al.,

2010; Wildhagen et al., 2013), but is induced in young leaves with increased N availability and repressed by SD treatment (Coleman et al., 1994; Pettengill et al., 2013). It has been suggested that WIN4 may play a role in short-term N storage and mobilization in leaves during growth while BSP is involved in seasonal N storage and storage during periods of excess nitrogen availability (Coleman et al., 1994) Recently, *Populus* WIN4 (PtdWIN4) was reported to be involved in herbivore resistance since PtdWIN4 transgenic *Arabidopsis* exhibited high anti-herbivore activity (Hu et al., 2012). Methyl jasmonate has also been reported to regulate the accumulation of both BSP and WIN4 in *Populus* (Beardmore et al., 2000; Zhu and Coleman, 2001a), as well as VSP accumulation in soybean (Anderson, 1991; Mason and Mullet, 1990; Staswick, 1994), alfalfa (Meuriot et al., 2004) and Arabidopsis (Berger et al., 1995) which may be indicative of possible role in herbivore resistance.

Other VSP in *Populus*: PNI288

PNI288 is another of the NP-like family of poplar VSPs, and is expressed in conditions similar to WIN4, supporting a possible role as a short-term storage protein (Lawrence et al., 2001). For example, like WIN4, PNI288 is also induced by both wounding and increased nitrogen availability, whereas its mRNA abundances decreased when exposed to either SD or low temperatures (Cooke et al., 2003; Lawrence et al., 2001; Pettengill et al., 2013; Rennenberg et al., 2010; Wildhagen et al., 2013). Similar to WIN4, PNI288 expression was also detected in shoot tips, leaves and bark (Pettengill et al., 2013). To date, studies on PNI288 are only limited to Populus (Cooke et al., 2003; Lawrence et al., 2001; Pettengill et al., 2013), and

future research needs explore the role of PNI288 in N storage and response to environmental stresses in other woody plants.

Nitrogen remobilization

In temperate deciduous trees seasonal N cycling involves two phases of N remobilization. N is mobilized from senescing leaves in the fall where it is transported to and stored in perennial tissues during winter. In the spring, as growth commences, this stored N is remobilized once again and partitioned to growing tissues. Although progress has been made towards understanding the molecular and physiological processes involved in autumn N remobilization from leaves and storage in perennial tissues such as bark, much less is known about the physiology and regulation of N remobilization during spring growth. The role of spring N remobilization to plant growth is mostly circumstantial and is based on the seasonal dynamics of BSP accumulation and disappearance. Few studies have directly assessed the contribution of stored N to spring growth. The importance of spring N remobilization from storage pools to N sinks is likely to be related to reduced N acquisition from soil in spring when soil temperatures are cold (Rennenberg et al., 2010). For example, 15N soil feeding experiments that assayed changes in xylem 15N content during the spring showed that 15N enrichment of xylem sap did not occur until 40 days after bud burst in poplar and 21 days after bud burst in cherry (Millard et al., 2006). Since 15N in xylem sap was dependent upon the uptake of soil applied 15N, this delay in the acquisition of soil N implies that initial spring growth relies upon N remobilization from stored N to developing N sinks such as expanding reproductive and vegetative buds and shoots.

Spring N remobilization involves the catabolism of stored BSP. Furthermore, since Gln is the major amino acid present in xylem sap during N remobilization then spring N remobilization must also involve metabolic processes involved in amino acid catabolism and biosynthesis, and amino acid transport to N sinks. Currently little is known about the physiology and regulation of these processes. In poplar, BSP catabolism and N remobilization is dependent upon the development of N sinks that occurs during bud break and shoot growth (Coleman et al., 1993). Further, the absence of expanding buds inhibits BSP catabolism even in plants with sufficient chilling to break dormancy, suggesting that N source (bark) and sink (expanding buds and young leaves) communication is an important aspect that coordinates BSP catabolism and N remobilization (Coleman et al., 1993). Because BSP catabolism depends upon expanding buds and the development of N sinks, it is likely that a signal originates in expanding buds and shoots and subsequently transported to storage tissues, such as bark phloem parenchyma, which in turn triggers BSP catabolism and N remobilization. Ongoing research in our lab is targeted towards identifying this signal and the molecular processes associated with BSP catabolism and N remobilization.

One of the key processes involved in spring N remobilization is the catabolism of BSP which is likely to involve the action of proteolytic enzymes. In apple, Kang and Titus (1980) partially purified an endopeptidase from dormant bark that appeared to be involved in protein catabolism. Moreover, the levels of exo- and endopeptidase activity in shoot bark coincided with ABA levels of bark where increased ABA levels seemed to suppress protease synthesis or activation (Mousdale,

1982, 1983). Thus, it was proposed that in the case of apple that storage protein catabolism is inhibited by increases in ABA that occur in bark during the winter.

Proteolysis is a complex process involving multifunctional proteases important to different stages in the plant life (van der Hoorn, 2008). The genome of *Populus* is predicted to contain 955 genes that encode proteases (García-Lorenzo et al., 2006) making the identification and study on proteases involved in N remobilization challenging. In an attempt to identify proteases that could play a role in poplar BSP catabolism during spring N remobilization, Islam et al. (2015) used multidimensional protein identification technology (MudPIT) to identify bark protein changes that occur during BSP catabolism. Over 4,000 proteins were identified in bark prior to and during BSP catabolism with the majority of the proteins associated with BSP catabolism. Thus, the bark proteome undergoes extensive changes as bark transitions to a N source in the spring. These extensive changes in the proteome of bark also included at least 30 proteases that increased in abundance during BSP catabolism and N remobilization (Islam et al., 2015). The identified proteases spanned a range of families including members of the papain-like cysteine proteases, serine carboxypeptidases and aspartyl proteases (Islam et al., 2015). Of these 30 proteases, 16 were predicted to be targeted to vacuole or secretory system which is likely to be necessary if they are involved in BSP catabolism. Half (8) of the proteases predicted to be targeted to the vacuole or secretory systems were classified as papain-like cysteine proteases (PLCPs; C1A), 3 as serine carboxypeptidases (S10), and 3 as eukaryotic aspartyl proteases (A1A and A1B) (Islam et al., 2015). Although the identified proteases may be involved in other process, such a xylem development

(Funk et al., 2002), it is likely that many are involved in BSP catabolism, especially given their possible location to vacuoles. It is also likely that multiple proteases, including exo- and endoproteases are required for BSP catabolism which would require coordination of protease synthesis or activation. Cysteine proteases also have a role in the mobilization of seed storage proteins that involves both the activation of proteases as well as de novo biosynthesis (Müntz, 2007; Müntz et al., 2001; Shutov et al., 2003; Tiedemann et al., 2001). It is possible that similarities exist between BSP and seed storage protein catabolism and research directed at uncovering these similarities would be informative towards uncovering conserved features of N remobilization in plants. Additional studies are required to thoroughly identify the role of C1A cysteine proteases during N remobilization in *Populus*, which could provide a basis to develop strategies to manipulate N remobilization in trees.

During N remobilization in the spring, glutamine is the predominate amino acid present in xylem sap of poplar, cherry and red beech (Millard et al., 2006; Sauter and Cleve, 1992; Schneider et al., 1994; Wildhagen et al., 2010). Some tree species appear to use different amino acids or compounds in N remobilization including citrulline in Betula pendula (Millard et al., 1998), arginine in *Juglans nigra* × *regia* (Frak et al., 2002) and asparagine in *Acer pseudoplatanus* (Millard and Grelet, 2010) and *Malus domestica* (Guak et al., 2003a; Malaguti et al., 2001). Irrespective of the chemical nature of N transport, catabolism of the respective storage proteins in different species requires catabolism of the amino acids produced from storage protein catabolism and the biosynthesis of the transport form of N. As an example, *Populus* BSP is rich in serine, leucine, phenylalanine and lysine, but not glutamine

(Coleman et al., 1992), yet glutamine is the major amino acid found in xylem sap during spring N remobilization. This implies that the breakdown of poplar BSP provides the C and N used in glutamine biosynthesis via glutamine synthetase (GS) before transport to developing buds and shoots. Thus, functional studies on specific glutamine transporters and GSs will advance our understanding of N source-sink mechanisms of seasonal N cycling.

Future directions

Nutrient accumulation, including N accumulation, is important to the productivity of both horticultural and forest trees. N fertilizers are an integral part of U.S. and global agricultural systems with over 90 million metric tons (MMt) of N fertilizer applied to soils globally (Frink et al., 1999) but global nitrogen use-efficiency (NUE) is only 42% (Zhang et al., 2015) and it is estimated that 50-70% of N fertilizers are lost following application (Good et al., 2004). Further, N lost from fertilization has major environmental costs including increased atmospheric N deposition in forest and other natural ecosystems, increased leaching and surface runoff leading to the onset of algal blooms, hypoxia and fish kills (Robertson and Vitousek, 2009). Thus, any gains in enhancing plant NUE will lead to lower N inputs and would directly impact long-term improvement and sustainability of U.S. agriculture and food and fiber systems. Because seasonal N cycling is the major factor that contributes the NUE in trees, deciphering this process would reveal strategies used by perennial plants to conserve and reuse N. Although progress has been made towards understanding the mechanisms of seasonal N cycling in trees there are still substantial knowledge gaps. The molecular signaling and regulatory pathways involved in seasonal N

accumulation and the factors involved in N transport for N sources to N sinks are poorly understood in trees. Understanding this process would also provide insight into long-distance source-sink communication in plants.

Chapter 2: Seasonal nitrogen remobilization and the role of auxin transport in poplar trees

Abstract

Nitrogen (N) is an essential nutrient for plant growth, development and reproduction as it is the basic constitute of amino acids, the building blocks of proteins. Seasonal N cycling in trees is an adaption to nutrient limitations and an important component of the perennial lifestyle. In *Populus,* Bark Storage Proteins (BSP) accumulate in bark during autumn and then decline when growth resumes in the spring. Although BSP catabolism is associated with spring regrowth and N remobilization that follows dormancy, little is known about the relative contribution of N remobilized from BSP to plant growth or the signals regulating N remobilization. Here, we used transgenic poplars with reduced BSP accumulation via RNAi knockdowns as well as sink manipulations to gain a better understanding of how N storage influences shoot growth. It was discovered that reduction of the BSP N storage-pool delayed the timing of bud break following dormancy. Further, growth of shoots following dormancy was significantly reduced when BSP accumulation was limited. Results from ^{13}N tracer studies revealed that BSP accumulation also contributes to the bark N sink development and N partitioning from senescing leaves to bark. Previous research has shown that BSP catabolism and N remobilization requires a signal from expanding shoots, yet the nature of this signal is unknown. To identify the possible

nature of this signal, bark transcriptome changes in gene expression during BSP catabolism and N remobilization were examined using DNA microarrays and discovered an enrichment in the expression of genes associated with auxin transport and signaling. Through a series of physiological studies that manipulated either the source of auxin or auxin transport indicated an association between bark localized expression of auxin transport and signaling genes and protease gene expression during BSP catabolism and N remobilization. Furthermore, the bark expression of specific protease genes appeared to be auxin inducible. Taken together, these results indicate that BSP accumulation is an important component involved in the establishment of bark sink strength during N remobilization from senescing leaves to bark. BSP accumulation is also important to the N budget of expanding shoots once growth commences following dormancy. In addition, N remobilization associated with BSP catabolism appears to be regulated by auxin that is produced in expanding buds and shoots and transported to bark where it induces the expression of protease genes that are likely to be involved in BSP catabolism.

Introduction

Resource allocation and partitioning mediated by source-sink interactions is fundamental to plant growth and development. Nitrogen (N) is a major nutrient that impacts plant growth and productivity. Growth of annual plants requires acquiring external N from soil and the internal redistribution of assimilated N. Forest trees and other perennial plants also acquire assimilate and redistribute N during growth but have the additional feature of N redistribution that occurs seasonally where N is mobilized from senescing leaves to perennating storage tissues and then remobilized

from these storage tissues when growth resumes. This seasonal cycling of N is a fundamental feature of the perennial habit (Cooke and Weih, 2005; Staswick, 1994). Because seasonal N cycling occurs annually in deciduous forest trees N is retained and reused for longer periods of time and influences overall N budgets (Millard and Grelet, 2010; Millard et al., 2006). This adaptive strategy contributes to the economics of N use and provides a competitive advantage in N limited conditions (Chapin et al., 1990; Millard and Grelet, 2010; Vitousek, 1982). Consequently, seasonal N cycling is important to the ecology of forest tree N use and is a major factor of N-use efficiency (NUE) (Aerts, 1990; Boerner, 1984; Chapin and Kedrowski, 1983; Ryan and Bormann, 1982; Vitousek, 1982). Because of the importance of internal N cycling to NUE this process is considered an important trait in the development of perennial lignocellulosic energy feedstock (Allwright and Taylor, 2016; Karp and Shield, 2008). Despite the importance of seasonal N cycling to tree N allocation and partitioning, the contribution of stored N to growth and the mechanisms involved in source to sink remobilization of stored N remains poorly understood in trees.

A central feature of seasonal N cycling in the deciduous temperate poplar (*Populus*) tree is the accumulation of 32 kDa proteins in protein storage vacuoles localized to bark phloem parenchyma and xylem ray cells during autumn and the disappearance of these proteins when shoot growth commences in the spring (van Cleve et al., 1988; Sauter et al., 1988; Wetzel et al., 1989). These proteins, termed bark storage proteins (BSP), are encoded by three genes in poplar (*BSPA*, *BSPB* and *BSPC*) and are members of a larger 13-member gene family (Pettengill et al., 2013).

BSP expression and protein accumulation is associated with environmental factors including short-day (SD) photoperiods, N availability and low temperature (Coleman et al., 1991, 1992, 1994; Pettengill et al., 2013; Zhu and Coleman, 2001a, 2001b).

Poplar seasonal N cycling involves two distinct phases of N remobilization that are accompanied by N source and sink transitions. During autumn leaf senescence leaves transition to N-sources with N transported from leaves to bark phloem parenchyma and xylem ray cells that act as N-sinks (Sauter et al., 1988; Wetzel et al., 1989). Poplar leaf senescence is characterized by the accumulation of glutamine (Gln) resulting from protein hydrolysis and is the predominate transport amino acid (Couturier et al., 2010; Hörtensteiner and Feller, 2002). Phloem loading of Gln in senescing leaves appears to be mediated by the cationic amino acid transporter CAT11 (Couturier et al., 2010) and this same transporter may also have a role in unloading Gln to bark phloem parenchyma (Babst and Coleman, 2018). Gln can also induce poplar *BSP* expression when fed to stems in long-day (LD) non-inductive conditions suggesting that Gln may have both signaling and transport roles (Zhu and Coleman, 2001a). Once growth commences in the spring, bark phloem parenchyma and xylem rays become N-sources and BSP is catabolized and stored N is remobilized to growing sink tissues (Coleman et al., 1993; Wetzel et al., 1989). BSP catabolism requires new shoot growth and the establishment of N-sinks (Coleman et al., 1993) and is accompanied by extensive changes in the bark proteome including increased abundance of papain-like cysteine proteases, serine carboxypeptidases, and aspartyl proteases (Islam et al., 2015).

The contribution of stored N to spring growth and the N budget of trees is largely based on their seasonal cycle of accumulation and disappearance (Wetzel et al., 1989), leaf defoliation studies (May and Killingbeck, 1992), or ^{15}N transport studies (Millard et al., 2006). Although these approaches have been informative they fail to directly address the contribution of the BSP storage-pool and N remobilization to growth. Moreover, BSP catabolism and N remobilization requires communication between the N-sink established by expanding buds and shoots to bark BSP storage tissues, yet the nature of this signal has remained elusive. Here, multiple approaches were used to further define the role of BSP storage and N remobilization to shoot growth. We also establish that the long-distance transport of auxin from expanding buds and shoots likely plays a significant role of BSP catabolism and N remobilization. Furthermore, transported auxin appears to be involved in mediating the expression of specific protease genes that maybe involved in BSP catabolism.

Materials and methods

Plant culture and growth conditions

Two poplar genotypes, *Populus trichocarpa* (Nisqually) and the *Populus tremula* × *P. alba* hybrid clone INRA 717-1B4 were used in this study. Rooted stem cuttings of plants were first grown in long-days (LD) (16h light/8h dark) at 20°C for 8 weeks. To induce BSP accumulation, leaf senescence and bud dormancy, LD grown plants were subjected to SD treatment by changing the photoperiod in controlled environmental chambers to SD (8h light/16h dark) for 8 weeks at 20°C after which the temperature was reduced (10°C day/4°C night) for additional 4 weeks. Bud dormancy was

overcome by treating plants in continuous darkness at 4°C for an additional 8 weeks. Bud break, shoot growth, BSP catabolism and N remobilization was triggered after the 8 week low-temperature treatment by transferring plants to LD (16hr light/8hr dark) at 20°C.

N availability treatment

The *Populus tremula X Populus alba* clone INRA 717 IB4 was used for all experiments related to N availability. Rooted *in vitro* cuttings were individually planted into 6.0L pots containing soilless media (Sunshine LC1) and grown in a LD (16 h light, 8 h dark) greenhouse at 20-25°C for 10 weeks at different N levels. Supplemental lighting to extend photoperiods to LD (minimum of 16 hrs of light) was provided by high-pressure sodium lamps. Plants were randomly assigned to N treatments with 3 replicates per treatment. Plants were fertilized 3 times per week with 500ml of a nutrient solution (8.3mM KCl, 8.3mM $CaCl_2.2H_2O$, 1mM $MgSO_4.7H_2O$, 0.5mM KH_2PO_4, 44.8uM EDTA Fe (III) [$C_{10}H_{12}FeN_2NAO_8$], 23.1uM H_3BO_3, 4.5uM $MnCl_2.4H_2O$, 4uM $ZnCl_2$, 2.7uM $CuCl_2.2H_2O$, 52nM $Na_2MbO_42H_2$) containing 1.5625mM, 3.12mM, 6.25mM, 12.5mM or 25mM NH_4NO_3. Plants were destructively harvested after the 10-week treatment period and shoot growth parameters including leaf area, stem diameter, plant height and sylleptic shoot number and sylleptic shoot length were measured.

Shoot competition

Populus trichocarpa clone Nisqually was used for this study. Rooted softwood cuttings of *Populus trichocarpa* were grown in 6.0L pots containing soilless media (Sunshine LC1) in a LD (16 h light, 8 h dark) greenhouse for six weeks and fertilized once at the beginning of LD growth with 2g of 30-day controlled release fertilizer (18-3-3, Nutricote). BSP accumulation and bud dormancy was induced by transferring plants to SD conditions (8 h light, 16 h dark at 20°C) using a 160ft^2-controlled environment chamber (EGC, Chagrin Falls, OH). After 6 weeks of SD treatment at 20°C the temperature was reduced (LT) (10°C light, 4°C dark) for an additional 8 weeks of SD to induce leaf senescence and abscission. After 8 weeks of SD combined with LT leaf senescence and abscission was complete and plants were moved to refrigerated storage (4°C) with continuous darkness for 10 weeks to provide sufficient chilling to release bud dormancy. Following LT release of bud dormancy plants were pruned to 100 cm in height so that the pool of stored N was consistent between treatments. Plants were then randomly assigned to one of the various treatments used to compare sink competition between lateral shoots, sylleptic shoots or between lateral and sylleptic shoots. To compare the effect of different sink numbers on resulting shoot growth from lateral buds, plants were treated such that they either consisted of the most apical 1, 3, 6, 9 or 12 lateral buds by surgically removing the remaining lateral buds appropriate for each treatment. In addition, all sylleptic shoots were also surgically removed. To determine the effect of sink competition between sylleptic shoots on shoot growth the lateral buds of plants were surgically removed and plants were treated such that they either consisted of 1, 5 or

10 sylleptic shoots. The effect of sylleptic shoot competition on the growth of lateral shoots was also examined using treatments consisting of either 1 or 10 lateral buds combined with either 1 or 10 sylleptic shoot. This resulted in 4 different treatments, 1 lateral shoot and 1 sylleptic shoot, 1 lateral shoot and 10 sylleptic shoots, 10 lateral shoots and 1 sylleptic shoot and 10 lateral shoots and 10 sylleptic shoots. The effect of lateral shoot competition on sylleptic shoots was evaluated using plants consisting of 1 or 10 sylleptic shoots with either 1 or 10 lateral buds. Similar to the previous treatments, this regime resulted in 4 different treatments, 1 sylleptic shoot and 1 lateral shoot, 1 sylleptic shoot and 10 lateral shoots, 10 sylleptic shoots and 1 lateral shoot and 10 sylleptic shoots and 10 lateral shoots. Following plant manipulation to create the various treatments, plants were placed in a LD greenhouse and after 5 weeks leaf number, leaf area, stem length, number of new sylleptic shoots and length of new sylleptic shoots were determined. For experiments focused on sylleptic shoot growth the attributes consisted of leaf area, number of sylleptic shoots and length of sylleptic shoots.

Generation of BSP-RNAi poplars

A 229 bp DNA fragment of the BSPA gene from *Populus trichocarpa* clone Nisqually was amplified using the forward primer 5'-CACCCCAGAGAATGGAGAGAACTTG-3' and reverse primer 5'-TGGTGATGGGAAGCCAGAAAAC-3', and a 103 bp DNA fragment of BSPB gene from Nisqually was amplified using the forward primer 5'-CACCTCGCTTAGGGCTTGTTTTTACG-3' and reverse primer 5'-

GATGACTCCGTGAATGCTGAATC-3'. Purified DNA fragments were cloned into pENTR D-TOPO entry vector using pENTR™ Directional TOPO Cloning Kits (Invitrogen by Life Technologies). The entry clones were combined into the binary vector pB7GWIWG2(II) (Karimi et al., 2002) using Gateway LR ClonaseII enzyme mix (Invitrogen by Life Technologies). The destination clone was transformed into *Agrobaterium tumefaciens* strain C58/PMP90 using heat-shock method. Stem sections from the hybrid poplar (*Populus tremula* x *Populus alba*, INRA 717 IB4) were transformed by co-cultivation with *Agrobacterium tumefaciens* strain C58/pMP90 harboring the binary vectors (Leple et al., 1992). Transformed plants were selected on Murashige and Skoog (MS) media containing 5mg/L glufonsinate ammonia (Basta).

^{13}N labeling study

Wild-type (WT) and BSP_{RNAi} (*bsp*) poplars were used in the experiments. WT is the hybrid poplar *Populus tremula* x *Populus alba*, INRA 717 IB4 and BSP_{RNAi} (*bsp*) is a BSP RNAi transgenics produced in the same hybrid poplar genotype. WT and BSP_{RNAi} (line BSM9) plantlets grown from micro-cuttings cultured on hormone-free 1/2 MS medium (Murashige and Skoog 1962). Shoot cultures were maintained on this medium and grown at 23 °C under a 16-h photoperiod. Light was provided by fluorescent tubes (F40PL/AQ/ECO 49893 40Watt T12, GE) at a photon flux density of ~100 – 130 μmol m^{-2} sec^{-1} measured at the top of the culture box. 7-8 week old in vitro-grown plantlets were transplanted into potting soil (Professional growing mix, Sungro®) in plastic pots (8cm x 8cm x 7cm). After transplanting, plants were grown in a plant growth chamber (A1000, CONVIRON) under a long-day (LD) photoperiod

(16-h light, 24°C daytime, 22°C dark) for 5 weeks and then a subset of the plants were used for ^{13}N experiments. When LD plants were removed, the remaining plants were exposed to short-day (SD) photoperiod (10-h light, 24°C daytime, 22°C dark) for 6 weeks, and then the SD treatment was supplemented with cold treatment (SD-LT) (10-h photoperiod, 12°C daytime, 7°C dark) for 3 weeks before SD-LT ^{13}N experiments. At each time point, ten poplar plants of each genotype that were fairly similar in size were chosen for experiments.

Each poplar plant was transferred to a growth chamber containing the positron emission tomography (PET) scanner and positioned at the center of the PET field of view (Wang et al. 2014). A single load leaf at approximately leaf plastochron index (LPI) 10-12 was clamped inside a cuvette fitted with LED lights. The ^{13}N was produced by bombarding a water target in a cyclotron to produce $[^{13}N]NH_3$. The $^{13}NH_3$ solution was basified with KOH and injected into the cuvette onto an absorbent pad at the bottom of the cuvette. The delivered activity was measured in a dose calibrator/gamma radiation well counter (CRC-258, Capintec, Florham Park, NJ, USA) (~0.16-0.3 MBq per dose), and the time was recorded for decay correction (half-life of ^{13}N = 9.965 minutes). A pump was attached to the cuvette outlet to provide airflow through the cuvette. The leaf was treated for 15 minutes before removing the cuvette, and then the PET scanned continuously for an hour. The plant was taken out from the scanner, dissected to 4 parts: upper stem including the apex; lower stem; petiole and the half of the load leaf not in the cuvette; and the load zone, which is the part of the leaf in the cuvette. The radioactivity of each plant part was measured in a calibrated gamma radiation well counter (Shielded Well Gamma

Sample Counter Head: Model 203, NATS Inc., Middletown, CT, USA; Scaler/Ratemeter Model 2200, Ludlum Measurements, Inc., Sweetwater, TX, USA) and the time was recorded for decay correction.

To test how much of the ^{13}N in the leaf had been assimilated, a piece of the load zone was excised and the radioactivity was measured before and after volatilization of $^{13}NH_3$, as described by Hanik et al. (Hanik et al. 2010). Briefly, the leaf piece was ground in 1M KOH solution to raise the pH and convert any $^{13}NH_4^+$ to the volatile form $^{13}NH_3$, and the solution was sparged with compressed air for 20min to remove any $^{13}NH_3$. After 5, 10 , and 20 minutes of sparging, we found no decrease in the decay-corrected radioactivity, indicating that there was no free $^{13}NH_3/^{13}NH_4^+$ in the leaf by the end of the 1 hr plant incubation.

The ^{13}N export was calculated as a percentage of total ^{13}N in the plant, after decay correction. Partitioning to the lower stem was calculated using the activity measured in the lower stem compared to the total activity detected in plants. Total export was calculated using the combined activity of apex/upper stem and lower stem as a percentage of the total activity in the plant.

Morphology measurements were taken 3 days before the first day of each set of ^{13}N experiments, including stem height, and total number of leaves (upper leaves with length > 2cm were counted; lower leaves with length > 7cm were counted). Load leaf length (cm) from tip to petiole was measured, as well as width (cm) at the widest part of the leaf. Load leaf average chlorophyll content (mg/m^2) was measured *in vivo* using a chlorophyll fluorescence meter (CCM-300, OPTI-SCIENCES, Hudson, NH, USA), based on the method of Gitelson et al. (Gitelson et al. 1999).

Chlorophyll measurements were taken prior to ^{13}N experiments at three different positions on each leaf and averaged for the leaf.

RNA preparation and microarray analyses

Total bark RNA was purified from plants after 12 weeks of treatment with SD+LT (dormancy breaking treatment) and after 1, 2 and 3 weeks of LD treatment following dormancy breaking. Total RNA was purified using Qiagen RNeasy plant mini kit (Qiagen, USA) with modifications and on-column DNA digestion using DNase I (Qiagen, USA) as previously described (Pettengill et al., 2012). RNA quality was assessed using the Exprion RNA StdSens Analysis Kit (Bio-Rad Laboratories, CA) and spectrophotometric analysis (Eppendorf BioPhotometer plus; Eppendorf, NY). Biotinylated cRNA was prepared according to the standard Affymetrix protocol (GeneChip 3' IVT expression kit) from 100 ng of total RNA. Following fragmentation, 12.5 µg of cRNA was hybridized for 17 h at 45 °C on Affymetrix GeneChip® Poplar Genome Arrays, and washed and stained in the Affymetrix Fluidics Station 450 and scanned using GeneChip Scanner 3000 according to the manufacturers protocols. Microarray data was analyzed using R and Bioconductor. Log2-transformed expression values were obtained for each probe set. For the filtering process, we first applied a similar filtering process based on threshold fractions of "present" calls as described previously (McClintick and Edenberg, 2006), which effectively eliminated probe sets that are unlikely to be reliable while preserving the most significant probe sets as well as those that are differentially expressed between experimental conditions. Subsequently, probe sets that had a median absolute deviation smaller than or equal to 0.1 were excluded from further

analysis. This filtering process resulted in 30410 probe sets retained for further statistical analysis for the regrowth experiment.

Statistical analysis of probe sets passing the filtering process was carried out using the limma package (Smyth, 2004) where variances were adjusted by the empirical Bayes (eBayes) method and adjusted *P*-values for multiple tests were calculated using Benjamini-Hochberg's method (Benjamini and Hochberg, 1995). Annotations for the probe sets were obtained from Affymetrix and the corresponding *Populus* gene models for each probe set were extracted. For gene models with multiple matching probe sets, the average expression values, average $\log_2$ ratios for each comparison, and average adjusted *P*-values were calculated based on all matching probe sets. Gene models with an adjusted *P*-value ≤ 0.01 and a $\log_2$-fold change ≥ 1.585 (3-fold change on linear scale) were considered differentially expressed in LD samples compared to the 12 SD-LT control.

Pathway analysis was performed using the corresponding *Arabidopsis* locus for each *Populus* model as obtained from Phytozome. The mean $\log_2$-ratios for all *Populus* gene models matching single *Arabidopsis* orthologues were then imported into CIMminer to generate color-coded Clustered Image Maps (CIMs) ("heat maps") with the default parameters (https://discover.nci.nih.gov/cimminer/home.do) (Weinstein et al., 1997). Enrichment of GO terms in the up- and down-regulated genes in the differentially expressed genes (DEGs) were generated from AgriGO (Du et al., 2010) where singular enrichment analysis was performed with a hypergeometric test and Yekutieli FDR (0.05) under dependency for multiple test adjustment. All microarray data and expression values for all probe sets were

submitted to Gene Expression Omnibus (GEO) at NCBI http://www.ncbi.nlm.nih.gov/geo under the accession GSE49982.

Phylogenetic tree construction

Protein sequences were obtained from Phytozome and aligned using ClustalW. The aligned sequences were used for constructing an unrooted phylogenetic tree using the Neighbor-Joining method (Saitou and Nei, 1987). The percentage of replicate trees in which the associated taxa clustered together in the bootstrap test (10000 replicates) are shown next to the branches (Felsenstein, 1985). The tree is drawn to scale, with branch lengths in the same units as those of the evolutionary distances used to infer the phylogenetic tree. The evolutionary distances were computed using the Poisson correction method (Zuckerkandl and Pauling, 1965) and are in the units of the number of amino acid substitutions per site. The analysis involved 10 amino acid sequences. All positions containing gaps and missing data were eliminated. There were a total of 114 positions in the final dataset. Phylogenetic analyses were conducted in MEGA7 (Kumar et al., 2016).

Auxin manipulation

To determine a possible role for auxin in BSP catabolism and N remobilization two approaches were used to manipulate auxin levels and transport. In the first approach we eliminated the possible source of auxin by removing apical and lateral buds after the combined 12 week SD + LT treatment. Control plants consisted of plants also treated with the combined 12 week SD + LT to overcome bud dormancy with the uppermost 5 lateral buds and the apical bud were left intact while the remaining

lateral buds were surgically removed from the stem of plants. Plants with and without buds were placed in a LD greenhouse at 20-25°C and bark from the middle of the stem was collected at the beginning of the LD treatment (day 0) and after 1, 2, and 3 weeks of LD treatment. At each sampling interval four biological replicates were collected. Bark was peeled from stems and immediately frozen in liquid N_2 and stored in -80°C freezer until used for protein or RNA extraction.

In a second approach poplar auxin transport was inhibited during LD mediated N remobilization using the auxin transport inhibitor, 1-*N*-naphthylpthalamic acid (NPA). Following the 12 week combined SD +LT treatments plants and prior to treatment with LD all of the lateral buds except the uppermost 5 lateral buds and the apical bud were removed from the stem of plants and then a subset of the plants were treated with either 1) a ring of 50 mM NPA in lanolin paste applied 20 cm below the proximal lateral bud, or 2) a ring of lanolin paste with 0 mM NPA also applied 20 cm below proximal lateral bud. Plants were randomly assigned each treatment. NPA (Chem Services, West Chester PA) was first dissolved in DMSO and then mixed with lanolin paste to give a final concentration of 50mM. The lanolin paste control (without NPA) contained the same volume of DMSO. The area of application was immediately covered with aluminum foil and plants were transferred to LD greenhouse conditions at 20-25 °C. Lanolin paste treatments were reapplied at weekly intervals. Bark tissue above and below the site of NPA treatment was collected separately at the beginning of the LD treatment (day 0) and after 5, 10 15 and 21 days of LD treatment. At each sampling date four biological replicates were

collected. Bark was peeled from stems and immediately frozen in liquid N_2 and stored in -80°C freezer until used for protein extraction or RNA extraction.

In vitro auxin treatments

Stems from tissue-cultured *Populus tremula* x *Populus alba*, INRA 717 IB4 were used for auxin treatment as described by Schrader et al., (2003). Appropriately 6-cm-long and 3-mm-thick stems were defoliated and immediately transferred into ½x Murashige and Skoog (MS) medium lacking agar. Samples were harvested after being incubated at 100rpm at 20°C for 0, 2, 4, 8, and 16h. After 16 hr of incubation 20μM IAA was added into the medium, and the samples were further incubated for 0.5, 1, 2 and 4h in the same condition before harvesting. Three biological replicates were harvested at each time interval and stems were immediately frozen in liquid N_2 and stored in -80°C freezer until used for RNA extraction.

Auxin quantification

Poplar bark tissues were pre-ground and stored at -80 °C prior to analysis. Samples (approximately 20-23 mg per sample) were triple-ground in liquid nitrogen, and 1 mL 50 mM sodium-phosphate buffer (pH 7.0, containing 1% DETC) was immediately added into each tube. 10 ng [$^2H_5$] indole-3 acetic acid (d5-IAA, OlChemIm, Ltd., Olomouc, Czech Rebuplic, part #0311532), 1 μg [$^2H_3$] tryptophan (d3-Trp, CDN isotopes, Quebec, Canada, part #D-7419), 2.5 ng [$^2H_5$] Indole-3-[^{15}N] acetamide (DN-IAM, olchemIm Ltd, Olomouc, Czech Republic, part #0311541), 5 ng [$^2H_4$] indole-3-acetonitrile (d4-IAN, olchemIm Ltd, Olomouc, Czech Republic, part #0311851), 2.5 ng [$^2H_5$] indole-3-acetyl-L-[^{15}N] alanine (DN-IAAla, olchemIm Ltd,

Olomouc, Czech Republic, part #0311581), 2.5 ng [$^{2}H_5$] indole-3-acetyl-L-[^{15}N] phenylalanine (DN-IAPhe, olchemIm Ltd, Olomouc, Czech Republic, part #0311621), 2.5 ng [$^{2}H_5$] indole-3-acetyl-L-[^{15}N] valine (DN-IAVal, olchemIm Ltd, Olomouc, Czech Republic, part #0311641), 2.5 ng [$^{2}H_5$] indole-3-acetyl-L-[^{15}N] leucine (DN-IALeu, olchemIm Ltd, Olomouc, Czech Republic, part #0311612), 2.5 ng [$^{2}H_5$] indole-3-acetyl-L-[^{15}N] aspartic acid (DN-IAAsp, olchemIm Ltd, Olomouc, Czech Republic, part #0311592), 2.5 ng [$^{2}H_5$] indole-3-acetyl-L-[^{15}N] glutamic acid (DN-IAGlu, olchemIm Ltd, Olomouc, Czech Republic, part #0316132), 2.5 ng [$^{2}H_5$] indole-3-acetyl-L-[^{15}N] tryptophan (DN-IATrp, olchemIm Ltd, Olomouc, Czech Republic, part #0311632) were added into each tube as internal standards (ISTD). Samples were vortexed, extracted for 20 min at 4 °C on a lab nutator and centrifuged at 12,000 x G for 15 min at 4 °C. Supernatants were collected, and the pH was adjusted to 3 using 1N HCl. Auxinic compounds were further purified and concentrated by passing each supernatant over an HLB column (conditioned using 1 mL methanol (LC-MS/MS grade, Fisher Scientific, Pittsburgh, PA, part #A456-1) followed by 1 mL water and 0.5 mL 50 mM Na-Phosphate buffer, pH 2.7). After sample loading, HLB columns were washed with 2 mL 5% methanol and finally eluted with 2 mL 80% methanol. Eluates (containing auxins and auxin metabolites) were dried under nitrogen gas, re-dissolved with 1.00 mL methanol and filtered through 4 mm 0.2 μm PTFE filters (Phenomenex, Inc., Torrance, CA, part# AF0-3202-52). 0.2-0.5 μL of each sample was injected for LC-MS/MS analyses.

RNA extraction and qRT-PCR

Total RNA was extracted from three biological replicates using Qiagen RNeasy plant mini kit as previously described (Pettengill et al., 2012). Purified RNA was used for cDNA synthesis according to manufacturer's instructions (*iScript*™ cDNA Synthesis Kit, Bio-Rad). The cDNA was used for determination of relative transcript levels of target genes using qRT-PCR. Amplification reactions consisted of 30 sec at 95 °C followed by 40 cycles of 5 sec at 95 °C and 15 sec at 60 °C. Reference gene sand relative expression analysis was performed using qbasePLUS as previously described (Pettengill et al., 2012). All qRT-PCR primers for target genes and reference genes (Table 1.) were designed and validated as previously described (Pettengill et al., 2012).

Protein extraction and SDS-PAGE

Bark tissues were ground using a Freezer/Mill 6970EFM (Spex SamplePrep Metuchen, NJ). Ground bark samples (0.2-0.4g fresh weight) from three biological replicates were used for protein extraction. Protein was extracted from bark as previously described (Coleman et al., 1991; Wetzel et al., 1989), but with minor modifications. Frozen bark was mixed with 10 volumes of extraction buffer (50mM sodium borate, 50mM ascorbic acid, [pH 9.0] 1% β-mercaptoethanol and 1mM PMSF added just before homogenizing), vortexed for 10 seconds and then homogenized for 30 seconds and maximum speed using a tissue homogenizer (PowerGen 125, Fisher Scientific). The homogenized mixture was then centrifuged for 30 minutes at 15,000g and the supernatant was transferred to a clean 50ml

centrifuge tube and five volumes of 0.1M ammonium acetate in -20°C methanol was added to each protein sample. Proteins were then precipitated overnight at -20°C. Precipitated proteins were collected by centrifuging for 25 minutes at 15000g, washed twice with 0.1M ammonium acetate in -20°C methanol and twice with -20°C acetone. The protein pellet was resuspended in Laemmli lysis buffer, held in boiling water bath for 5 minutes and cooled at room temperature. Proteins were stored at -20°C for long-term storage.

Proteins were quantified using the Bicinchoninic acid (BCA) assay with minor modifications (Brown et al., 1989; Smith et al., 1985). Duplicate protein samples were prepared by mixing 5ul of total protein with water to a volume of 1ml solution. Triplicates of protein standards were prepared from the Pierce BCA protein assay kit. Samples and standards were precipitated from Laemmli buffer with 100ul of deoxycholate (DOC) (0.15%, w/v) and 100ul trichloroacetic acid (TCA) (72%, w/v) followed by centrifugation at 5000 x g for 15 minutes. Protein pellets were then resuspended in 50ul solution containing 5% SDS and 0.1N NaOH. BCA working reagent (BCA Reagent A product No. 23227 and BCA Reagent B; WR ratio = 1:8) (225ul) was then added, the samples were vortexed and incubated at 37°C for 30 minutes. The absorbance of each sample was measured using μQuant spectrophotometer (Bio-Tek Instruments, Inc). Linear regression using Prism software was used to calculate protein concentrations. Proteins were separated by SDS-PAGE using 12% resolving and 4% stacking gels. 5ug of total protein was electrophoresed at 180V for 1 h. Gels were stained with Commassie Brilliant Blue R-

250 and destained in water. Gel images were visualized using a VersaDoc imaging system (Bio-Rad).

Western Blotting

Proteins were transferred to nitrocellulose membranes from mini-gels with the Genie Electrophoretic Blotter (Idea Scientific Company, Minneapolis, MN) according to the manufactures instructions. The blotting time was 30 min at 24 volts in a standard Tris-glycine buffer in 20% v/v methanol. Membranes were washed for 10 min in TBS (20 mM Tris-HCl, pH 7.5, 150 mM NaCl) and blocked overnight at 4°C with 3% Bovine Serum Albumin (BSA) in TTBS (TBS, 1% Tween-20). The membranes were then washed for 15 min in TBS. BSP antibodies were diluted 1:2000 (Research Genetics, Inc., Huntsville, AL, USA) in 1% BSA in TTBS. The membranes were incubated with the BSP antibody overnight at room temperature, then washed three times for five minutes in TTBS at room temperature before incubating with the secondary antibody solution (goat anti-rabbit conjugated alkaline phosphatase, diluted 1:5000) (Santa Cruz Biotechnology Inc., Santa Cruz, CA, USA) for 1 hour. The membranes were then washed three times in TTBS and once in TBS at room temperature. The membranes were stained with nitro-blue tetrazolium (NBT) chloride and 5-bromo-4-chloro-3'indolylphosphate p-toluidine salt (BCIP) for 30 minutes. Membranes were imaged with the VersaDoc (Bio-Rad Laboratories, Hercules, CA, USA).

Results

Nitrogen availability impacts leaf area, sylleptic shoot production and stem growth

Prior to examining how levels of BSP accumulation influence growth, we first examined the relationship between N availability and growth of *Populus tremula* x *Populus alba* clone 717-1B4 (WT-717). Similar to previous studies using a different poplar genotype (Cooke et al., 2005), we observed that increased N availability results in increased leaf area, greater sylleptic shoot production, and increased stem diameter (Figure. S2-1 A-F). It is noteworthy that sylleptic shoot production appeared to have a threshold N level above which sylleptic shoots production was significantly enhanced (Figure. S2-1C and E).

BSP accumulation influences shoot growth following dormancy

To examine the influence of BSP storage on shoot growth, we used two approaches that manipulate N sources or sinks. The first approach reduced BSP accumulation via RNAi gene suppression (i.e. reduced N source) while the second approach altered the number of sinks that compete for stored N and we then examined the effect of these manipulations on shoot growth following dormancy. RNAi knockdowns of *BSP* were used to produce poplars with reduced BSP accumulation and after screening more than 40 independent transgenic events from two different *BSP* RNAi constructs we identified 3 events for each of the two different *BSP* RNAi constructs which showed reduced levels of BSP accumulation after SD induced dormancy and leaf senescence (Figure. 2-1A-B). Shoot growth was then measured for the *BSP* RNAi transgenics

following low-temperature dormancy release (*Materials and Methods*). To eliminate confounding effects of shoot competition for stored N, all but a single bud was removed from both excised stems and intact plants prior to growth. Unexpectedly, we observed that bud break was delayed for the majority of *BSP* RNAi events of both excised stems and intact plants (Figure. 2-1C-D) indicating N storage levels influence bud expansion and bud break. Since leaf area and stem growth are influenced by N status, we measured these growth parameters as outputs of N status after 6 weeks of growth following bud break (adjusted for differences in timing of bud break among BSP RNAi lines) using both excised stems (Figure. 2-2A-B, S2-2A) and intact plants (Figure. 2-2C-D, S2-2 E). After 6 weeks of growth we found a 40-60% reduction in leaf area for excised stems and a 50-60% reduction for intact plants. Similar to leaf area, stem growth was also reduced by 50% or more for both excised stems and intact plants (Figure. 2-2B and D). Similar reductions in leaf DW (Figure S2-2B and F), stem DW (Figure. S2-2C and G) and shoot biomass (Figure. S2-2D and H) also occurred for all of the BSP RNAi lines. These results demonstrate that remobilization of N from BSP significantly contributes to shoot growth and reduced BSP accumulation levels reduce initial shoot growth.

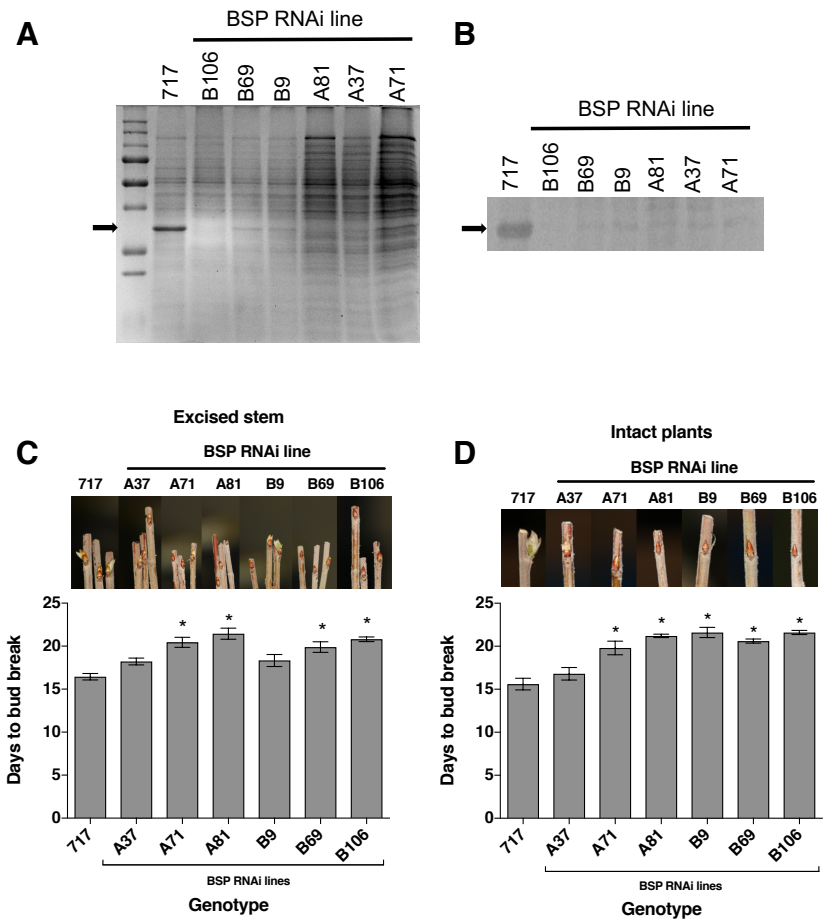

Figure. 2-1. Reduced poplar BSP accumulation delays bud break following dormancy. (A) SDS-PAGE gel of soluble bark proteins following low-temperature treatment to overcome dormancy and immediately prior to LD treatment. The location of the 32 kDa BSPs are indicated by the arrow. Control wild-type plants (717) and the BSP-RNAi lines (B106, B69, B9 A81, A37 and A7) are independent transformation events where the RNAi construct used for the B-lines targets a different region of *BSP* than the A-lines (see methods and materials). (B) Western blot analysis of BSP abundance in the bark of control (717) and BSP-RNAi lines immediately prior to LD treatment at 20°C. Days to visible bud break of control and BSP-RNAi in (C) excised stems or (D) intact plants after treatment in LD at 20°C. Error bars indicate mean ± SE and * indicates values significantly different from control at $p<0.01$.

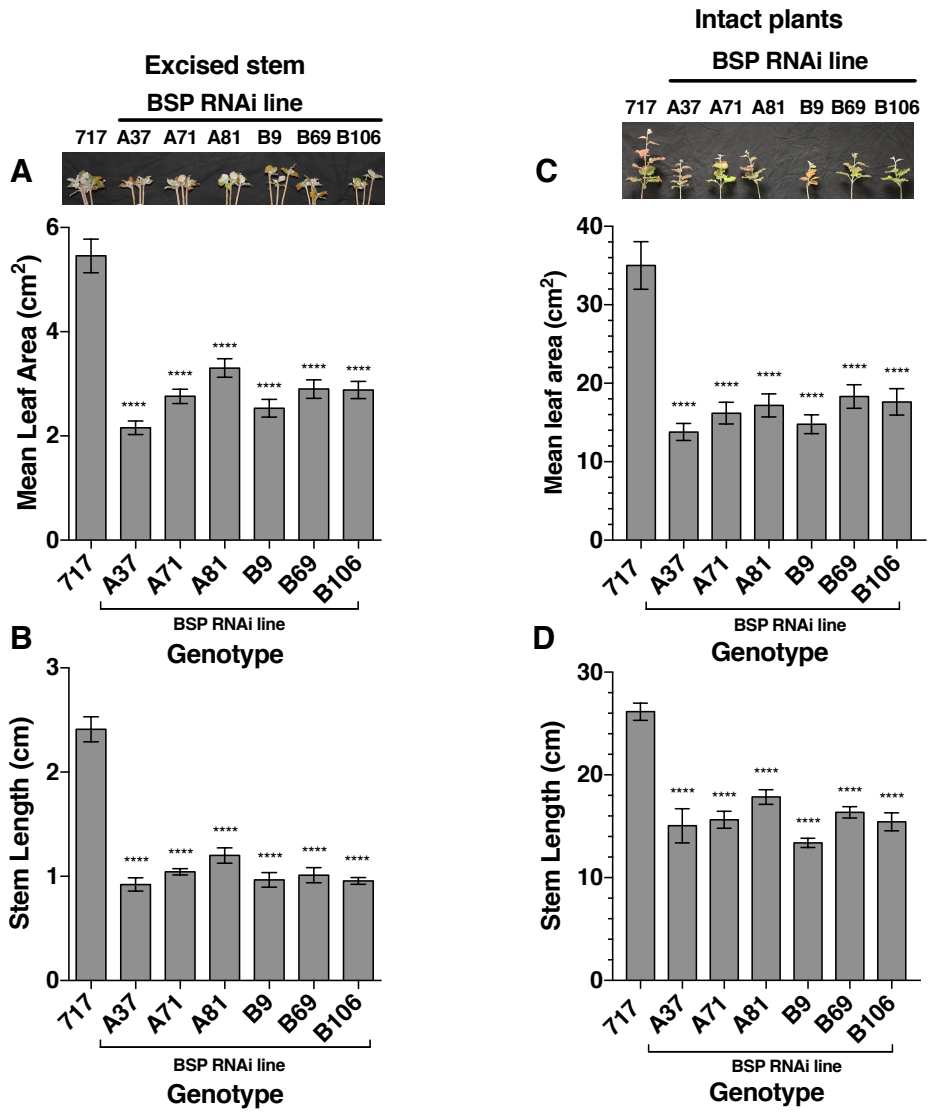

Figure. 2-2. Reduced BSP accumulation via RNAi knockdown reduces growth following bud break. (A) Mean leaf area and (B) length of new stem growth 6 weeks after bud break of excised stems for control (717) and BSP-RNAi lines (A37, A71, A81, B9, B69, B106). Each BSP-RNAi line is an independent transformation event with the RNAi constructs for the A and B lines targeting different regions of *BSP*. (C) Mean leaf area and (D) length of new stem growth 6 weeks after bud break for intact plants. Error bars indicate mean ± SE and **** indicates means significantly different from control at $p<0.0001$.

In the second approach, shoot sink demand was manipulated to provide different levels of sink competition for stored N while BSP storage levels were unchanged and then we determined how sink demand and competition influence

shoot growth following dormancy (Figure. S2-3A-C). Increasing sink demand from 1 to 3 shoots reduced leaf area by 43% (107.2 cm^2 versus 61.41 cm^2) (Figure. 2-3S A). Continued increases in sink number (6, 9 or 12 shoots) further decreased leaf area and at the highest level of sink competition (12 axillary shoots) leaf area was reduced by 70% compared to plants with a single shoot (Figure. S2-3 A). A similar trend was also observed for stem length (Figure. S2-3 B), although differences were only significant for plants with 1, 3 or 6 shoots compared to plants with 9 or 12 shoots, indicating that stem length is less influenced by sink competition than leaf area. We also found that the number of sylleptic shoots arising from re-growing shoots was also related to sink competition (Figure. S2-3 C) with the greatest number of sylleptic shoots (9.8) produced from plants with a single re-growing shoot while significantly fewer sylleptic shoots were produced from plants with 6, 9 or 12 growing shoots (Figure S2-3 C). A similar trend of reduced leaf area, stem length and sylleptic shoot number was also observed when sink competition was limited to sylleptic shoots formed during the previous growth cycle (i.e. prior to dormancy induction and release) (Figure. S2-3 D-F). Combined with the BSP RNAi studies, these results support that BSP accumulation and N storage play a major role in providing N to newly expanding shoots following dormancy and growing shoots compete for stored N.

Since poplar can produce both proleptic and sylleptic shoots, we were also interested if these shoots compete with each other for stored N. To examine this we varied the ratio of proleptic and sylleptic shoots while BSP storage was kept constant and then measure growth following dormancy (Figure. S2-4 A-E). Unexpectedly, we

found that there were no differences in leaf area or stem growth of shoots from axillary bud when sylleptic shoot competition increased from 1 to 10 shoots, although these growth traits were significantly reduced by competition from shoots arising from axillary buds (Figure. S2-4 A and B). This same pattern was also observed for new sylleptic shoot production from the shoots arising from axillary buds (Figure. S2-4 C). When we examined growth traits of the previously formed sylleptic shoots when subjected to competition from shoots arising from axillary buds, both leaf area and stem length were significantly reduced for shoots arising from sylleptic shoots when the number of shoots developing from axillary buds was increased from 1 to 10 shoots or when the sylleptic shoot number was increased (Figure. S2-4 D and E). This indicates that competition for stored reserves depends upon the shoot type whereby shoots growing from axillary buds appear to compete amongst themselves and previously formed sylleptic shoots for stored reserves while previously formed sylleptic shoots compete little with shoots growing from axillary buds. Thus complex interactions between different shoot-types are likely to mediate N allocation during stored N remobilization.

BSP accumulation contributes to sink demand and N export from leaves during autumn

Prior to examining N transport dynamics from leaves to stems during SD induced BSP accumulation we first determined if there were any differences in growth between wild-type and BSP-RNAi plants during SD induced growth cessation and we found that there were no significant differences associated with plant height, number of leaves, leaf area and chlorophyll content between wild-type and BSP RNAi plants

(Figure. S2-5). The plants continued to grow substantially in height after switching from LD to SD (54% increase for WT, and 67% for *bsp*) and produced 3-4 additional leaves. By the 6th week of SD treatment, the plants stopped growing in height, ceased producing new leaves, and formed a terminal bud. Leaf senescence occurred upon exposure to LT resulting in reduced chlorophyll contents (Figure. S2-5).

N partitioning during SD-induced BSP accumulation was examined using ^{13}N labeling and positron emission tomography (PET). A relatively small portion of the ^{13}N was exported from the leaf during the 1 h incubation period of our experiments. Most of the ^{13}N was detected in the upper part of the lower stem (Figure. 2-3A). Based on previous experiments with carbon-11 (^{11}C), 1hr is plenty of time for the phloem transport stream to reach the roots of small poplar plants like these (Babst et al. 2005), suggesting that N is removed from the phloem for use or storage in the stems of poplars. Total partitioning of ^{13}N to the stem was lower in the BSP-RNAi than WT poplars (Figure. 2-2B). This suggests that N sink strength was reduced in BSP-RNAi plants, and that BSP normally makes a significant contribution to maintaining N sink status in WT poplars. Partitioning of ^{13}N to the upper stem increased substantially after short-day+low-temperature treatment (Figure. 2-3C), but the total export did not change significantly. This may indicate that the upper stem shifts from a weak N sink during growth, to become a stronger N sink during SD-induced leaf senescence. This is consistent with the general pattern that stem N/protein tends to be low during the growth season, and higher during winter dormancy (Wildhagen et al., 2010). In the BSP-RNAi

line, partitioning of ^{13}N to the lower stem decreased after SD-LT treatment. Also, the ^{13}N partitioning to lower stem became significantly less in BSP-RNAi than WT after the short-day+low-treatment. This fits with the fact that the stem N/protein tends to be high during winter dormancy, and the BSP-RNAi line has less BSP for N storage in the lower stem. However, there was still substantial N partitioning to stems in BSP-RNAi plants, suggesting that other mechanisms also contribute partially to N sink strength during dormancy induction.

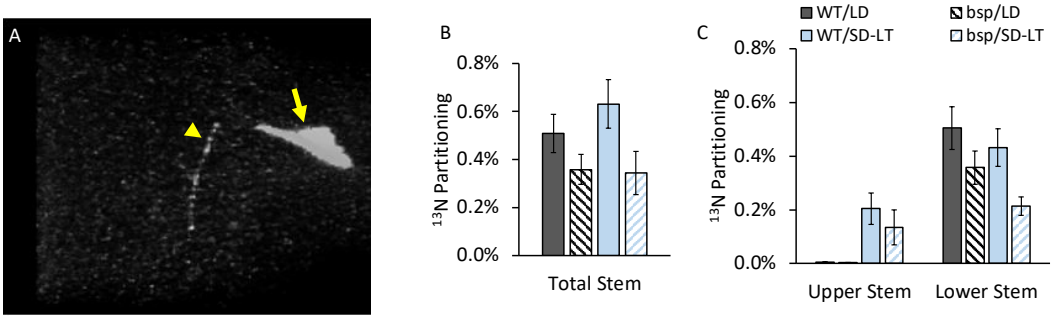

Figure. 2-3. ^{13}N partitioning in poplars. (**A**) PET image of ^{13}N distribution in a representative poplar plant. $^{13}NH_3$ was fed to the load zone (yellow arrow), the portion of the load leaf clamped inside a leaf cuvette, and the plant was imaged 1 hr later. Arrowhead points to 13N labeling in the stem. (**B**) ^{13}N partitioning in wild-type (WT) and BSP-RNAi (*bsp*) poplar stems, and (**C**) separated into the regions of the stem below the load leaf (lower stem) and above the load leaf (upper stem). Plants were grown in long day photoperiod (LD), or grown in LD first followed by 6 weeks in short-day photoperiod plus another 3-5 weeks in short-day and low temperature (SD-LT). Bars indicate mean ± SE ^{13}N partitioning to the stem as a percentage of total ^{13}N in the plant.

BSP catabolism and N remobilization involve extensive changes in bark gene expression

In order to gain insight into the molecular events associated with BSP catabolism and N remobilization during growth following dormancy we used DNA microarrays to study transcriptome changes. We identified differentially expressed genes (log_2-fold>1.5 and adjusted *P*-value ≤ 0.01) by comparing expression in the bark of plants

after 1, 2 or 3 weeks of LD growth to the bark of plants that had received sufficient chilling to overcome dormancy prior to transfer to LD conditions. After 1 week of LD-growth a total of 2,227 genes were differentially expressed with 3 times as many genes exhibiting increased expression compared to genes with reduced expression (Figure. S2-5). After 3 weeks of LD-growth the number of differentially expressed genes increased to 5,643 with 2 times as many genes showing increased expression compared to genes with reduced expression (Figure. S2-6). Therefore, LD-induced BSP catabolism and N remobilization during renewed shoot growth is associated with major changes in the bark transcriptome. Functional classification of the differentially expressed genes by gene ontology (GO) analysis (supplemental table 1) revealed a wide range of processes that were significantly enriched in bark during renewed shoot growth. Enriched biological processes included ontologies such as receptor-linked protein signaling, transport, cellular response to hormone stimulus, hormone-mediated signaling pathways, while enriched functional processes included activities related to catalytic, transporter, and peptidase activity.

We also used MapMan to map differentially expressed genes to various processes and discovered that 25% of genes that mapped to hormone BINS (Bin 17) were related to auxin-related process (42 of 168 genes). Because of the prevalence of auxin-related genes we queried the microarray data for expression of genes encoding auxin transporters and auxin signaling (Aux-IAA, ARF and GH3) during LD-associated BSP catabolism and N remobilization (Figure. S2-7). Except for 1 auxin transporter (Potri.008G050400; ABCB18) all the remaining transporter genes that were differentially expressed during LD-induced BSP catabolism and N

remobilization showed increased expression (Figure. S2-7). Two putative auxin transporter genes, Potri.005G187500 (Aux7/Lax8) and Potri.009G132100 (Aux6/Lax3), clustered together and were induced the greatest (Figure. S2-6A). Similar to auxin transporters, the majority of differentially expressed Aux/IAA repressors were induced during LD treatment (Figure. S2-7 B) while only two genes (Potri.008G161100; IAA3.5 and Potri.018G127800; IAA29.2) showed reduced expression. One cluster of 8 Aux/IAA genes (IAA3.2, IAA12.1, IAA12.2, IAA19.3, IAA20.1, IAA26.2, IAA27.2, IAA28.2) were highly induced during renewed shoot growth (Figure. 2-S7B). The expression patterns of auxin response factors (ARFs) clustered into 3 major groups (Figure S2-7 C). The largest group (9 genes) included ARFs whose expression increased during LD treatment; a second group (6 genes) included genes whose expression declined and the third group (6 genes) included genes whose expression changed little during the LD treatment. Although GH3 gene expression patterns were clustered into 2 major groups, all of the genes showed a generalized pattern whereby expression increased after 2 weeks of LD treatment and then declined in week 3. Expression of two GH3 genes (GH3-9, Potri.002G206400 and GH3-5, Potri.011G129700) that clustered together showed the greatest increase in expression after 2 weeks of LD treatment. In summary, results from bark transcriptome analysis during N remobilization suggest that auxin transport and signaling may play a role in this process.

Because BSP catabolism and N remobilization involves the action of proteolytic enzymes (Islam et al., 2015) and the reallocation of N from bark to expanding buds and shoots involves amino acid transport we also queried the

microarray data to characterize the expression of genes involved in these processes. The poplar genome is estimated to contain 955 genes encoding proteases (García-Lorenzo et al., 2006). DNA microarray analysis of gene expression during LD-induced N remobilization indicated that a large number of protease genes are expressed in bark with the majority showing either little change or a decline in transcript abundance (Figure. S2-8). A cluster of 37 putative protease genes grouped together that showed increased transcript abundance during N remobilization (Figure. S2-8) and within this cluster 6 genes that included 4 putative aspartic proteases (Potri.001G028200, Potri.002G104600, Potri.015G051800 and Potri.018G014600) and 2 putative serine proteases (Potri.002G120400 and Potri.009G133400) were highly induced (Log_2-fold increase ranged from 2.1-7.5) and may represent proteases that play important roles in BSP catabolism. Since glutamine is the major form of N that is transported during N remobilization (Millard et al., 2006; Sauter and Cleve, 1992) we also queried the microarray data for changes in amino acid transporter expression (Figure. S2-9) including the ATF-AAP superfamily (Figure. S2-9A), PTR-NRT family (Figure. S2-9B), APC family (Figure. S2-9C), UmaniT family (Figure. S2-9D) and the OPT family (Figure. S2-9E). Differential gene expression was observed for many members of all the amino acid families. In general, a greater proportion of genes belonging to the ATF-AAP and APC families showed increased expression levels during N remobilization while a greater proportion of members of the PTR-NRT and OPT families appeared to be repressed during N remobilization (Figure. 2-9S). In the ATF-APP family a cluster of 4 genes (Potri.010.G128300, Potri.005G174000, Potri.005G181600 and Potri.009G132100) were highly induced

and showed a steady increase in expression during the 3 weeks of LD treatment that ranged between a log_2-fold increase from 4.8 to 7.6. The APC family included a cluster of 8 genes whose expression increased during LD treatment (Figure. S2-9C) and the increases ranged from log_2-fold increase of 0.68 for Potri.001G378500 to 2.4 for Potri.01G24100. CAT11 (Potri.012G131300) has been reported to be involved in glutamine transport from senescing leaves to bark during autumn (Babst and Coleman, 2018; Couturier et al., 2010) and our results revealed that CAT11 is repressed during N-remobilization (Figure. S2-9C). In contrast to CAT11, CAT10 (Potri.01G24100) is induced in LD and repressed during SD-induced N storage (Babst and Coleman, 2018). This raises the possibility that CAT11 might be involved in glutamine transport when bark serves as an N sink while CAT10 is involved in transport when bark serves as an N source.

Shoot growth may involve auxin production and transport which regulates BSP catabolism

Previous research demonstrated that shoot growth is necessary for BSP catabolism which involves a signal produced in expanding buds and shoots that is transported to bark that triggers BSP degradation (Coleman et al., 1993). Since our microarray results suggest that auxin transport and signaling could have a role in N remobilization we suspected that auxin could be the signal from expanding buds and shoots. To examine this we characterized the expression of genes involved in auxin production in expanding buds and shoots (Figure. 2-4). We identified 4 genes that are similar to TAA1/TAR genes (Figure. 2-4A) and found that expression of 2 genes (Potri.008G187800 and Potri.010G044500) increased in expanding buds and shoots

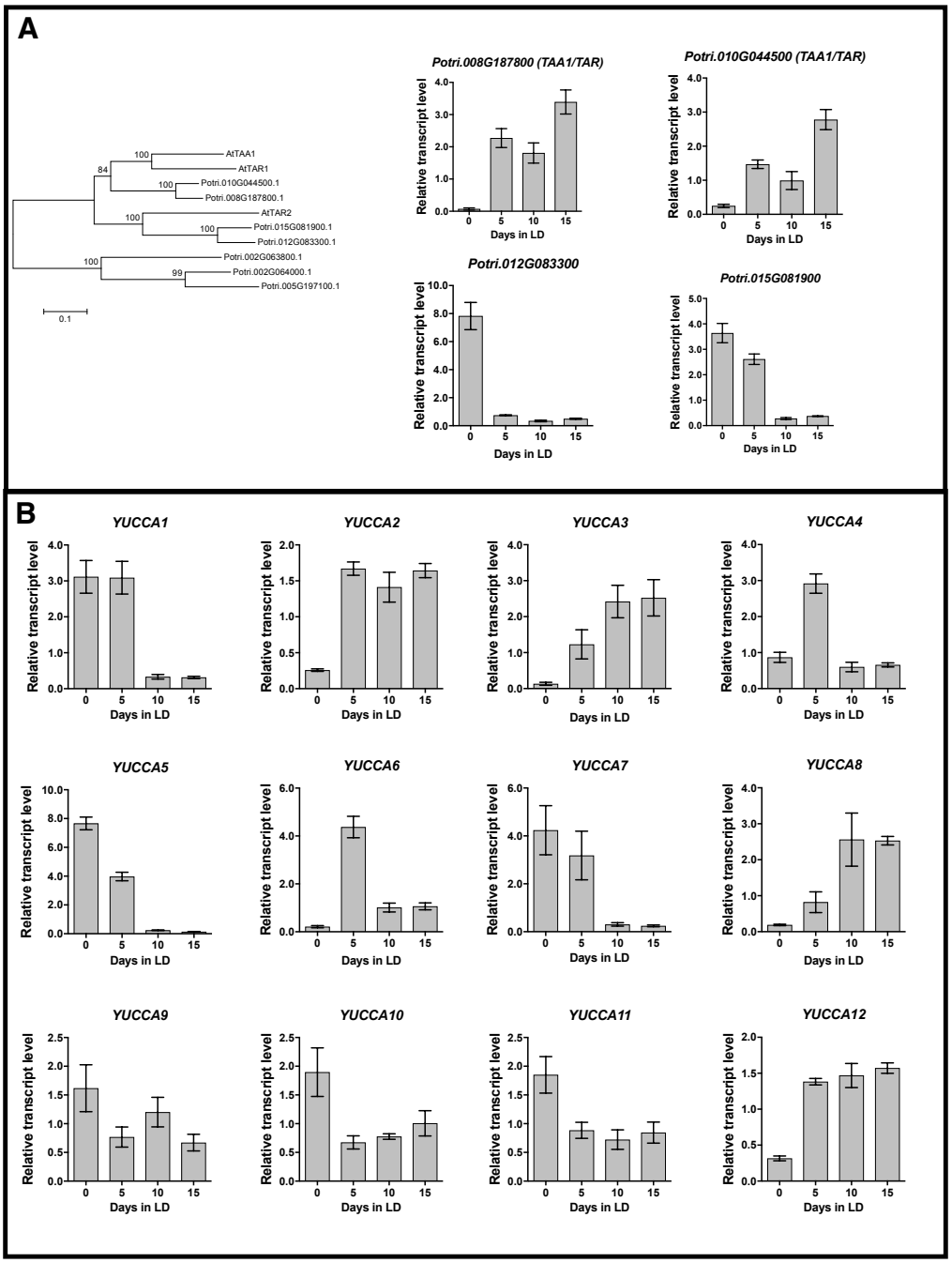

Figure. 2-4. Expression of auxin biosynthesis genes in expanding buds and shoots of poplar. Relative expression of (A) TAA1/TAR and (B) YUCCA genes were determined by qRT-PCR. Plants (*Populus trichocarpa*, Nisqually) were first grown in LD for approximately 6 weeks followed by SD treatment for 8 weeks at 20°C to induce dormancy. Leaf senescence and abscission was then induced with 6 weeks of further SD at low-temperature (LT) (10°C, light; 4°C dark). After leaf senescence and abscission the plants were place in the dark at 4°C for 7 weeks to release buds from dormancy. Renewed shoot growth was then initiated by placing plants in LD at 20°C. Three independent replicates were collected for RNA purification at the start of the LD treatment and at 5 day intervals for 15 days. Error bars indicate mean ± SE.

during LD N remobilization while expression of the other 2 genes declined. We also characterized the expression of poplar YUCCA genes during N remobilization and found that 6 (YUCCA2, YUCCA3, YUCCA4, YUCCA6, YUCCA8, and YUCCA12) of the 12 genes showed increased expression during LD-treatment and the remaining 6 genes showed a decline in expression (Figure. 2-4B). These results confirm that specific genes associated with auxin production are expressed in expanding buds and shoots that may account for auxin production that is then transported to bark during N remobilization.

Since shoot growth is necessary for BSP degradation and genes involved in auxin production are expressed in expanding buds and shoots during LD-treatment, we were interested in whether removal of the source of auxin would affect bark expression of genes associated with BSP catabolism and N remobilization. We selected a set of auxin transporter, Aux/IAA, GH-3, protease and amino acid transporter genes, based on microarray expression patterns, to determine if their expression differed between intact plants and those whose buds were removed after treatment with LT to overcome dormancy and prior to LD treatment. Auxin transporter gene expression increased after 1 week of LD treatment and continued to increase during the 3-week treatment interval in intact plants (Figure. 2-5A). Auxin transport gene expression also increased to some extent during the 3 week LD treatment in plants lacking buds, but the magnitude of the increase was greatly reduced at each weekly time point compared to intact plants (Figure. 2-5A). Similar to auxin transporter gene expression, AUX/IAA gene expression also steadily

increased during LD treatment in intact plants while little to no increase was found in plants lacking buds when

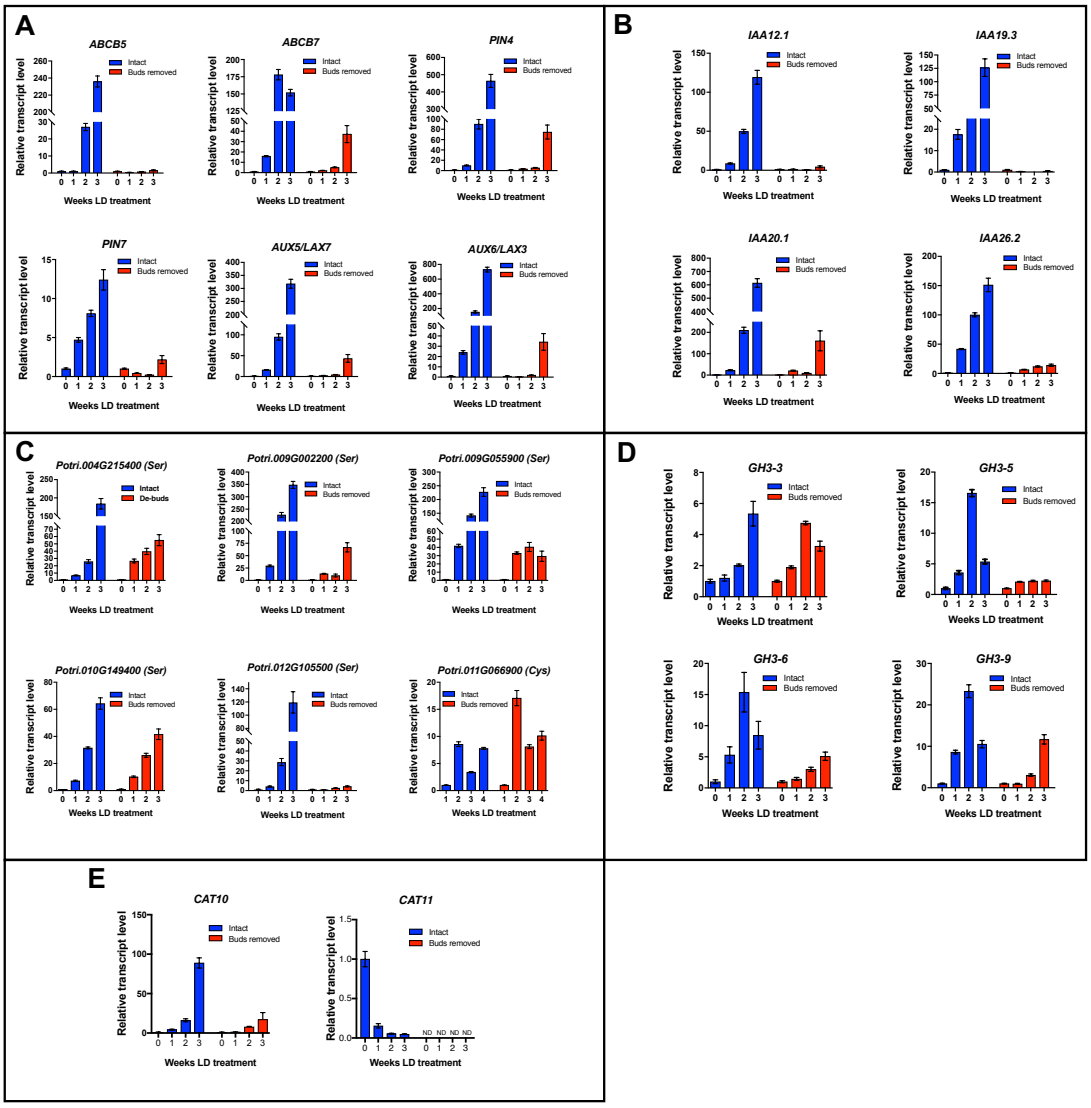

Figure. 2-5. Effect of bud removal on bark gene expression during growth following dormancy. The relative expression determined by qRT-PCR of selected (A) auxin transporter genes, (B) AUX/IAA signaling genes, (C) protease genes, (D) auxin responsive GH3 genes and (E) the amino acid transporters *CAT10* and *CAT11* for intact plants (blue bars) and plants with buds removed (red bars). Plants (*Populus trichocarpa*, Nisqually) were first grown in LD for approximately 6 weeks followed by SD treatment for 8 weeks at 20°C to induce dormancy. Leaf senescence and abscission was then induced with 6 weeks of further SD at low-temperature (LT) (10°C, light; 4°C dark). After leaf senescence and abscission, the plants were place in the dark at 4°C for 7 weeks to release buds from dormancy. Prior to placing plants in LD at 20°C to initiate bud break and shoot growth, buds were removed from a set of plants and another set was left intact. At least 3 independent bark replicates were collected for RNA purification at the start of the LD treatment and at weekly intervals for 3 weeks. Error bars indicate mean ± SE and ND indicates not detected.

compared to intact plants (Figure. 2-5B). In general, the expression pattern of proteases genes was similar to auxin transporter and AUX/IAA genes where expression generally increased during the 3 week LD treatment but the differences between intact plants and those lacking bud was more variable (Figure. 2-5C). Three of the selected protease genes (Potri.009G002200, Potri.009G055900, Potri.012G105500) were expressed at much greater levels in intact plants compared to plants lacking buds. The expression patterns 2 of the protease genes (*Potri.004G215400* and *Potri.010G149400*) were similar between intact plants and those lacking buds although the levels were greater in intact plants after 3 weeks of LD treatment. The exception to the patterns of protease gene expression was for the gene encoding a putative cysteine protease (*Potri.011G066900*) whose expression increased in LD treatment and was greater in plants lacking buds compared to intact plants. Interestingly, all of the protease genes with reduced expression in plants lacking buds are annotated as putative serine proteases while only one protease gene with increased expression in these plants is a putative cysteine protease. We also found that the expression of the auxin induced GH3 genes differed between intact plants and plants lacking buds (Figure. 2-5D). In intact plants, expression of GH3-5, GH3-6 and GH3-9 peaked after 2 weeks of LD treatment and declined by the third week while in plants lacking buds the expression of these three genes showed a gradual increase in LD, although the levels were greatly reduced compared to intact plants. Unlike GH3-5, GH3-6 and GH3-9, GH3-3 showed similar patterns and levels of expression between intact plants and those lacking buds (Figure. 2-5D). *CAT10* and *CAT11* showed contrasting patterns of gene expression where *CAT10* expression

increased during the 3 week LD treatment in both intact plants and plants lacking buds but the transcript abundance was significantly greater for intact plants (Figure. 2-5E) whereas *CAT11* transcript abundance declined during LD treatment for intact plants and was not detected in plants lacking buds. The expression patterns of *CAT10* and *CAT11* are consistent with the concept that *CAT10* is expressed in bark that serves as a N source while *CAT11* bark expression is associated with bark sink status. The results for plants lacking buds also are consistent with *CAT10* being induced by auxin during N remobilization while *CAT11* expression is repressed by auxin.

Auxin transport is involved in BSP catabolism and N remobilization

Since our microarray analysis combined with the results from bud removal experiments are consistent with a possible role for auxin in BSP catabolism and N remobilization we further investigated this possibility. Although it would be desirable to use approaches that perturb expression (knockdown or knockouts) of auxin transport or signaling genes, this is likely to be difficult due to the potential number of genes involved and functional redundancy. Instead we used NPA to inhibit or block polar auxin transport and determined if this affected BSP catabolism and the expression of genes associated with N remobilization. We theorized that if polar auxin transport was inhibited or blocked, BSP catabolism would be inhibited as well as the expression of genes associated with N remobilization. First, we determined if and at what concentration NPA would inhibit BSP catabolism during growth following dormancy and found that 50mM of NPA applied in a lanolin paste to the stem consistently inhibited BSP catabolism (Figure. S2-10). This NPA concentration is consistent with the concentration used by Spicer et al. (Spicer et al.,

2013) to block polar auxin transport in poplar stems. We then treated poplar stems during regrowth following dormancy with 50mM NPA and found that after 15 days in LD differences in BSP abundance were observed between the bark of stem located above and below the site of NPA treatment while control treatments showed no difference (Figure. 2-6A). After 21 days of treatment BSP was not detected in bark above the site of NPA treatment while BSP levels below the site of treatment were similar to those at the beginning of the LD treatment (Figure. 2-6A). We then measured IAA levels from bark samples above and below the site of NPA treatment and found that IAA levels increased in bark above the site of treatment by 5 days of LD and after 21days IAA levels in bark above the site of treatment averaged 61 ng/g FW (Figure. 2-6B). For comparison, IAA levels below the site of treatment were below the threshold of detection (Figure. 2-6B) throughout the LD treatment period.

Since stem NPA treatment during regrowth results in differential IAA and BSP levels between bark above and below the treatment site, we then examined the expression of selected genes (based on microarray analysis) involved in auxin transport and signaling, genes encoding proteases as well as the CAT10 and CAT11 genes to determine if they were also differentially expressed. We found that transcript levels for the selected auxin transporters were significantly reduced in bark below the site of NPA treatment compared to bark above the treatment site or when compared to control plants treated with a lanolin pasting lacking NPA (Figure. 2-6C). We also observed similar patterns of differential expression for transcripts of 3 AUX/IAA (IAA12.1, IAA19.3, IAA201) genes while one gene, IAA16.2, showed no differences in expression related to NPA treatment (Figure. 2-6D). In addition, we

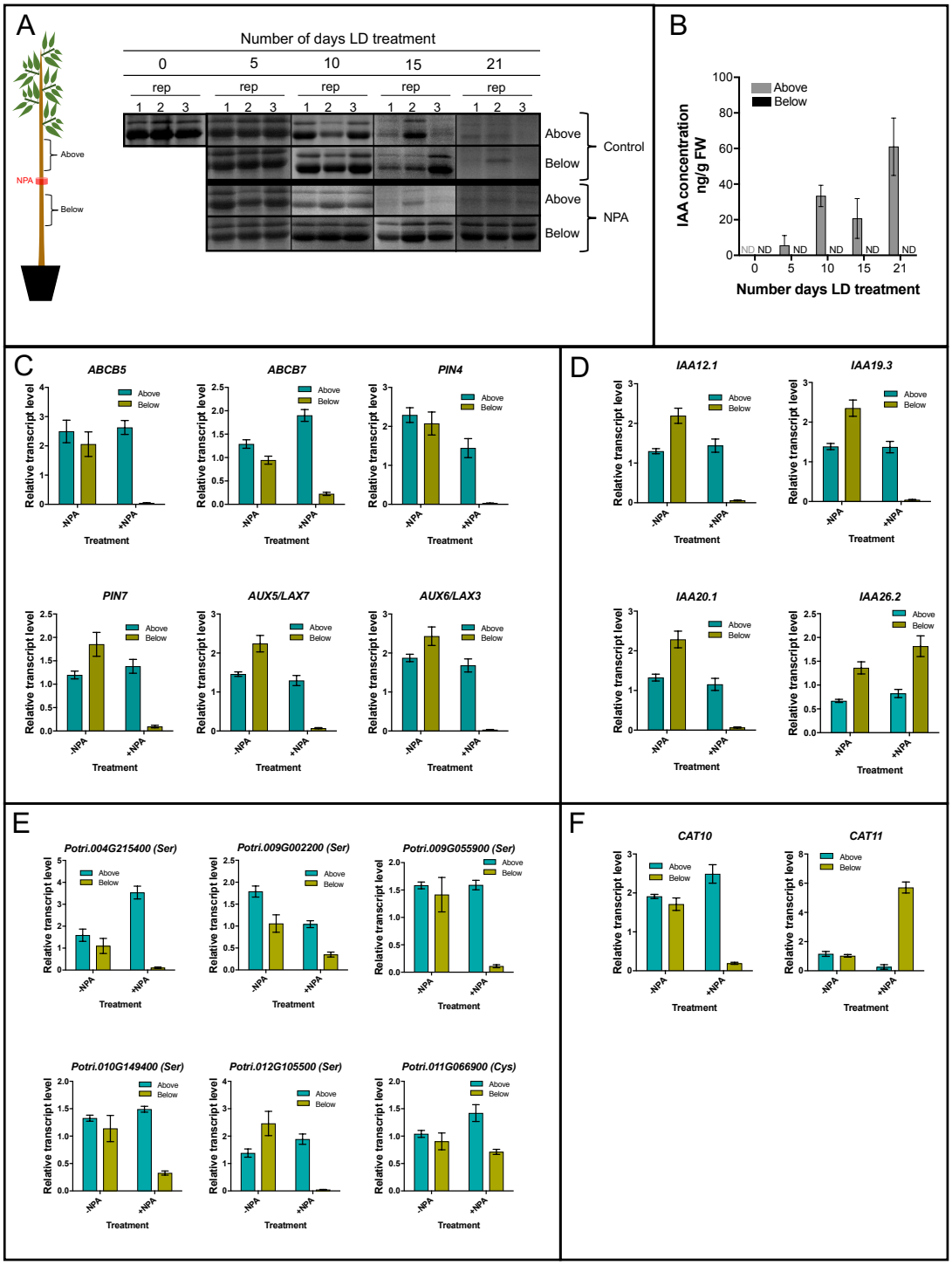

Figure. 2-6. Inhibiting auxin transport alters bark gene expression during growth following dormancy. (A) Diagram of NPA treatments and SDS-PAGE analysis of BSP abundance above and below the site of the stem ringed with lanolin paste containing 50 mM NPA during LD-mediated BSP catabolism and N remobilization. (B) IAA levels measured by LC-MS in bark above and below the site of NPA treatment during the LD-treatment. Relative gene expression determined by qRT-PCR in bark of plants (*Populus trichocarpa*, Nisqually) above and below (the site of NPA treatment (+NPA) and plants ringed with lanolin paste lacking NPA (-NPA) after 3 weeks of LD-treatment (C) auxin transporter gene, (D) AUX/IAA

signaling genes,(E) protease genes and the amino acid transporters *CAT10* and *CAT11*. Plants were first grown in LD for approximately 6 weeks followed by SD treatment for 8 weeks at 20°C to induce dormancy. Leaf senescence and abscission was then induced with 6 weeks of further SD at low-temperature (LT) (10°C, light; 4°C dark). After leaf senescence and abscission, the plants were place in the dark at 4°C for 7 weeks to release buds from dormancy. Prior to placing plants in LD at 20°C to initiate bud break and shoot growth, all buds except the apical and uppermost 5 axillary buds were removed and the stem was ringed with lanolin paste containing 20 mM NPA or lanolin lacking NPA. At least 3 independent bark replicates were collected for RNA purification after 3 weeks of LD treatment. Error bars indicate mean ± SE and ND indicates below detection limits.

also found that protease gene expression also showed a differential pattern of expression between bark above and below the location of NPA application (Figure. 2-6E). However, the putative cysteine protease (*Potri.011G066900*) was affected to a lesser extent that the other protease genes and expression of this gene was also unaffected by bud removal which may indicate that this protease gene may not be regulated by auxin levels. Interestingly, we also found that expression of the amino acid transporters *CAT10* and *CAT11* differed when polar auxin transport was blocked with NPA. *CAT10* expression was significantly reduced in bark below the location of NPA treatment while *CAT11* was induced (Figure. 2-6F). This result further supports the possible relationship between bark N sink-source status and *CAT10* and *CAT11* expression whereby bark *CAT10* expression is associated with bark acting as an N source while bark *CAT11* expression is associated with bark sink status. Furthermore, *CAT10* and *CAT11* may also be differentially regulated by auxin since *CAT10* expression was reduced in bark with reduced auxin levels while *CAT11* expression was induced.

Protease genes associated with N remobilization are auxin inducible

The proteolytic digestion of BSP is a critical feature of spring N remobilization in poplar. Results from blocking auxin transport using NPA as well as the results involving bud removal suggest that auxin produced in expanding buds and shoots is transported to bark which in turn induces the expression of protease genes involved in BSP catabolism. To determine if selected protease genes were auxin inducible we used stems of *in vitro* cultured poplars that were first incubated in growth medium lacking auxin to deplete endogenous IAA and then after 16 h of depletion the stems were treated with IAA as previously described (Schrader et al., 2003). Throughout the depletion and IAA addition periods we assayed transcript levels of the same set of protease genes that were also assayed in the NPA and bud removal experiments. Concurrently, we also examined the expression of auxin inducible AUX/IAA genes and found that transcript levels steadily declined over the 16 h depletion period (Figure. 2-7A). With the addition of 20 μM IAA to the growth medium transcript levels of the AUX/IAA genes rapidly increased several-fold (Figure. 2-7A) demonstrating auxin inducible expression in this assay system.

Expression analysis of the protease genes revealed a general decline in expression, however, the level of the decline varied among the genes (Figure. 2-7B). For half of the genes (Potri.004G215400, Potri.010G149400, Potri.011G066900) the decline was gradual and stabilized after about 4 h of auxin depletion. The remaining 3 genes (Potri.009G002200, Potri.009G055900, Potri.012G105500) also showed a steady decline, but the decline continued during the entire 16 h auxin depletion period (Figure. 2-7B). The addition of 20 μM IAA to the growth medium induced gene

expression within 30 min for all of the protease genes assayed. However, the level of the induction varied among the genes with Potri.004G215400 showing a low level of induction while Potri.012G105500 and Potri.011G066900 showed the greatest level

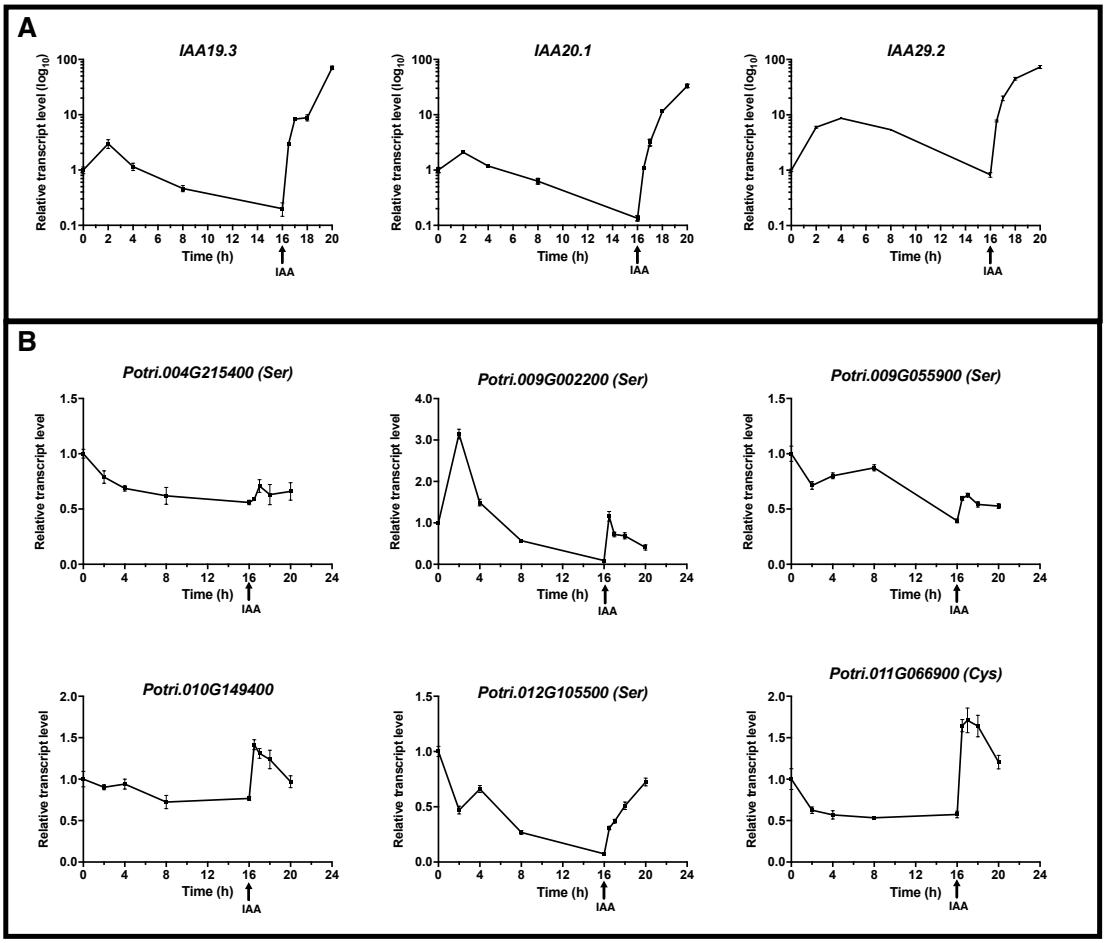

Figure. 2-7. Auxin responsiveness of poplar protease genes. *In vitro* grown defoliated stems of poplar (*P. tremula* × *P. alba* hybrid clone INRA 717-1B4) were incubated in growth medium to deplete endogenous auxin. After 16 h of depletion 20 μM IAA was added and incubation was continued for 4 h. Stems were collected at the indicated time points and the relative expression of (A) auxin responsive AUX/IAA genes and (B) protease genes was determined by qRT-PCR. At least 3 biological replicates were collected at each time point and error bars indicate mean ± SE.

of induction. With the exception of Potri.012G105500, gene expression increased rapidly within 30 min and then began to decline. This decline in expression was not detected for the AUX/IAA genes suggesting differences in auxin inducible expression between the protease and AUX/IAA genes. This difference may reflect the relative location in the signaling-response pathway with the AUX/IAA genes in early steps of auxin signaling while the protease genes are likely to the be the endpoint of the pathway.

Since both *CAT10* and *CAT11* showed differential expression during regrowth in LD and under NPA treatment, their expression may be associated with auxin level or N status. Different from AUX/IAA and protease genes that showed steady declines in transcripts level during auxin depletion period, *CAT10* showed a rapid decline in 2 h of auxin depletion and then gradual induction within the remaining depletion period. However, with the addition of IAA the transcript level was rapidly reduced within 30 min and continued the reduction. *CAT11* showed gradual increase in transcript level during auxin depletion period and a subtle decline by 1 h of IAA addition. These changes indicated that *CAT11* was negatively regulated by auxin which is consistent the results in the NPA and bud removal experiments. Nevertheless, *CAT10* seemed to be also negatively regulated by auxin, which is inconsistent with previous results in the NPA and bud removal experiments. This inconsistence suggests that the expression of CAT10 may be complexly regulated not only by auxin but also other signal, e.g. N status (Figure S2-11).

Bark N remobilization is associated with plastid glutamine synthetase expression

Spring N remobilization involves BSP catabolism and amino acid transport to expanding buds and shoots. Glutamine is the primary amino acid transported during spring N remobilization in poplar (Millard et al., 2006; Sauter and Cleve, 1992), yet poplar BSP is composed of less than 2.5% glutamine suggesting that proteolytic and hydrolytic activities directed at BSP likely yield ammonium which is used in the synthesis glutamine and other amino acids via the activity of glutamine synthetase (GS) , NADH-glutamate synthase (GOGAT) and possibly glutamate dehydrogenase (GDH). Because of the pivotal role of GS in glutamine synthesis we determined if N remobilization was associated with bark expression of GS genes. In poplar, GS is encoded by a gene family of 8 genes that includes cytosolic (GS1) and chloroplastic (GS2) isoforms (Castro-Rodríguez et al., 2011). We examined the expression of 4 genes encoding GS1 isoforms and the 2 GS2 isoforms since our microarray data showed differences in expression for these genes during N remobilization. The expression of remaining 2 GS1genes (Potri.004G085400 and Potri.012G043900) was not examined since we failed to detect their expression on the microarrays. We found little difference in the expression of GS1 isoforms during N remobilization (Figure. 2-8) except GS1.1 (Potri.017G131100) that showed a gradual decline in expression during LD-mediated N remobilization. In contrast to GS1 genes, both genes for the GS2 isoforms (Potri.008G200100 and Potri.010G029100) showed increase expression during N remobilization with the greatest increase in expression occurring for Potri.008g200100. Thus it appears that the synthesis of glutamine for N transport

during N remobilization involves mostly chloroplast isoforms as opposed to cytosolic isoforms.

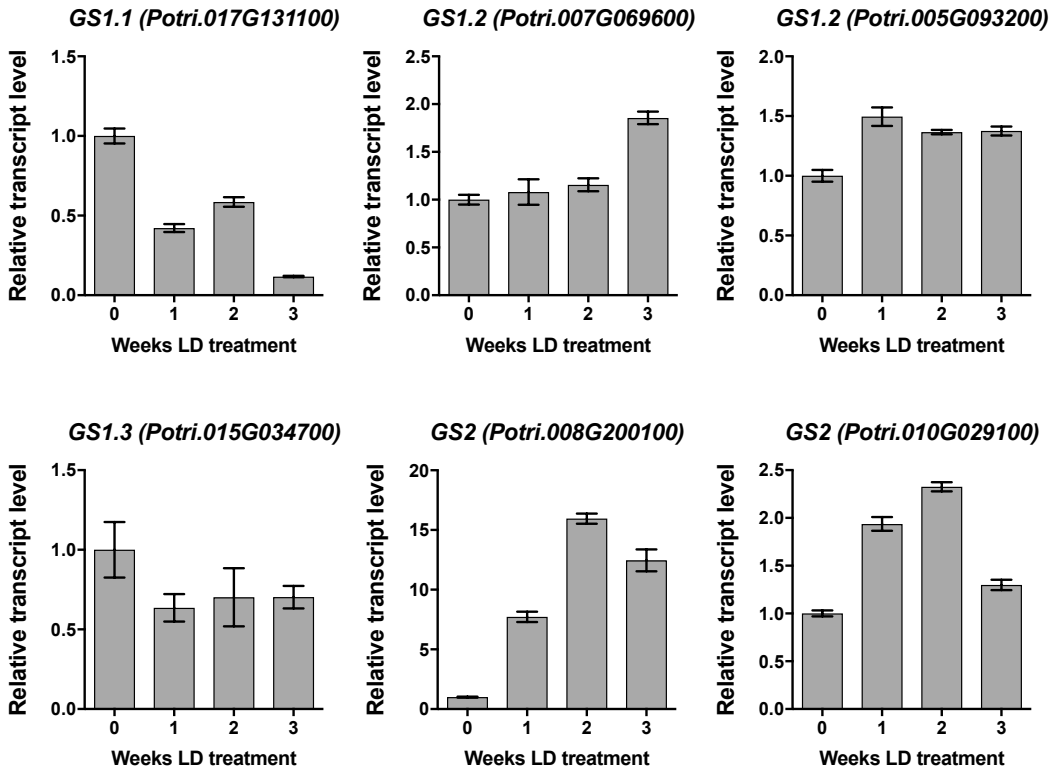

Figure. 2-8. Glutamine synthetase (GS) expression in bark during N remobilization. Relative expression of GS genes encoding cytosolic (GS1) and plastid (GS2) forms of GS were determined by qRT-PCR at weekly time points during LD-mediate N remobilization. Plants (*Populus trichocarpa*, Nisqually) were first grown in LD for approximately 6 weeks followed by SD treatment for 8 weeks at 20°C to induce dormancy. Leaf senescence and abscission was then induced with 6 weeks of further SD at low-temperature (LT) (10°C, light; 4°C dark). After leaf senescence and abscission the plants were place in the dark at 4°C for 7 weeks to release buds from dormancy. Renewed shoot growth was then initiated by placing plants in LD at 20°C. Three independent replicates were collected for RNA purification at the start of the LD treatment and at weekly intervals for 3 weeks. Error bars indicate mean ± SE.

Discussion

BSP accumulation influences bud break and shoot growth following dormancy

Numerous studies have demonstrated the importance of internal N stores to meet the N demand of trees (Guak et al., 2003; Millard, 1994; Millard and Proe, 1991; Millard et al., 2006; Neilsen et al., 1997; Weinbaum and Van Kessel, 1998). Utilization of internal N stores has the advantage of uncoupling growth from N uptake (Cooke and Weih, 2005; Millard and Grelet, 2010). These previous studies demonstrate the importance of N stores to the N budget of trees, yet the relative contribution of different N storage pools such as proteins and amino acids has not be studied. In the research we present here, we used a transgenic approach and RNAi mediated gene knockdowns to reduce bark accumulation of BSP and then determine the effect on growth following dormancy. We found that initial growth was reduced when BSP accumulation was reduced, supporting a role for BSP N storage as an important N store that is remobilized and used to support new shoot growth. Besides storing BSP, amino acids including arginine also accumulate in poplar bark during overwintering (Wildhagen et al., 2010). It is likely that amino acid stores were the predominate storage pool utilized since BSP levels were reduced. It is also possible that amino acid stores may increase if BSP accumulation is inhibited which would partially compensate for reduced protein stores. Additional research is needed to determine if such compensatory mechanism occurs when N store pools are altered.

The BSP RNAi transgenic studies reduce BSP accumulation and therefore N sources that are remobilized during shoot regrowth, we also performed a set of studies where we instead manipulated the N sinks during regrowth while N sources remained the same. This was accomplished by manipulating the number of shoots that would be competing for a given level of stored N and then examining how that influenced their growth. The underlying assumption is that initial growth competes for N stores, although we cannot exclude that C stores can also contribute to shoot growth. However, by measuring growth parameters known to be strongly influenced by N availability (i.e. leaf area, stem length) (Cooke et al., 2005) it is likely that differences in growth are a consequence of competition for N. As expected, when the number of growing shoots increased growth was reduced irrespective of the shoot type (proleptic or sylleptic). Sylleptic shoot production was one of the most affected parameters as shoot competition of N stores increased. We also found that competition between shoot types was not uniform. There was little competition for N stores from shoots originating from previously formed sylleptic shoots with shoots originating from axillary buds. However, shoots originating from axillary buds were very effective in competing with shoots from previously formed sylleptic shoots. Thus, initial shoot growth following dormancy seems to be source limited, suggesting that strategies to increase N stores could reduce source limitations to growth. Poplar sylleptic and proleptic shoots are known to differ in their physiology. Sylleptic shoots/branches export C mainly to the lower stem and roots while carbon from the leaves on the main stem (proleptic) partition C that is used mostly for height growth (Scarascia-Mugnozza et al., 1999). In addition, sylleptic shoots were reported have a greater

translocation efficiency than proleptic shoots (Scarascia-Mugnozza et al., 1999). Our results also suggest that besides differences in C partitioning that sylleptic and proleptic shoots also differ in respect to physiological responses related to tree N budgets.

We also discovered that the timing of bud break was delayed in the majority of transgenic poplars with reduced levels of BSP. This suggests that N stores also impact the timing of bud break in addition to shoot growth. The timing of bud break in poplar involves APETALA2/ERF EBB1 (EARLY BUD-BREAK1) (Yordanov et al., 2014). It was reported that most enriched GO category for putative targets for EBB1 were genes associated with N metabolism (Yordanov et al., 2014). Thus it appears that N metabolism, including remobilization from reserve stores, has an important role in the timing of bud break following dormancy.

BSP accumulation also contributes to sink status during N partitioning from leaves

^{13}N tracer experiments using BSP RNAi lines showed a reduction of ^{13}N partitioning in stems during leaf senescence. In addition ^{13}N partitioning from leaves was also observed in in poplar stems during growth. The fact that ^{13}N partitioning to the lower stem did not increase under SD-LT conditions suggests that the stem may become a direct sink for exported leaf N as the stem matures, even while growth in younger parts of the stem is still under way. It was surprising that the total export of ^{13}N from leaves to stems did not increase when the photoperiod was switched from LD to SD/LT, as we had expected. Given that leaf N content declines during SD-

induced senescence, this suggests that N export begins during leaf development and that N uptake into the leaf continues well beyond the point at which the leaf reaches maturity in order to maintain the level of N in the leaf. Then during senescence, rather than up-regulating N loading into the phloem, the leaf ceases N uptake, and the decrease in N uptake is a component of declining leaf N. Alternatively, the lack of apparent increase in N export from leaves could be due to isotopic dilution (Babst et al., 2013) since the concentration of glutamine in poplar leaves increases during SD-induced senescence, especially in the veins (Couturier et al., 2010).

Polar auxin transport is required for N remobilization from bark during regrowth

We found BSP catabolism and N remobilization during shoot regrowth was associated with induction of specific auxin transporter genes including *ABCB5, ABCB7, PIN4, PIN7, AUX5/LAX7* and *AUX6/LAX3*. In accordance with our findings, *PttLAX3,* the ortholog of *AUX5/LAX7* and *AUX6/LAX3,* was also induced in wood forming tissues of hybrid aspen (*Populus tremula* × *tremuloides*) during regrowth in spring (Schrader et al., 2003). Similar induction was also observed during wood formation for *PttPIN1* and *PttPIN2* in hybrid aspen, which are orthologs of *PIN4* and *PIN7*, which appears to be related to increases in auxin transport capacity (Schrader et al., 2003). Moreover, the expression of these auxin transporter genes was regulated by auxin via a positive feedback (Carraro et al., 2012; Schrader et al., 2003), which may explain the reason that auxin transporter genes were gradually induced during regrowth. During active growth, young and expanding leaves serve as a major source of auxin (Ljung et al., 2001; Schrader et al., 2003; Sundberg and Uggla, 1998).

Consistent with these tissue serving as an auxin source we found that specific auxin biosynthesis genes in the *TAA/TAR* and *YUCCA* families were also induced in the young and expanding leaves during regrowth and removal of buds which eliminated the sites of auxin production significantly reduced expression of auxin transporter and response genes. Stem auxin is also radially transported in poplar stems and proposed to by synthesized by dividing cambial cells (Schrader et al., 2003; Spicer et al., 2013; Sundberg and Uggla, 1998) in addition to longitudinal polar auxin transport (Kramer et al., 2008; Schrader et al., 2003; Spicer et al., 2013; Sundberg and Uggla, 1998). Since blocking polar auxin transport inhibited BSP degradation suggests that polar auxin transport is required for BSP catabolism and radial transport from dividing cambium appears to contribute little to BSP catabolism. Thus BSP catabolism requires long distance auxin transport from shoots to bark rather than a stem-localized source of auxin.

BSP catabolism involves induction of protease genes by auxin

The BSP catabolism during regrowth involves the action of proteolytic enzymes in poplar bark. It is predicted that there are 955 protease genes in the genome of *Populus* (García-Lorenzo et al., 2006). In order to identify proteases responsible for poplar BSP catabolism during regrowth, multidimensional protein identification technology (MudPIT) was used to analyze bark protein changes during the period of BSP catabolism (Islam et al., 2015). 30 proteases showed increased abundance in bark during BSP catabolism, including papain-like cysteine proteases, serine carboxypeptidases and aspartyl proteases. Among those proteases, four of them showed increased transcript abundance in our DNA microarray, including two serine

protease genes Potri.002G120400 and Potri.014G018900, one cysteine protease gene Potri.006G232900 and one aspartyl protease gene Potri.018G014800 (Islam et al., 2015). However, a notable number of protease genes that showed induced gene expression by DNA microarray analysis were not detected in proteome analyses using MudPIT. There could be multiple reasons for these differences. First, the proteome analyses were limited to samples of two time points (LD for 1 week and 3 weeks), while the DNA microarray analysis involved bark samples of four time points. Second, the activation of some proteases involves post-translational processes (van der Hoorn, 2008).which would not involve changes in genes expression. Thus the proteases by accumulate along with BSP in bark phloem parenchyma but remain inactive until spring remobilization. We also found that specific proteases were auxin inducible which supports the role of polar auxin transport in regulating BSP catabolism through auxin-mediated induction of the expression. Thus polar transport of auxin from shoots to bark appears to regulate BSP catabolism and N remobilization by regulating the expression of specific proteases.

Glutamine synthesis and transport is involved in N remobilization

Glutamine synthetase (GS) contains two major isoforms, GS1 (cytosolic) and GS2 (chloroplastic) in poplar (Castro-Rodríguez et al., 2011). Previous studies have shown that the expression of GS genes is seasonally regulated in poplar (Castro-Rodríguez et al., 2011). In our study, two GS2 genes *Potri.008G200100* and *Potri.010G029100* showed increased transcript levels in bark during regrowth. Changes in *GS2* expression have been previously reported in poplar bark during spring regrowth (Castro-Rodríguez et al., 2011). These data together suggest that bark serves as a

strong N source during regrowth and GS2 isoforms play an important role in N metabolism and remobilization and in particular in the production of glutamine since it is the major amino acid transported during N remobilization In addition, a slight increase of *GS1.2* transcript level was observed during regrowth suggesting that *GS1.2* is not the major isoform for N remobilization. It has been reported that the transcript level of *GS1.1* was mainly abundant in older leaves and increased during summer and autumn, indicating that GS1.1 may be involved in N metabolism and remobilization during leaf senescence (Castro-Rodríguez et al., 2011). This may explain why the transcript levels of *GS1.1* were reduced in bark during regrowth. However, the transcript level of *GS1.3* was slightly reduced in bark during regrowth while it was increased during spring regrowth in a previous report (Castro-Rodríguez et al., 2011). These results suggest that GS1.3 may play a role in N metabolism during active growth after N is remobilized from bark.

Glutamine is the predominant amino acid that is transported from bark to leaves during spring N remobilization (Millard et al., 2006a; Sauter and Cleve, 1992; Wildhagen et al., 2010). Pt-CAT11 has previously been shown to transport glutamine and appears to be involved in N remobilization from senescing leaves to bark during autumn (Couturier et al., 2010a). Our results showed that *CAT11* expression was negatively related to N remobilization from poplar bark during regrowth. Moreover, we found *CAT10* was induced in bark during regrowth and reduced when BSP catabolism was inhibited by bud removal or NPA treatment. It appears that CAT11 is involved in glutamine import to bark during leaf senescence while CAT10 may be involved in the export of glutamine during N remobilization from bark to shoots.

Thus CAT11 appears to be associated with bark sink status while CAT10 is related to bark source status.

In summary, the results of this research suggest that spring N remobilization from bark to shoots during the spring is, at least in some part, regulated by auxin (Figure 2-9). This process likely involves the production of auxin in expanding buds and shoots that is transported to bark. Auxin then induces the expression of specific proteases that are involved in the catabolism of BSP. The products of this catabolism are used in the biosynthesis of glutamine that is then loaded into phloem and transported to expanding shoots that act as N sinks. This phloem loading appears to involve CAT10. There are many unanswered questions about this process, but the results from this research provides a foundation from which further research can define important factors involved in N remobilization in trees.

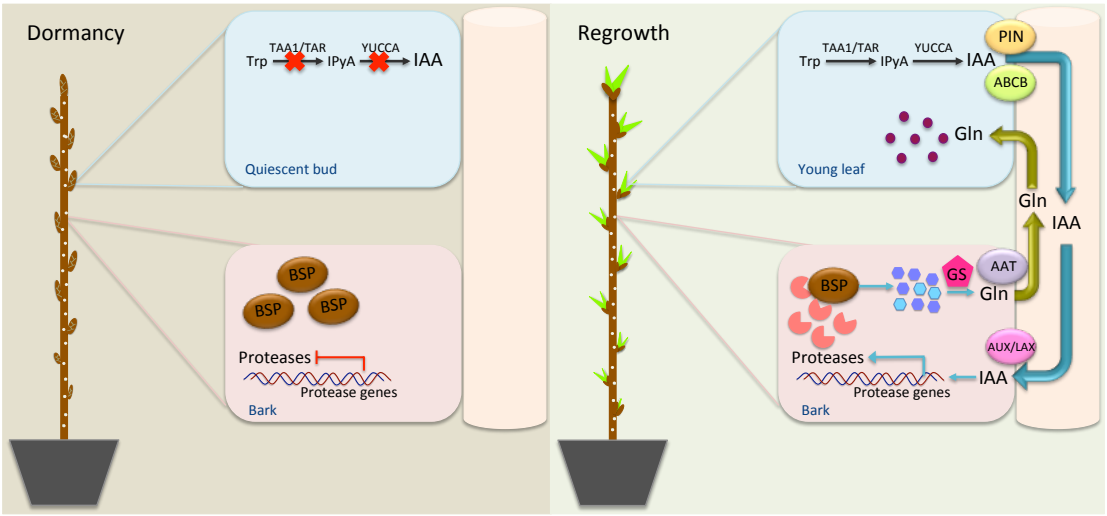

Figure 2-9. Proposed working model for the role of auxin in N remobilization during regrowth in poplar. During dormancy, there is no active growth and auxin activity, thus no BSP catabolism and N remobilization occurs. During active regrowth, yound and expanding leaves serve as an auxin source and then auxin is transported to bark and activate protease-mediated BSP catabolism and N remobilization. Remobilized N is then converted to glutamine by GS, the currency of N transport, and transported to young and expanding leaves.

Chapter 3: Ethylene plays a role in nitrogen sink status and storage in poplar trees.

Abstract

Photoperiod is an environmental signal that impacts many aspects of plant growth and development. In poplar, short-day (SD) photoperiod is the major environmental factor regulating Bark Storage Protein (BSP) accumulation and N storage. However, the mechanism underlying this process remains unclear. To identify potential candidate genes involved in SD-mediated N storage, changes in transcript abundance was investigated in poplar bark using poplar whole genome DNA microarrays. Analyses of gene expression profiles revealed changes in the expression of genes associated with ethylene synthesis and signaling during SD treatment. Stem ethylene production was also found to be repressed during SD treatment and this repression was accompanied by a decline in expression of specific ethylene signaling genes. Through stem feeding experiments with ACC, ethephon and AVG we found that both ACC and ethephon repressed BSP gene expression while AVG enhanced expression. Furthermore, ACC and ethephon repression of BSP gene expression was reduced in poplars expressing the dominant gain-of-function allele (*etr1-1*) of the *Arabidopsis* ethylene receptor. Two transcription factors belonging the ERF family, ERF12 and ERF4, were found to be the two transcription factors that were induced the greatest in SD treatment. Transient expression of *ERF12* and *ERF41* in tobacco transformed with the *BSPA* promoter fused to GUS resulted in increased GUS activity supporting a role for these transcription factors in the induction of poplar BSP gene expression.

Taken together, our findings suggest a mechanistic model whereby photoperiod may regulate BSP gene expression through alterations in ethylene production and signaling.

Introduction

Light is an important factor involved in plant photomorphogenesis. Phytochrome, the photoreceptor for red and far-red light, exists in two forms: a red light-absorbing inactive form (Pr) and a far-red light-absorbing active form (Pfr) (Chen and Chory, 2011). Because of the red/far-red reversability of phytochrome plants are able to perceive light conditions to regulate plant growth and development processes by mediating the degradation of the PIF (phytochrome interacting factors) family of basic helix-loop-helix (bHLH) transcription factors (Lorrain et al., 2008). A wide-range of processes are influenced by phytochrome-mediated signaling including respiration (Igamberdiev et al., 2014), germination (Shinomura et al., 1994, 1996), de-etiolation (Smith et al., 1997; Weller et al., 2001), shade avoidance (Casal, 2013), circadian rhythms (Somers et al., 1998) and stress tolerance (Carvalho et al., 2011). In addition, phytochrome is also involved in modulating levels of various plant hormones including gibberellin, auxin, cytokinin, abscisic acid, brassinosteroid and ethylene which are involved in signaling light-regulated developmental processes (Jeong et al., 2007; Lau and Deng, 2010; Seo et al., 2009; Shi et al., 2016).

Ethylene, a gaseous phytohormone, is involved in plant response to diverse environmental cues. Major components in ethylene signaling pathway have been identified and characterized in recent years (Kendrick and Chang, 2008; Merchante et al., 2013; Stepanova and Alonso, 2009; Yoo et al., 2009). In *Arabidopsis*, ethylene is

perceived by the receptors ETR1, ETR2, ERS1, ERS2 and EIN4, which subsequently prevents the phosphorylation of the positive regulator EIN2 by inactivating CTR1, a kinase that suppresses ethylene response (Merchante et al., 2013). The activation of EIN2 results in cleavage of its C-terminal end, which moves to the nucleus and stabilizes transcription factors EIN3/EIL1, which in turn activates or represses the expression of down-stream ethylene response genes (Merchante et al., 2013). The F box proteins, EBF1 and EBF2, target EIN3/EIL1 for proteasome-mediated degradation through the SCR E3 ligase complex (Binder et al., 2007; Gagne et al., 2004; Guo and Ecker, 2003; Potuschak et al., 2003) and ethylene stabilizes EIN3/EIL1 by inhibition of transcription and protein stability of EBF1/EBF2 (An et al., 2010; Merchante et al., 2015; Qiao et al., 2012).

Photoperiod is a major environmental cue in the growth and development of perennial plants. In poplar, growth cessation, terminal bud formation, and bud dormancy is induced by short-day (SD) photoperiod. In addition, SD photoperiod is the major environmental cue that triggers seasonal N storage that involves the mobilization of N from leaves and storage in perennial tissues. Central to poplar seasonal N storage is the accumulation of Bark Storage Proteins (BSP) in bark phloem parenchyma (Black et al., 2001; Coleman et al., 1991a, 1992; Langheinrich and Tischner, 1991; Pettengill et al., 2013; Zhu and Coleman, 2001a, 2001b). Poplar BSP is encoded by 3 genes (*BSPA*, *BSPB*, *BSPC*) that are members of a 13-member gene family with homology to nucleoside phosphorylases (Pettengill et al., 2013). Previous studies have shown that SD photoperiod-induced expression of *BSP*s involves phytochrome signaling (Langheinrich and Tischner, 1991; Zhu and Coleman,

2001a). The importance of this storage pool of N during regrowth following dormancy is supported by the observation that external or soil sources of N does not occur until 40 days and 21 days after bud burst in poplar and cherry respectively (Millard et al., 2006a). Although it is well known that SD photoperiod induces BSP expression and BSP accumulation in poplar, the regulatory mechanism of this process remains unclear. In this study, we investigated possible regulatory mechanisms to bridge the link between SD photoperiod with *BSP* expression. To this end, genome-wide transcriptome analysis of poplar bark from plants treated with SD reveal major changes in the bark transcriptome. We found that gene expression of the majority of ACS and ACO ethylene biosynthesis genes were reduced in SD-treated poplar bark. Furthermore, ethylene repressed *BSP* expression and ethylene insensitive poplars showed less repression of *BSP* expression when treated with either ACC or ethephon compared to the wild type plants. We also found that the two ethylene response factors ERF12 and ERF41 were repressed by ethylene and induced by SD photoperiod. These two ERFs were also found to enhance the expression of a *BSPA* promoter::GUS chimeric gene in transient assays in tobacco. This study provides insights into possible mechanism that involve ethylene signaling in the photoperiod regulation of *BSP* expression and accumulation in poplar.

Materials and methods

Plant materials and growth conditions

Two poplar genotypes, *Populus trichocarpa* (Nisqually) and the *Populus tremula X tremuloides* (T89) were used in this study. Nisqually was used in all short-day (SD)

photoperiod treatments and low temperature (LT) experiments. Briefly, Nisqually plants were first grown in long-day (LD) condition (16h light/8h dark) at 20°C for 8 weeks. After growth in LD, SD treatments were conducted by changing the photoperiod in controlled environmental chambers to SD (8h light/16h dark) for 6 weeks at 20°C. LT treatments involved reducing the temperature during SD to 10°C day/4°C night for additional 4 weeks. Depending on the experiment, bark and leaves were harvested at weekly intervals, immediately frozen in liquid N and then stored at -80°C until used for further analysis. Transgenic poplar 1E transformed with the *Arabidopsis etr1-1* (Chang et al., 1993) mutant allele (35s::*etr1-1*) in *Populus tremula X tremuloides* T89 background and the T89 wild-type were obtained from the Umeå Plant Science Centre (Love et al., 2009).

RNA preparation and microarray hybridization

Total RNA from bark and leave tissues for all experiments was performed with the Qiagen RNeasy plant mini kit (QIAGEN, USA) using a Qiacube with modifications and on-column DNA digestion as described by Pettengill et al. (2012). For DNA microarray analysis RNA quality was assessed using Experion RNA StdSens Analysis Kit (Bio-Rad Laboratories, CA) while spectrophotometric analysis (Eppendorf BioPhotometer plus; Eppendorf, NY) was used for RNA used in qRT-PCR. DNA microarray analysis was performed by the University of Maryland, Baltimore Genomics Core facility. Briefly, biotinylated cRNA was prepared according to the standard Affymetrix protocol (GeneChip 3' IVT expression kit) from 100 ng of total RNA. Following fragmentation, 12.5 µg of cRNA was hybridized for 17 h at 45 °C on the GeneChip® Poplar Genome Array. GeneChips were washed and

stained in the Affymetrix Fluidics Station 450 and scanned using GeneChip Scanner 3000 according to procedures of the manufacturer.

Statistical analysis of microarray data

Microarray data analysis was completed using R and Bioconductor. Log_2-transformed expression values were obtained for each probe set. Initial filtering of probe sets using a process based on threshold fractions of "present" calls as described previously (McClintick and Edenberg, 2006), which proved to effectively eliminate probe sets that are unlikely to be reliable and while preserving the most significant probe sets as well as those turned on and off in different experimental conditions. Probe sets with a median absolute deviation smaller than or equal to 0.1 were excluded from further analysis. This filtering process resulted in 32,617 probe sets retained for further statistical analysis for the SD treatment experiment.

Statistical analysis of probe sets passing the filtering process was carried out using the limma package (Smyth, 2004) where variances were adjusted by the empirical Bayes (eBayes) method and adjusted *P*-values for multiple tests were calculated using Benjamini-Hochberg's method (Benjamini and Hochberg, 1995). Annotations for the probe sets were obtained from Affymetrix and the corresponding *Populus* gene models for each probe set were extracted. For gene models with multiple matching probe sets, the average expression values, average $\log_2$ ratios for each comparison, and average adjusted *P*-values were calculated based on all matching probe sets. Gene models with an adjusted *P*-value $\leqslant 0.01$ and a $\log_2$-fold change $\geqslant 2$ (4-fold change on linear scale) were considered differentially expressed in SD treatment samples over the control.

For pathway analysis the corresponding *Arabidopsis* locus for each *Populus* model was obtained from Phytozome. The mean log_2-ratios for all the *Populus* models matching single *Arabidopsis* orthologues were then imported into CIMminer to generate color-coded Clustered Image Maps (CIMs) ("heat maps") with the default parameters (https://discover.nci.nih.gov/cimminer/home.do) (Weinstein et al., 1997). All microarray data and expression values for all probe sets were submitted to Gene Expression Omnibus (GEO) at NCBI http://www.ncbi.nlm.nih.gov/geo under the accession GSE49983.

Chlorophyll quantification

Leaf discs (1.12 cm diameter) were collected from 3 leaves of each plant from leaves at LPI 5-10. Chlorophyll was extracted by gently shaking in a vial containing 5ml of 80% acetone at 4°C in darkness for 24h. After the 24h extraction, absorbance at 645nm and 663nm was measured. The concentration of Chl a, Chl b and total Chl was calculated using following equations. The final concentration was expressed using μg per cm^2 leaf area.

Chl a= 12.7*OD663-2.69*OD645

Chl b= 22.9*OD645-4.68*OD663

Chl total= 20.2*OD645+8.02*OD663

Excised stem feeding

Stems approximately 50 cm in length were removed from greenhouse grown stock plants and immediately placed in water. Stem cuttings were subsequently trimmed to

remove all but the apical 5 leaves and a fresh cut was made at the stem base and immediately place in 500ml flasks containing 400 ml of H_2O. The stems were then incubated for 24h in a controlled environmental chamber with continuous light at 20°C. After the 24h preincubation period cuttings were transferred to a 500ml flask containing 400ml of 100µM ACC (1-aminocyclopropane-1-carboxylic acid) (Sigma, St. Louis MO), 100µM Ethephon (2-chloroethylphosphonic acid) (Sigma) or 2µm AVG (aminoethoxyvinylglycine) (Cayman Chemical, Ann Arbor MI). Bark was harvested from at least 3 replicate stems at various time intervals as detailed in the results and immediately frozen in liquid N and then stored at -80 °C until used for RNA purification. N feeding experiments consisted of 20mM NH_4NO_3 and 25mM glutamine either alone or in combination with ACC, Ethephon or AVG.

Measurement of ethylene production

Stem ethylene production was measured by gas chromatography as described previously (Li et al., 2014). Briefly, 3 stem segments (3-4 cm in length) were collected and placed into a sealed glass vial with 1ml distilled water to minimize dehydration. The vials were incubated in light condition at room temperature for 2h. Ethylene was sampled from the vials with a 1ml syringe and injected into a gas chromatograph. Ethylene production was reported as nL per gram of fresh weight per hour.

RNA extraction and RT-qPCR

Total RNA was extracted from three biological replicates using as described for microarray analysis. Purified RNA was used for cDNA synthesis using iScript™

cDNA synthesis kit (BioRad, Hercules CA) according to manufacturer's instructions. The cDNA was used for determination of relative transcript level of target genes using qRT-PCR. Amplification reactions consisted of 30 sec at 95 °C followed by 40 cycles of 5 sec at 95 °C and 15 sec at 60 °C. Reference gene and relative expression analysis was performed using qbasePLUS as previously described (Pettengill et al., 2012). All qRT-PCR primers for target genes and reference genes are listed in Table S3-1 and were designed and validated as previously described (Pettengill et al., 2012).

Transient expression of ERF12 and ERF41 in tobacco leaves

Full-length cDNAs of ERF12 and ERF41 were amplified with the forward primer 5'-CACCATGAACGAGATTAGCTCATTG-3' and reverse primer 5'-CTAACTAGCCAATAATTGCTCGCC-3' and forward primer 5'-CACCATGTACCCACCCCTAACC-3' and reverse primer 5'-TCAAAAGAGTGGTGCCGGCA-3' respectively. The full-length cDNAs were cloned into the pENTR D-TOPO entry vector using the pENTR^{TM} Directional TOPO Cloning kit following the manufacturer's instructions (Invitrogen, Life Technologies). Plasmids were transformed into *E. coli* (DH5α) and plated and grown on LB media supplemented with 50 mg/l kanamycin. Colonies were selected and the insert was verified by PCR and DNA sequencing (Macrogen). Plasmids in the pENTR D-TOPO entry vector consisting of the correct DNA sequences were mobilized to the Gateway binary vector pB7WG2 (Karimi et al., 2002) using Gateway LR Clonase II enzyme mix (Invitrogen by Life Technologies) following the manufacturer's instructions. Following the Clonase reaction, plasmids were transformed in to *E. coli* (DH5α) and

grown on LB plates supplemented with 75 mg/l spectinomycin. Colonies were selected and the plasmid DNA purified, the insert size determined by PCR and the DNA sequence verified by DNA sequencing. Validated clones were then transformed into *Agrobaterium tumefaciens* strain C58/PMP90 using the heat-shock method. Agrobacterium transformants were selected on LB media containing 20µg/mL gentomycin and 50µg/mL spectinomycin.

Transient expression of *ERF12* and *ERF41* was conducted as described previously (Sparkes et al., 2006). Briefly, 5ml culture of Agrobacteria, previously transformed with ERF12 and ERF41, was separately grown overnight at 28 °C at 200 rpm and then 1ml of culture was pelleted in a sterile microcentrifuge tube at 5,000g for 5 min at the room temperature. The supernatant was removed, and the cells washed with 1ml of infiltration medium and then resuspended in infiltration medium. This was repeated twice after which the cells resuspended in infiltration medium at a 1 in 10 dilution of cells and then diluted with infiltration medium to an OD600 = 0.1. Diluted cells were taken up in a 1ml sterile syringe and infiltrate against the underside of the tobacco (line B6-9-1) leaves that had been previously transformed with *BSPA*-promoter::uidA (Zhu and Coleman, 2001b). Transfected plants where then incubated in a growth chamber with long-photoperiods and 20 °C for 3 days. After this 3 day incubation period, infiltrated leaf regions were collected, frozen and liquid N and stored at -80 °C until used for analysis.

Assay for GUS activity

Fluorometric assay of GUS activity was performed as described previously (Jefferson, 1987; Jefferson et al., 1987; Zhu and Coleman, 2001b). The concentration

of soluble protein was measured using the BCA protein assay kit (Sigma). GUS activity was expressed as nmol 4-methylumbelliferone (4-MU) per minute per mg protein.

Subcellular localization of ERF12 and ERF41

cDNA sequences (without stop codons) corresponding to ERF12 and ERF41 were amplified using the forward primer 5'- CACCATGAACGAGATTAGCTCATTG-3' and reverse primer 5'- ACTAGCCAATAATTGCTCGCC -3' and forward primer 5'- CACCATGTACCCACCCCTAACC-3' and reverse primer 5'- AAAGAGTGGTGCCGGCAAGTT -3' respectively. The cDNA fragments were cloned into pENTR D-TOPO entry vector and selected as described above. The entry clones were moved into the binary vector pK7FWG2 (Karimi et al., 2002) using Gateway LR Clonase II enzyme mix and selected as describe above. After verification by DNA sequencing the binary vectors were transformed into *Agrobacterium tumefaciens* strain C58/PMP90 as and used to transfect leaves of transgenic tobacco (line B6-9-1) as described above. After 3-5 days of incubation the infiltrated leaves were stained with 1μg/ml 4′ 6-diamidino-2-phenylindole (DAPI) by vacuum infiltration for 10 min and then examined using the LSM 710 Laser Spectral Scanning Confocal Microscope (Zeiss) with a 40× water immersion lens. Images were processed using ZEISS software.

Results

The timing of SD-induced BSP expression and leaf senescence differ

SD photoperiod is the primary environmental cue for the regulation of *BSP* expression and BSP accumulation. Since photoperiod is also involved in the induction of poplar leaf senescence (Fracheboud et al., 2009) it is possible that photoperiod may indirectly regulate *BSP* expression via the transport of N from senescing leaves. To determine if a relationship between leaf senescence and BSP expression exists, we examined the timing of *BSP* expression relative to leaf senescence. Bark transcript levels of *BSPA*, *BSPB* and *BSPC* started to increase after 2 weeks of SD treatment and continued to increase with continued SD treatment (Figure 3-1A). Between 4 to 6 weeks SD-treatment the relative transcript levels increased substantially. In contrast to *BSP* expression leaf chlorophyll contents changed little over a 6-week SD treatment and rather than decrease they increased slightly. After 8 weeks of SD treatment and the addition of low temperature (LT), chlorophyll levels declined significantly within 1 week of SD combined with LT treatment (Figure 3-1B). After 12 weeks of SD treatment where the last 4 weeks included LT leaf chlorophyll levels declined further to undetectable levels. The expression of senescence associated genes (SAG) also showed little change during the 6 weeks SD period during which *BSP* gene expression increased (Figure 3-1C). After 8 weeks of SD treatment the transcript levels of these senescence associated genes steadily increased over the addition 4 weeks of SD (12 weeks total) combined with LT. These results demonstrate that SD-induced *BSP* expression precedes leaf senescence suggesting that N remobilization from leaves to bark may not play a

regulatory role in SD-induction of *BSP* expression. Thus, SD-induced BSP expression appears to be independent of senescence-associated N transport from leaves to bark.

Transcriptome analysis of poplar bark during SD treatment

To investigate SD-responsive gene expression in poplar bark, genome-wide transcriptome analysis was performed using Affymetrix DNA microarrays. A total of 3188 genes were found to be differentially expressed in the bark during SD treatment compared to the bark of LD control plants. We then queried this set of differentially expressed genes for gene models of transcription factors with at least a $\log_2$-fold ≥ 2 (p value ≤0.01) and found approximately equal proportions of transcription factors that were repressed (67 genes) or induced (53 genes) during SD-treatment, including a range of transcription factor families. Two genes in the ERF family *ERF12* (*Porti.001G079900*) and *ERF41* (*Potri.002G043300*) showed a pattern where expression steadily increased during SD treatment and after 6 weeks of SD these two transcription factors were expressed at the greatest ($\log_2$-fold= 5.2 for *ERF12* and 5.6 for *ERF41*) of any of the transcription factors that were induced by SD (Figure 3-2). Furthermore, comparison of the microarray expression patterns of other ERF genes that were differentially expressed in bark were consistent with those of Vahala et al. (2013) in that ethylene-induced *ERFs* tended to be down-regulated in SD-treated bark whereas ethylene-repressed *ERFs* tended to be induced in SD-treated bark (Figure 3-3). These expression patterns suggest that SD treatment may repress bark ethylene production and signaling. We also queried the microarray data to see if genes involved in bark ethylene biosynthesis were also differentially expressed during

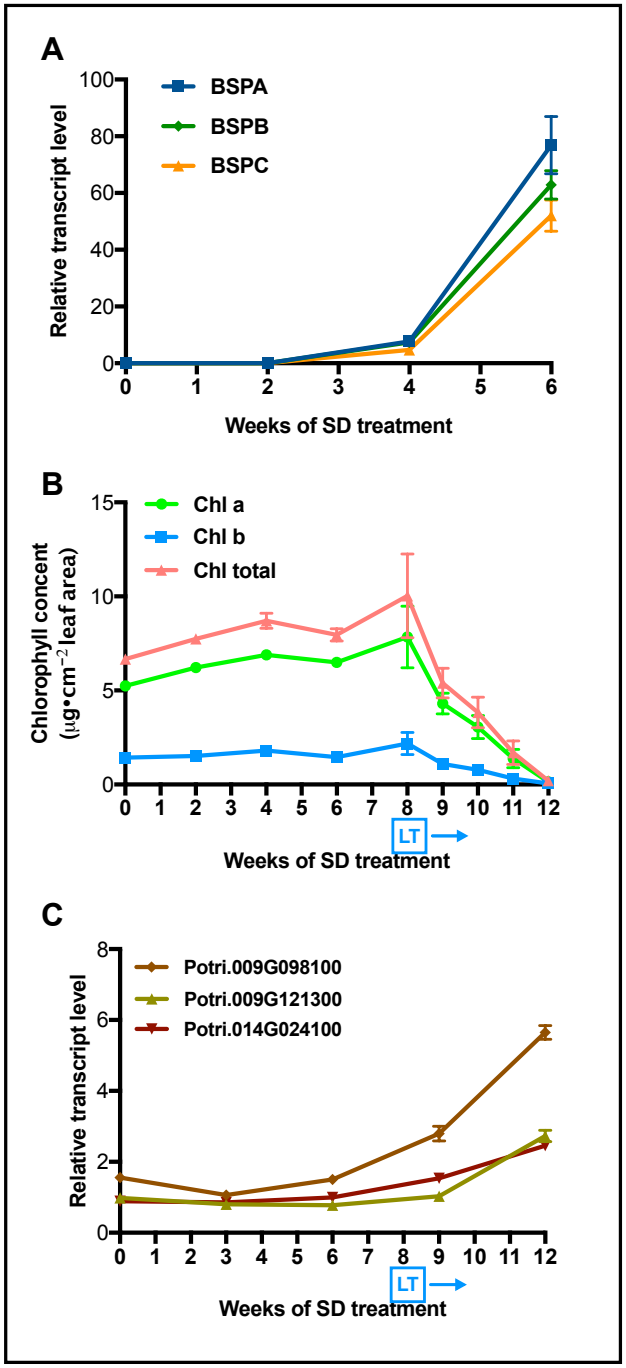

Figure 3-1. Induction of *BSP* genes occurs before leaf senescence during SD treatment. (A) Relative transcript levels of *BSPA*, *BSPB*, *and BSPC* in bark during 6 week of SD treatment. (B) Leaf chlorophyll contents and (C) leaf relative transcript level of three senescence associated genes during 8 weeks of SD followed by an additional 4 weeks of SD plus low-temperature (SD+LT) treatment (see material and method for details).

SD-treatment and found that *ACS1* (*Potri.001G099400*), *ACO2* (*Potri.002G224100*) and *ACO6* (*Potri.004G003000*) expression significantly declined (Figure 3-4). To further verify the observed changes from the DNA microarray, analysis by qRT-PCR for genes of interest was performed.

Expression of ethylene biosynthesis genes and ethylene production is repressed in poplar bark during SD treatment

To further characterize the expression of genes involved in ethylene biosynthesis bark and leaf expression of *ACS1-8* and *ACO1-7* were examined using qRT-PCR of poplars during SD treatment (Figure 3-5). Similar to the DNA microarray data, transcript abundance of *ACS2*, *ACS7* and *ACS8* declined in bark by two weeks of SD treatment while the remaining genes showed little difference in bark expression (Figure 3-4A). In contrast to bark, all of the ACS genes except *ACS1* showed significant increases in leaf tissue after 6 weeks of SD treatment. Among the 3 *ACSs* that declined in expression in SD, *ACS2* declined the greatest with a decrease of 98% of transcript level within the second week of SD treatment (Figure 3-5A). Similarly, transcript abundance of the majority of *ACO*s decreased in bark during SD treatment while *ACO3*, *ACO4*, *ACO5* and *ACO7* increased in leaves (Figure 3-5B). These results show that regulation and expression of ethylene biosynthetic genes differs between leaves and bark during SD treatment which may have important implications in the production of ethylene in these two tissues. We also measured ethylene evolution in bark during SD treatment and observed a steady decline during SD

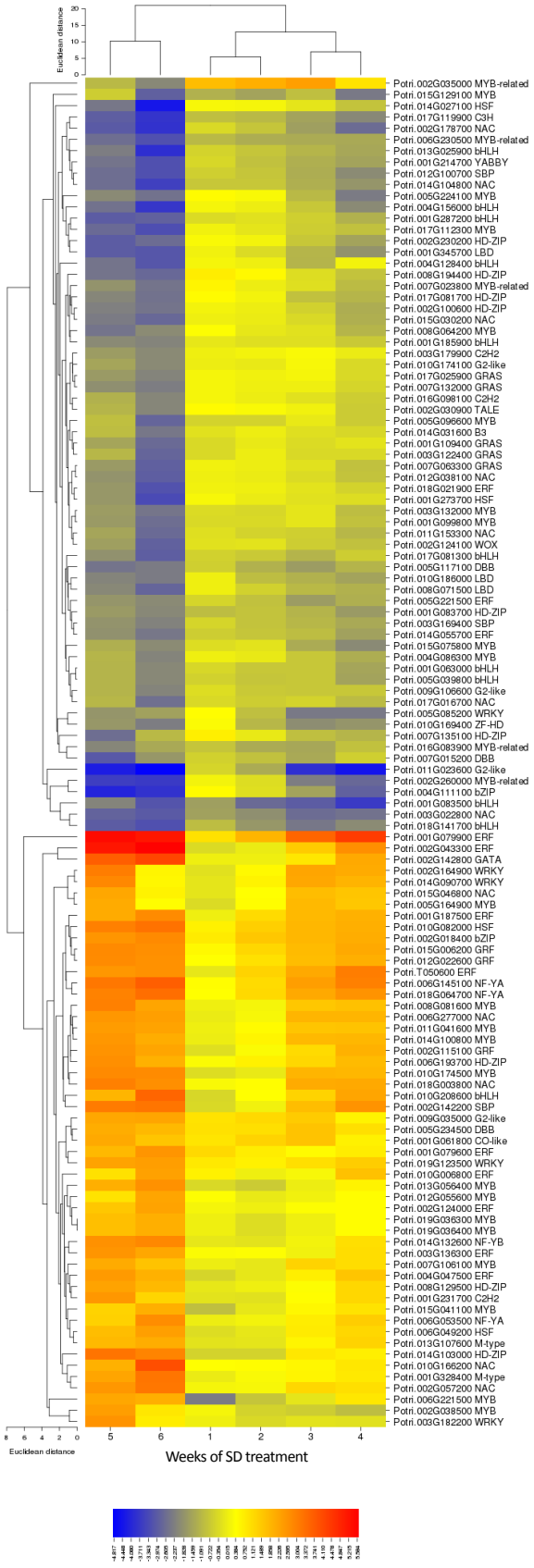

Figure 3-2. Expression profile of transcription factors in poplar bark during SD-treatment. Clustering is based on log_2fold values using DNA microarrays of plants treated with SD photoperiods relative to LD treated plants. Clustered heat map was produced using CIMminer.

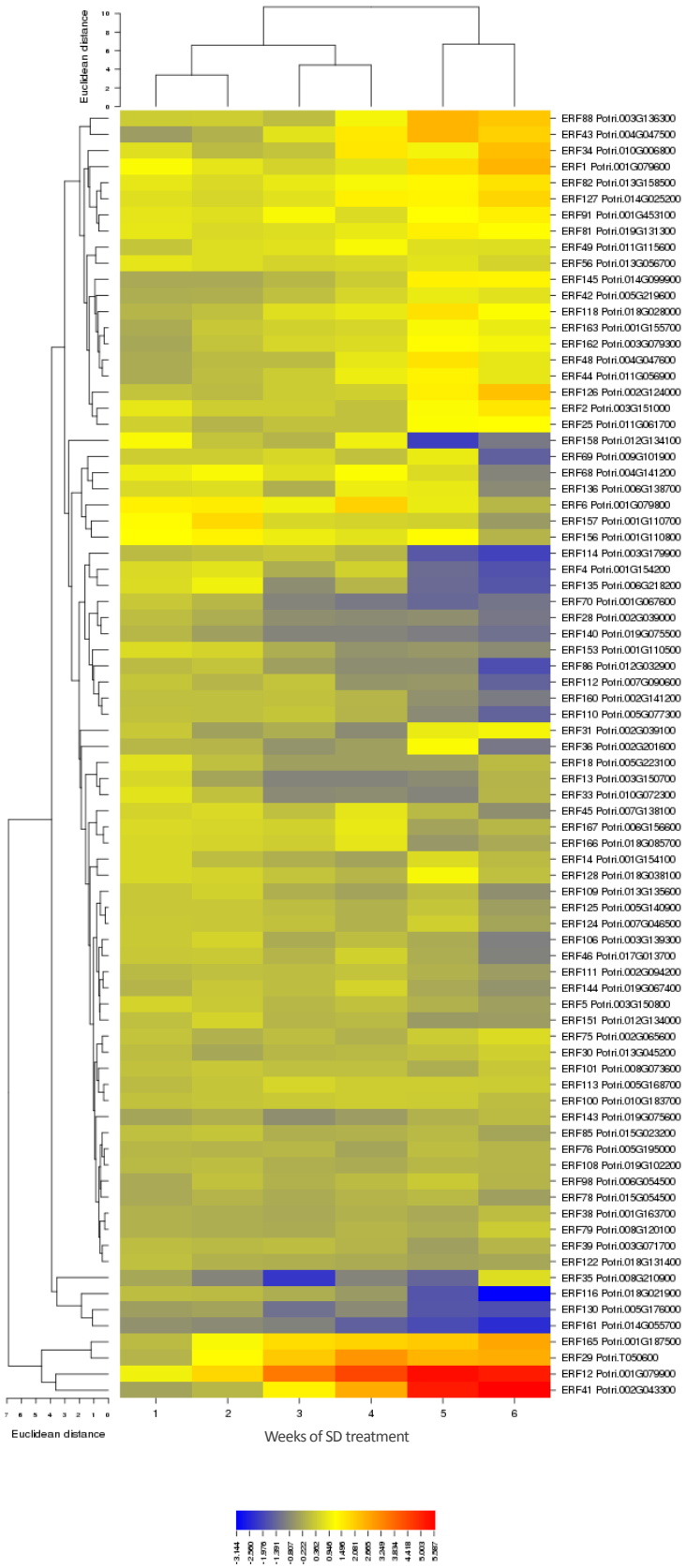

Figure 3-3. Expression profile of members of the ERF transcription factors family in poplar bark during SD-treatment. Clustering is based on log_2fold values using DNA microarrays of plants treated with SD photoperiods relative to LD treated plants. Clustered heat map was produced using CIMminer.

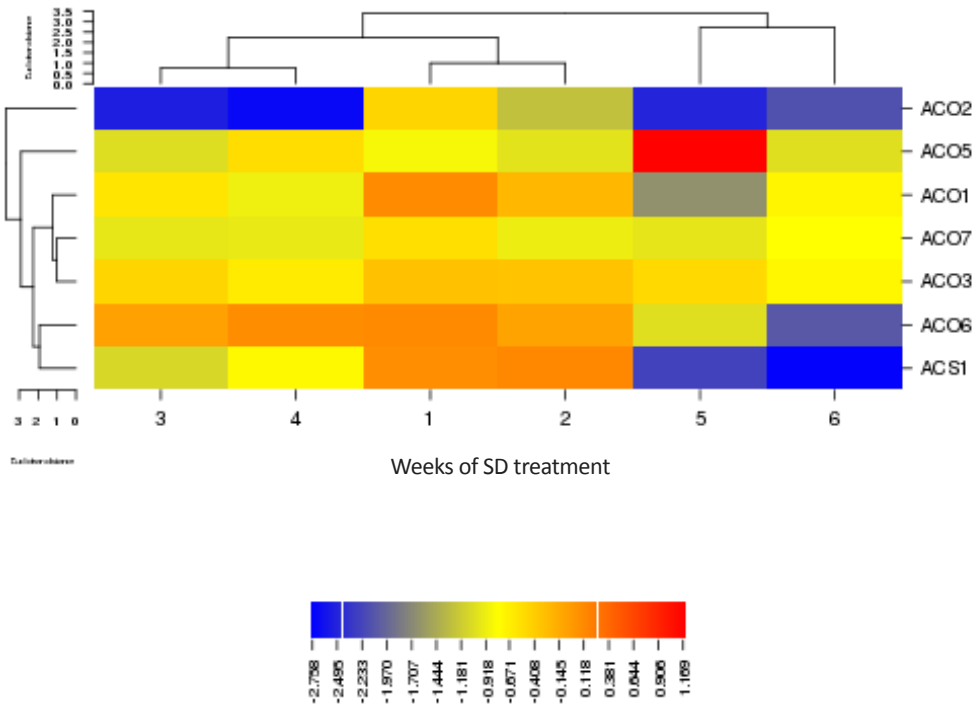

Figure 3-4. Expression profile of ethylene biosynthesis genes (*ACS* and *ACO*) expressed in poplar bark during SD treatment. Clustering is based on log_2fold values using DNA microarrays of plants treated with SD photoperiods relative to LD treated plants. Clustered heat map was produced using CIMminer.

treatment with significantly reduced levels after 28 and 42 days of treatment (Figure 3-5C). Since ethylene evolution declined in the bark of SD treated plants it is possible that bark ethylene production may be controlled by the ACS and ACO genes that declined in bark during SD.

Ethylene represses BSP expression in bark

Since *BSP* expression during SD coincides with a decline in bark expression of specific ACO and ACS genes and reduced bark ethylene production, experiments were undertaken to determine if feeding poplar stems ACC, ethephon or AVG influenced *BSP* expression. When excised poplar stems were incubated in a 100µM

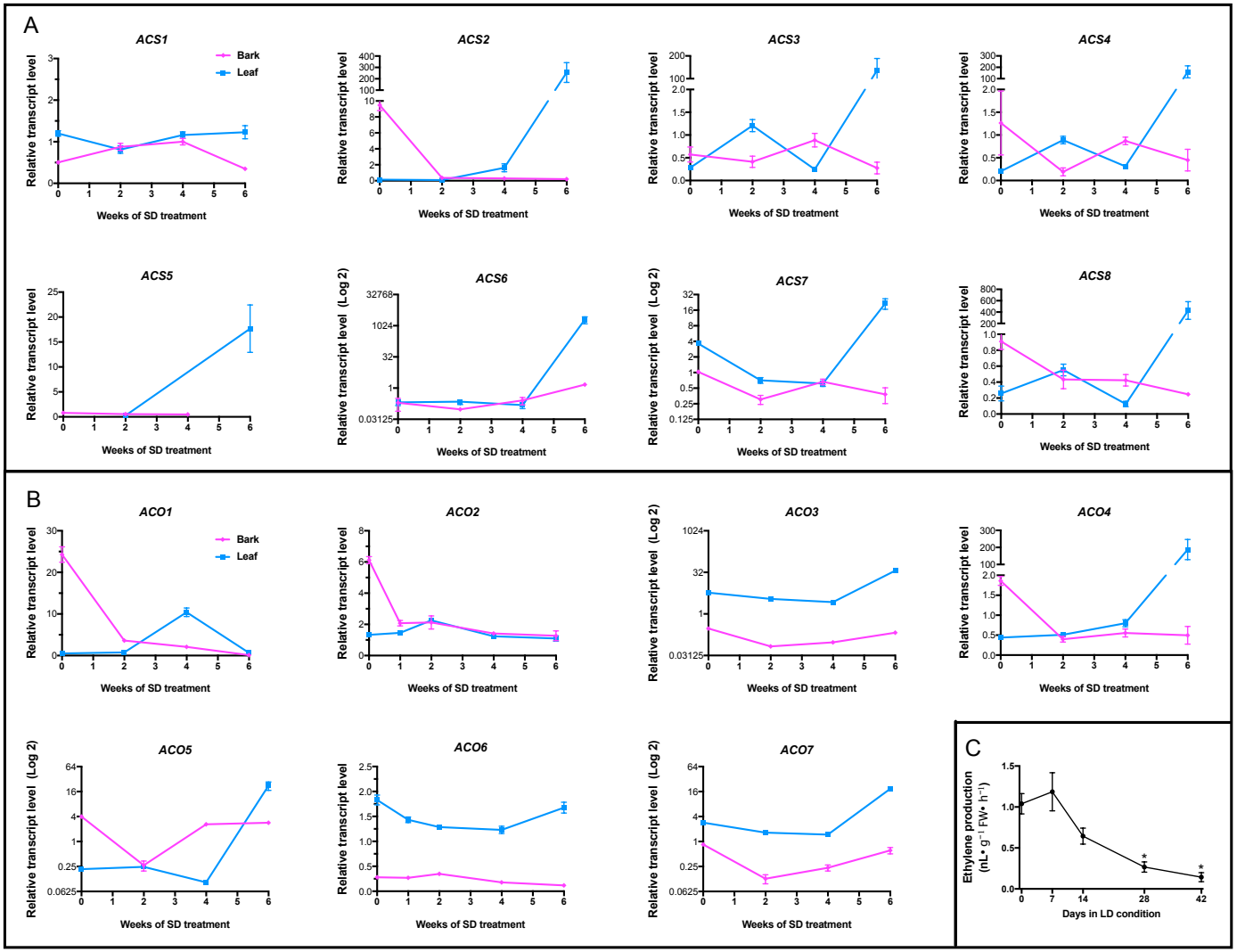

Figure 3-5. Expression of the ACS and ACO ethylene biosynthetic genes in bark and leaves of poplar and ethylene evolution in poplar bark during SD treatment. Relative transcript levels of (A) *ACSs* and (B) *ACOs* in bark (pink) and leaf (blue) during 6 weeks of SD treatment determined by qRT-PCR. (C) Ethylene production from bark during 6 weeks of SD treatment. * indicates means significantly different from control at $p<0.05$.

ACC solution transcript levels of both *BSPA* and *BSPB* significantly declined within 1h of treatment (Figure 3-6A). *BSPC* transcript levels also declined but the magnitude of the decline was not as great as *BSPA* and *BSPB*. With continued ACC feeding transcript levels continued to decline and changed little after 4 hours of treatment. As a positive control for ethylene induced expression we examined the expression of *ERF17*, *ERF21*, *ERF31* and *ERF33* which have been reported to be ethylene induced (Vahala et al., 2013) and found that transcript abundance of all 4 of these genes increased within 1h of treatment and reach maximum levels after 4h of treatment (Figure 3-6B). We then determined if feeding stems either 100μM ethephon or 2μM of the ethylene biosynthesis inhibitor AVG influenced *BSP* expression. After 16h of ethephon, ACC or AVG feeding bark RNA abundance for *BSPA*, *BSPB*, and *BSPC* declined compared to the control treatment of only water, while levels of both *BSPA*, *BSPB* and to a less extent *BSPC* significantly increase in the bark of stems fed with AVG (Figure 3-6C). Expression of the ethylene-induced *ERF17* showed increased expression with either ethephon or ACC treatment while AVG treatment showed a decline in expression (Figure 3-6D). Together, these results show that *BSP* expression is repressed by either ACC or ethephon and induced by AVG which further supports a possible role for ethylene in repressing *BSP* expression in LD conditions while reduced ethylene production in SD derepresses *BSP* expression.

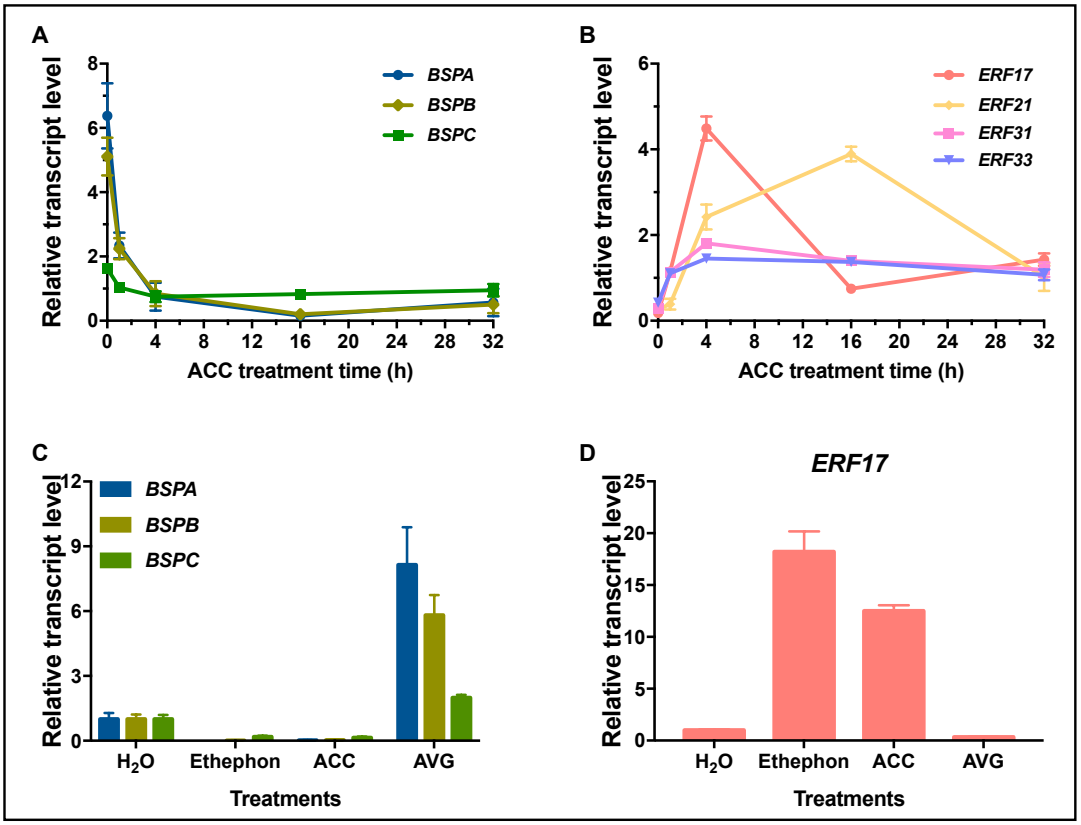

Figure 3-6. *BSP* genes expression is repressed in the bark of poplar stems fed with ACC or ethephon and induced by AVG. Relative transcript levels of (A) *BSPA*, *BSPB* and *BSPC* or (B) *ERF17*, *ERF21*, *ERF31* and *ERF33* in stems fed with 100µM ACC for 1, 4, 16 or 32h. Relative transcript levels of (C) *BSPA*, *BSPB* and *BSPC* or (D) *ERF17* in the bark of stems fed with either 100µM ethephon, 100µM ACC or 2µM AVG for 16h. Relative transcript levels were determined by qRT-PCR.

Ethylene inhibits N-induced BSP expression in bark

BSP expression is induced in poplar stems fed either NH_4NO_3 or glutamine (Zhu and Coleman 2001a). To determine if ethylene can influence N-induced *BSP* expression we fed poplar stems 20mM NH_4NO_3 or 25mM glutamine either alone or in combination with 100µM ACC, 100µM ethephon or 2µM AVG. Treatment with either NH_4NO_3 or glutamine for 24h significantly induced *BSPA* expression and to a lesser extent *BSPB* expression while *BSPC* was less affected by either N treatment

(Figure 3-7). When either N treatment was combined with either ACC (Figure 3-7A) or ethephon (Figure 3-7B) N-induced BSP expression was inhibited. N treatments combined with AVG had a small effect on NH_4NO_3 induced *BSP* expression while glutamine induced expression was enhanced by AVG treatment (Figure 3-7C). The difference between AVG modulation of NH_4NO_3 and glutamine induced *BSP* expression may be related the role that glutamine as the major transport amino acid from senescing leaves to bark as opposed to NH_4NO_3 (Couturier et al., 2010a; Sauter and van Cleve, 1992; Schneider et al., 1994; Wildhagen et al., 2010).

ACC and ethephon inhibition of BSP expression is reduced in transgenic poplar expressing the *Arabidopsis etr1-1* allele

To further investigate the role of ethylene-sensing and signaling in regulating *BSP* expression we used transgenic *Populus tremula* x *tremuloides* genotype T89 transformed with the dominant gain-of-function allele of *Arabidopsis etr1-1* (Love et al., 2009). When wild-type (T89) and etr1-1 transgenic plants (1E) were treated with 100μM ACC *BSPA* expression was reduced by 83% in wild type plants but only 47% in transgenic plants (Figure 3-8A). *BSPB* was reduced by 66% in wild-type plants while no significant reduction was observed in transgenic plants (Figure 3-8B). In the case of *BSPC*, expression was reduced by 85% with ACC treatment in wild-type plants but only 47% in transgenic plants (Figure 3-8C). When these plants were fed with ethephon instead of ACC a similar trend was observed

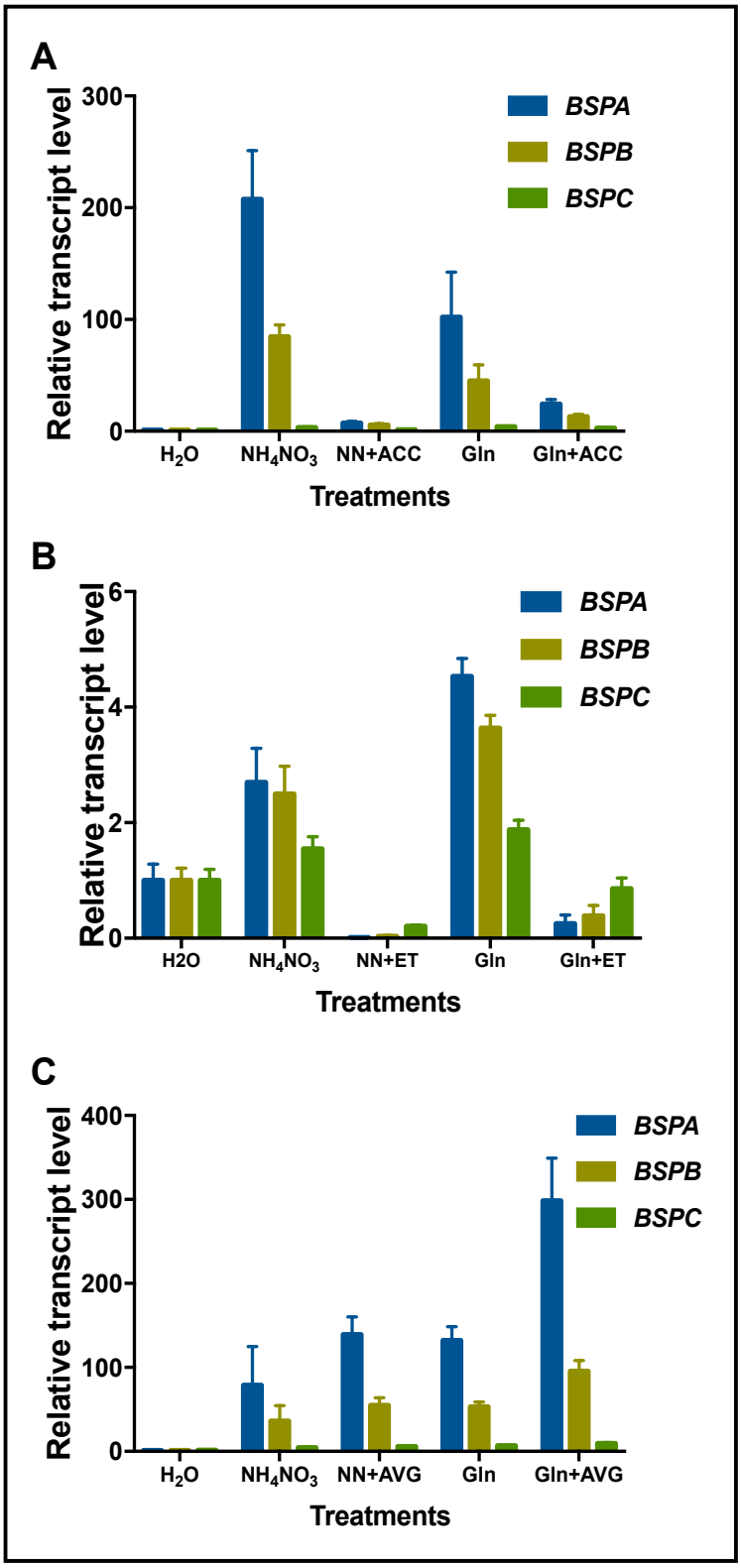

Figure 3-7. ACC and ethephon inhibit N-induced *BSP* expression. Relative transcript level of *BSP* genes in bark of stems fed with either 20mM NH_4NO_3 or 25mM glutamine with or without (A) 100µM ACC, (B) 100 µM ethephon, or (C) 2µM AVG for 24h. Relative transcript levels were determined by qRT-PCR.

where *BSPA* (Figure 3-9D), *BSPB* (Figure 3-9E) and *BSPC* (Figure 3-9F) expression was reduced to a lesser extent in transgenic plants compared to wild-type plants. These results suggest that ethylene sensing by ETR1 and ethylene signaling are likely to be involved in the repression of *BSP* expression by ethylene.

Glutamine-induced BSP expressed is enhanced in transgenic poplar expressing the *Arabidopsis etr1-1* allele

Since feeding poplar stems ACC or ethephon inhibited glutamine-induced *BSP* expression (Figure 3-7) we wanted to determine if glutamine-induced expression was altered in the *etr1-1* transgenic poplars. Glutamine induced *BSPA* expression was greater in the *etr1-1* transgenic poplars than the wild-type plants (6.85 fold versus 5.19 fold) (Figure 3-9A). *BSPB* did not increase in wild type plants yet significant increase occurred in the transgenic plants (1.26 fold increase) (Figure 3-9B). The increase in *BSPC* expression was similar between the two genotypes (4.24 fold for wild-type versus 4.51 fold for *etr1-1* transgenic) (Figure 3-9C). The lack of glutamine induction of *BSPB* is in contrast to our previous results and may be a consequence of the genetic background since *Populus tremula* x *tremuloides* genotype T89 was used in this experiments while the other feeding experiments in this study used *Populus trichocarpa* (Nisqually), yet both *BSPA* and *BSPC* did show glutamine-induced expression in the *Populus tremula* x *tremuloides* genotype T89. These results suggest that at least for *BSPA* that glutamine-induced expressed is enhanced when ethylene perception and signaling is altered by expressing *Arabidopsis etr1-1*.

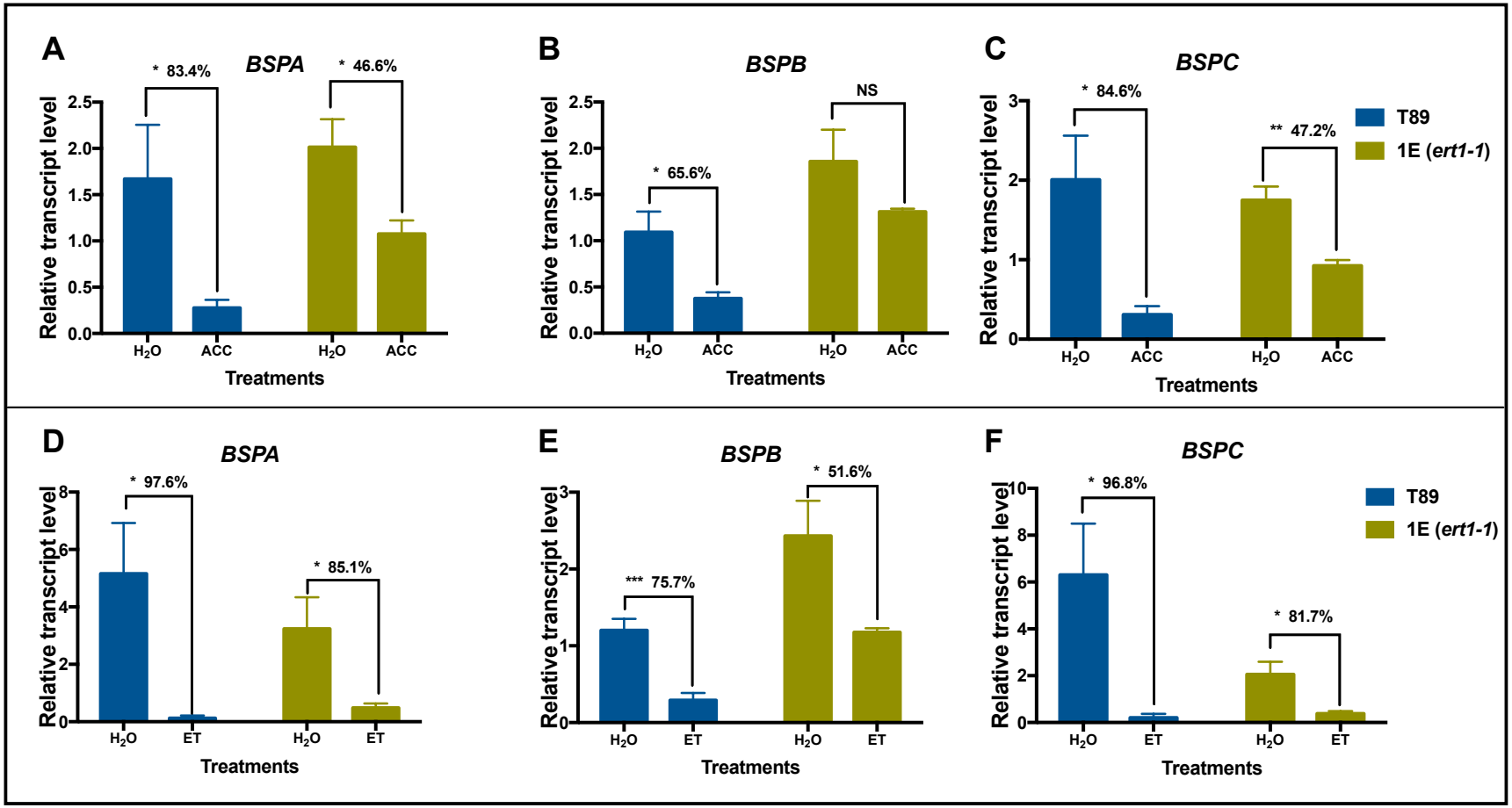

Figure 3-8. Inhibition of *BSP* expression is reduced in transgenic poplars expressing the *Arabidopsis etr1-1* allele. Relative transcript levels of *BSPA*, *BSPB* and *BSPC* in the bark of stems of control (T89) and transgenic (1E) plants fed either (A-C) 100μM ACC, or (D-F) 100 μM ethephon for 24h. * indicates means significantly different from control at $p<0.05$, ** for $p<0.01$ and NS for no significance, ET signifies ethephon. The percentage difference is calculated by $(Value_{H2O}-Value_{ACC})/ Value_{H2O}$ or $(Value_{H2O}-Value_{ET})/ Value_{H2O}$.

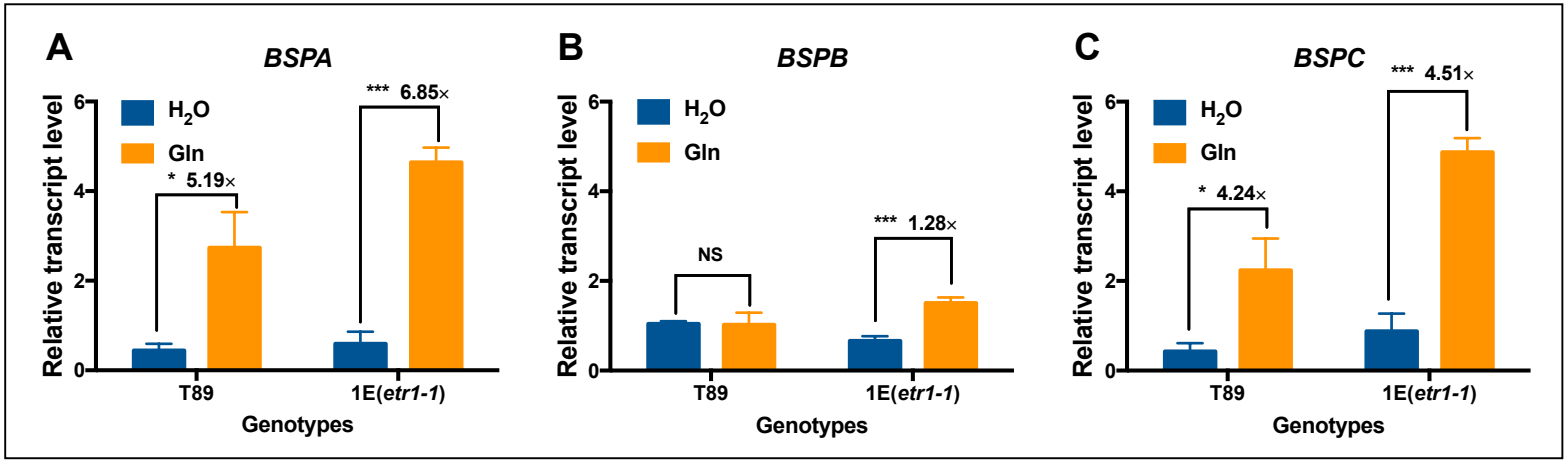

Figure 3-9. Glutamine-induced *BSP* expression in transgenic poplars expressing the *Arabidopsis* etr1-1 allele. Relative transcript levels of (A) *BSPA*, (B) *BSPB*, (C) *BSPC* in the bark of stems of control (T89) or transgenic (1E) plants fed with 20mM glutamine after 24h of feeding. * indicates means significantly different from control at $p<0.05$, *** for $p<0.001$ and NS for no significance. Numbers above each genotype represents the increase under glutamine treatment compared to water ($Value_{Gln}$-$Value_{H2O}$)/ $Value_{H2O}$).

Transient expression of ERF12 and ERF41 in tobacco transformed with a BSPApromoter::GUS chimeric gene results in increased GUS activity

The prior results indicate that ethylene signaling is involved in regulating *BSP* expression. Sequence analysis of the 5' upstream regions of the three *BSP*s revealed the presence of the DRE ethylene response element consensus sequence CCGAC (Liu Mingchun et al., 2018) in the promoter region of all three *BSP*s (Figure 3-10A). The locations and number of DRE elements varied among the three genes with *BSPA* possessing one copy, *BSPB* possessed 4 copies while *BSPC* contained 9 copies. It is interesting to note that in *Populus trichocarpa* (Nisqually) that the 3 *BSP*s are expressed at different levels during SD (Pettengill et al., 2013) with *BSPA>BSPB>BSPC*, thus there seems to be a negative correlation between the number DRE elements and the level of SD expression.

Gene expression analysis of both *ERF12* and *ERF41* by qRT-PCR was consistent with DNA microarray data (Figure 3-2 and 3-3) where SD treatments induced expression, however the qRT-PCR analysis revealed that induction of *ERF41* was more rapid than *ERF12* and reached a greater relative level of expression (Figure 3-10B). To determine whether ERF12 and ERF41 were targeted to the nucleus, a full-length cDNA was fused with a C-terminus EGFP tag. The vectors were then transiently expressed in tobacco leaves and subcellular localization was determined by confocal microscopy. We found that each of the *ERF*s localized to the nucleus based on colocalization with DAPI staining (Figure 3-10C). We also determined if transient expression of each of the *ERF*s in tobacco transformed with *BSPA*-

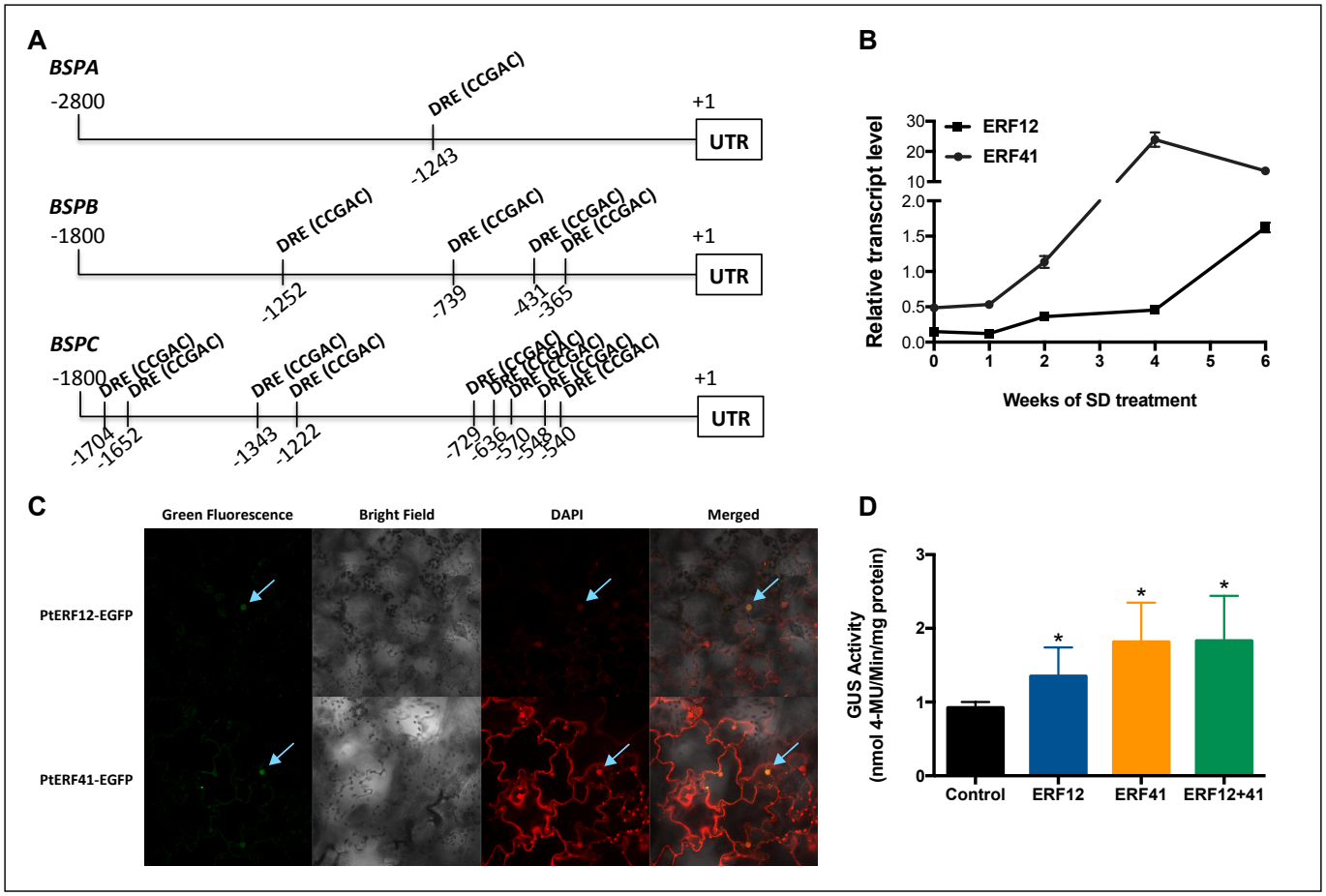

Figure 3-10. *ERF12* and *ERF41* serve as positive regulators of *BSP* expression. (A) Diagram of DRE (CCGAC) elements in the 5' upstream regions of *BSPA*, *BSPB* and *BSPC*. (B) Relative transcript level of *ERF12* and *ERF41* in bark of SD treated plants over a 6-week period as determined by qRT-PCR. (C) Subcellular localization of EGFP tagged ERF12 and ERF41 in transfected tobacco leaves visualized by confocal microscopy. (D) Induction of GUS activity in transfected leaves of tobacco plants transformed with *BSPA*-promoter::uidA. GUS activity was determined 3 days after transfection. * indicates means significantly different from control at $p<0.05$.

promoter::uidA would resulted in increased levels of GUS activity and found when each of the *ERF*s either alone or together were transfected into tobacco leaves, increased GUS activity was detected (Figure 3-10D). Transfection with *ERF41* tended to produce greater increases in GUS activity than *ERF12* and co-transfection with both was similar to *ERF41*. Therefore, it appears that these two ERFs can activate transcription via the *BSPA* promoter. Since they are both SD-induced, it is possible that they may act as positive regulators of *BSP* expression during SD.

Glutamine synthetase genes are differentially expressed in bark and leaves during SD treatment

Glutamine is the primary amino acid that is transported from senescing leaves to bark during autumn (Couturier et al., 2010a; Sauter and van Cleve, 1992; Schneider et al., 1994; Wildhagen et al., 2010). Because of the important of glutamine to remobilization of N from leaves to bark, the dynamics of glutamine synthetase gene expression was examined in leaves and bark of SD-treated plants. Transcript levels for 3 genes encoding the cytosolic isoform, GS1, as well as a plastid isoform, GS2, all increased in leaves after 4 weeks of SD treatment (Figure 3-11). In bark, the expression of only 2 of the GS1 genes, GS1.1 and GS1.3 increased in SD (Figure 3-11A & C) while GS1.2 and the GS2 changed little over the same time interval (Figure 3-11B and D). Therefore, GS gene expression differs between bark and leaves during SD which may reflect specialization associated with N sink status whereby leaves act as N sources while bark is an N sink.

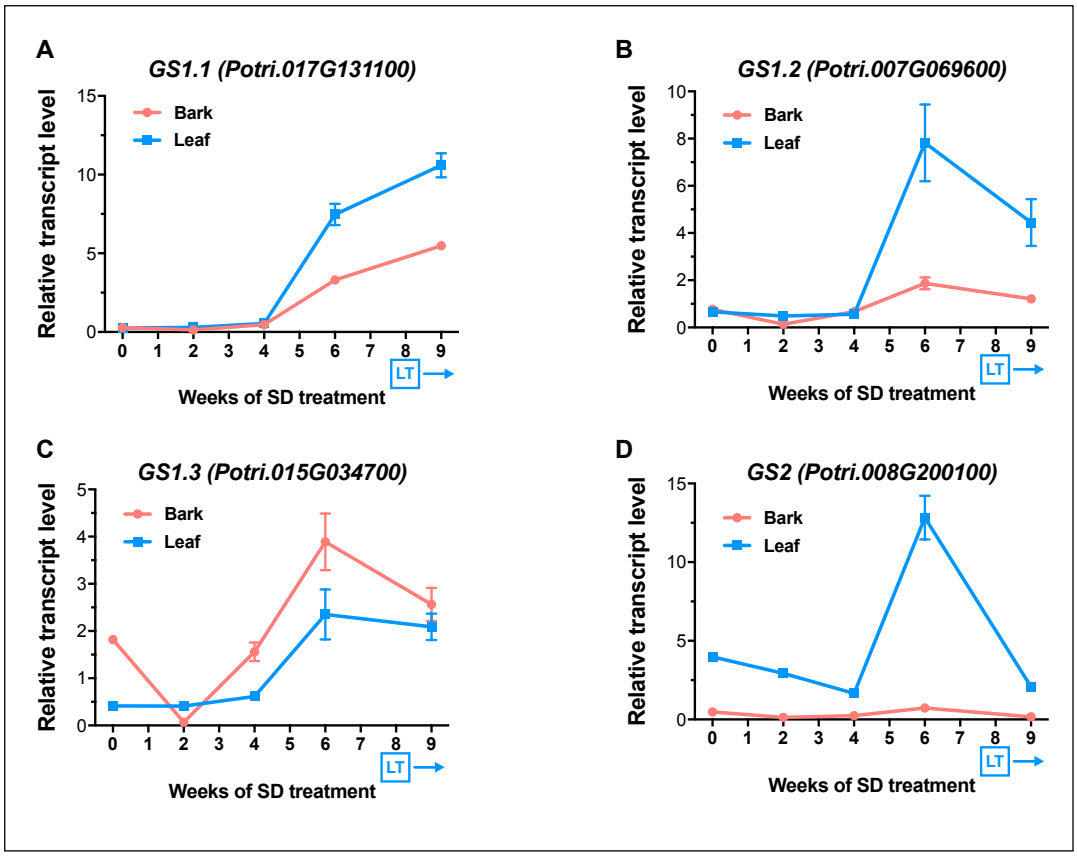

Figure 3-11. Differential expression of glutamine synthetase genes (GS) in leaves and bark during SD treatment. Relative transcript level of GS genes in leaf (blue) and bark (red) during 9 weeks of SD treatment where the last week was supplemented with LT.

Discussion

N partitioning from source to sink is influenced by multiple factors including N uptake, N metabolism in source organs, source strength, and sink status and strength (Tegeder and Masclaux-Daubresse, 2018). In temperate deciduous trees when the day length becomes shorter in autumn growth cessation and leaf senescence is triggered as well as the development of bark into an N sink. However, the mechanisms of bark N sink establishment induced by SD are poorly understood in trees. The establishment of bark as an N sink would be necessary for the translocation of N from leaves to bark. In poplar seasonal N cycling, N sink development involves changes in vegetative growth rather than reproductive growth

(Babst and Coleman, 2018). Thus, it is likely that the development of vegetative N sinks differs in trees compared to annual plants where N sink establishment is driven by reproductive development. BSPs which accumulate in bark during autumn are likely to major factors that establish bark as a N sink since these proteins account for up to 62% of total soluble bark protein during dormancy in autumn and winter (Coleman et al., 1991a). In this study, we attempted to gain insight into the regulatory factors that govern BSP accumulation to further advance our understanding of vegetative N sink development in trees.

Because SD photoperiod is the major environmental cue for BSPs accumulation in poplar bark (Black et al., 2001; Coleman et al., 1991a, 1992; Pettengill et al., 2013; Zhu and Coleman, 2001a, 2001b) we hypothesized that induction of *BSP* expression would be necessary for sink development prior to leaf senescence. To test this hypothesis, the timetable of leaf senescence during SD treatment was examined in relation to the timing of *BSP* expression. We found that bark *BSP* expression preceded leave senescence, based on the timing of leaf chlorophyll degradation and the expression of senescence-associated genes (Figure 3-1). The majority of studies related to leaf senescence in poplar have been performed outdoors making direct comparisons with our results difficult. A study of the timetable of poplar leaf senescence (Fracheboud et al., 2009) showed that in Sweden critical photoperiod for bud set and growth cessation occurred around July 20th with bud formation occurring around August 10th. Leaf senescence did not begin until a month later around September 10th. Although this study did not examine N storage, it is likely that BSP gene expression and accumulation also preceded the beginning of

leaf senescence. As we show in this study, *BSP* expression begins to increase after 3 weeks of SD treatment while leaf senescence occurred after 8 weeks of SD treatment when LT was added to the SD photoperiod. Therefore, the induction of *BSP* expression appears to be independent of leaf senescence which suggests that N export from leaves is not necessary for induction of *BSP* expression. However, we can't rule out that N export from the leaves occurs prior to measurable changes in leaf senescence. Thus the regulation of *BSP* expression may involve a signal different than leaf N export. Intuitively this makes sense since *BSP* expression and BSP accumulation may be necessary to establish bark N sink strength as a driving force for N transport from leaves.

In some tree species, xylem development is more sensitive than phloem to environmental stresses (Bannan, 1955). The xylem to phloem ratio usually declines when growth condition becomes unfavorable (Bannan, 1955). Several studies have also reported a circadian rhythm to ethylene production that peaks during the day and then declines during the night (Finlayson et al., 1998; Jasoni et al., 2000; Thain et al., 2004). Ethylene also stimulates cambium cell division and xylem growth in poplar (Junghans et al., 2004; Love et al., 2009) and genes encoding ethylene biosynthetic enzymes and ethylene responsive ERFs are expressed in wood tissues of poplar (Andersson-Gunnerås et al., 2003; Vahala et al., 2013). Gene expression networks centered around *EIN3D* and 11 *ERFs* during wood formation also support a role for ethylene signaling in xylem development (Seyfferth et al., 2018). Furthermore, photoperiod can also impact wood formation (Petterle et al., 2013), yet a relationship between photoperiod, xylem development and ethylene is lacking. The results

presented here show that stem ethylene production, expression of ethylene biosynthetic genes and components of ethylene signaling are influence by photoperiod (Figure 3-5). It may be possible that reduced ethylene production and signaling during SD may contribute to the negative regulation of xylem development that in turn could impact the transport of N and other nutrients to leaves affecting source-sink interactions.

Exogenous treatment of poplars with methyl jasmonate also induces *BSP* expression and GA treatment inhibits expression which may involve interactions with N source-sink status (Beardmore et al., 2000; Zhu and Coleman, 2001a). Since the endogenous levels of JA and GA have not been determined in relation to SD-induced *BSP* expression it is unknown if these phytohormones also play a role in ethylene-mediated *BSP* expression. However, analysis of the bark SD microarray data did not reveal an enrichment in genes associated with either JA or GA signaling suggesting these hormones are unlikely to play a major role in regulating SD-induced *BSP* expression.

Expression of poplar *BSPs* were found to be repressed within 1 h of ACC treatment in excised stem feeding experiments while ethylene-inducible *ERF*s (Vahala et al., 2013) were induced (Figure 3-6A and B). Furthermore, both ACC and ethephon treatment reduced *BSP* expression while the ethylene biosynthesis inhibitor AVG induced expression (Figure 3-6C). Using transgenic poplars with altered ethylene sensing and signaling via expression of the dominant gain-of-function *etr1-1* allele of Arabidopsis, we also found that ACC and ethephon inhibition of *BSP* expression was reduced (Figure 3-8). Although these results do not conclusively

establish that ethylene is an endogenous regulator of photoperiod-regulated *BSP* expression, they are consistent with this possibility. Further studies involving perturbation of ethylene signaling are necessary to further establish a role, but this may be limited by available methods (lack of forward genetics) and functional redundancy in poplar. However, even with these limitations, these results show for the first time the possible role of ethylene in regulating *BSP* gene expression and seasonal N cycling.

BSP gene expression is also induced by stem feeding N compounds NH_4NO_3 and glutamine (van Cleve and Apel, 1993; Coleman et al., 1994; Zhu and Coleman, 2001a). In the current study, we also found that feeding stems either ACC or ethylene could repress the induction of *BSP* expression by NH_4NO_3 or glutamine while AVG enhanced glutamine induced expression but had no effect on NH_4NO_3 induced expression (Figure 3-7). In addition poplar transformed with *Arabidopsis etr1-1* also showed enhanced *BSP* with glutamine feeding (Figure 3-9). The differences between NH_4NO_3 and glutamine induction when combined with AVG are not unexpected and could likely be a consequence of repression of either nitrate reductase, nitrate reductase and/or glutamine synthetase activity. This also suggests that NH_4NO_3 induction may actually occur via glutamine, yet more research is needed to determine if this is the case.

Since it appears that ethylene sensing and signaling are involved in the negative regulation of *BSP* gene expression in poplar bark, it would be informative to identify the signaling components regulating *BSP* gene expression. Promoter analyses indicated that the presence of the DRE ethylene response elements in *BSPA*, *BSPB*

and *BSPC* and the number of this element for each gene varied (Figure 3-10A). Interestingly the most highly expressed gene, *BSPA*, only possesses 1 copy of the element while the *BSPC* gene whose expression pattern differs for both *BSPA* and *BSPB* (Pettengill et al., 2013) contained the greatest number of copies (9 copies). The possible functional significance of these differences is not known but could be the basis for the difference in the expression patterns between these genes.

ERFs are components of the ethylene signaling pathways and recent studies suggest a broad regulatory role of poplar ERFs in root growth and development (Trupiano et al., 2013), stem growth and wood formation (Vahala et al., 2013), mutualistic symbiosis (Plett et al., 2014) and stress tolerance (Yao et al., 2016, 2017). We found a total of 80 *ERFs* expressed during SD treatment in bark based using DNA microarrays. For the vast majority of these *ERFs* their expression changed little compared to LD treated bark and only 15 *ERFs* were differentially expressed (log_2-fold ≥ 2 and p value ≤0.01). Among these *ERFs*, *ERF12* and *ERF41* were the two most highly induced among all the *ERFs* and other transcription factor families. Since the gene expression of these two *ERFs* are repressed by ethylene treatment (Vahala et al., 2013) combined with their increased expression in SD make them excellent candidates as regulators of *BSP* expression. These two ERFs were further found to be localized to the nucleus in transfected tobacco leaves, and transient expression of *ERF12*, *ERF41* or co-expression *ERF12* and *ERF41* enhanced the transcriptional activity of *BSP*A promoter::GUS gene in the stably transformed tobacco (Figure 3-10C and D). Together these results suggest that *ERF12* and *ERF41* may be positive regulators of SD-induced *BSP* expression. Since these expression of

these two ERF's is repressed by ethylene, the inhibition of *BSP* expression in LD-bark may be mediated by ethylene repression of *ERF12* and *ERF41* while during SD bark ethylene levels decline allowing for the derepression of *ERF12* and *ERF41* which in turn activates *BSP* expression.

The role of photoperiod perception in *Populus* growth cessation and bud set is well established (Howe et al., 1996; Olsen et al., 1997). Of particular note is the crucial role of SD photoperiod in BSP accumulation and N storage (Black et al., 2001; Coleman et al., 1991a, 1992; Langheinrich and Tischner, 1991; Pettengill et al., 2013; Zhu and Coleman, 2001a, 2001b). In this study we uncovered that ethylene signaling likely to be involved in SD-induced BSP accumulation in poplar bark through inhibition of ethylene production by SD which appears to links photoperiod, ethylene signaling and *BSP* expression.

Recent research suggests that PIF4 and PIF5 are involved in the regulation of ethylene biosynthesis by mediating transcription of *ACS* genes, and they can also activate *EIN3* expression by direct binding to the promoter of *EIN3* in Arabidopsis (Khanna et al., 2007; Sakuraba et al., 2014; Song et al., 2014). Moreover, phytochrome B (phyB) has been shown to regulate degradation of EIN3 by $SCF^{EBF1/EBF2}$ E3 ligases via direct interaction with EIN3 and enhanced association of phyB, EIN3 and EBF1/EBF2 proteins (Shi et al., 2016). Although there are no mechanistic findings for how SD photoperiod regulates ethylene production in poplar so far, previous studies revealed are role for phytochrome in regulation of the expression of *BSP*s by SD photoperiod (Langheinrich and Tischner, 1991; Zhu and Coleman, 2001a). Taken together, we propose that photoperiod regulates the

expression of *BSP*s via modulation of ethylene production and signaling by phytochrome (and PIFs). A possible model of this mechanism (Figure 3-12) involves LD ethylene production and activation of the ethylene signaling pathway. EIN3 could potentially act as a repressor of *ERF12* and *ERF41* expression which blocks *BSP* expression. In SD conditions, ethylene production declines and the ethylene signaling pathway is repressed resulting altered EIN3 repression of ERF12 and *ERF41* expression which in turn activates *BSP* expression.

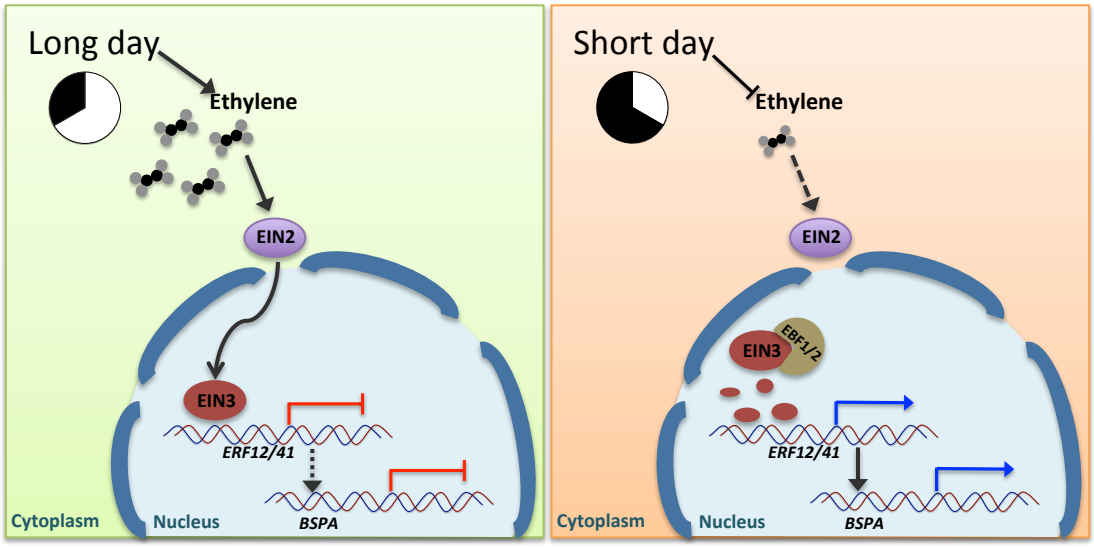

Figure 3-12. Theoretical model illustrating how photoperiod and ethylene signaling may regulate *BSP* expression. In long day condition, ethylene content is abundant in poplar bark, and ethylene signaling is transduced into nucleus to repress the expression of *BSPs* by inhibiting the expression of positive regulators *ERF12* and *ERF41*. However, in short day condition, the ethylene production is repressed in poplar bark, and thus ethylene signaling transduction is inactivated, which activates the expression of *BSPs* by de-repressing the expression of positive regulators *ERF12* and *ERF41*.

Chapter 4: The PII glutamine sensor plays a role in glutamine mediated BSP expression in poplar trees

Abstract

Seasonal N cycling is fundamental to the perennial lifestyle of *Populus* (poplars) and other tree species. Poplar seasonal N cycling involves the accumulation of Bark Storage Proteins (BSPs) in bark phloem parenchyma during autumn. This reallocation of N involves glutamine transport from senescing leaves to bark with glutamine serving as the primary N source for BSP synthesis. Previous research has suggested that in addition to serving as a source of N for BSP synthesis, glutamine may also serve as a metabolic signal regulating N storage. In the research presented here, we investigated the possible role of the PII sensor, a central integrator of cellular carbon and nitrogen metabolism, in glutamine mediated *BSP* expression. We found that *PII* expression was enhanced in poplar bark during SD-induced leaf senescence and was accompanied by increased expression of genes involved in arginine production. PII-RNAi knockdown poplars were altered in glutamine-mediated responses including anthocyanin accumulation and *BSP* expression. Further, 2-oxoglutarate (2-OG), which antagonizes PII interactions with NAGK, reduced glutamine-induced *BSP* expression. The results of this study suggest that PII is likely to play a role in sensing glutamine transported from senescing leaves during leaf N

remobilization to bark. This further supports the role of glutamine as both a metabolic signal and N source in seasonal N cycling of poplar.

Introduction

One of the crucial processes associated with perennial plants is the seasonal cycling of nitrogen (N) (Rennenberg and Schmidt, 2010). Temperate tree N dynamics involve a number of processes including 1) N uptake and assimilation from the soil, 2) N transport and assimilation associated with demands of plant growth and development, 3) N redistribution from leaves during senescence and storage in perennial sink tissue and 4) N remobilization mediated by proteolysis and transport from N storage tissue. Acentral feature of seasonal N dynamics in *Populus* is the autumn accumulation of Bark Storage Proteins (BSP) (Babst and Coleman, 2018; Cooke and Weih, 2005; Millard and Grelet, 2010).

Transient increases in stem glutamine levels peak during autumn leaf senescence and then again during spring N remobilization correlating with major developmental processes during the annual growth cycle of poplar (Sauter and Cleve, 1992; Wildhagen et al., 2010). These peaks in stem glutamine levels are indicative of autumn N transport from leaves to bark and spring remobilization from bark to growing shoots. During autumn senescing leaves become N sources that accumulate glutamine (Couturier et al., 2010a) that is transported via the phloem to bark which acts as an N sink (Babst and Coleman, 2018; Millard et al., 2006a; Sauter and van Cleve, 1992; Schneider et al., 1994; Wildhagen et al., 2010). Besides being a N source for the synthesis of BSP, glutamine also seems to act as metabolic signal

inducing the expression *BSP* (Babst and Coleman, 2018; Zhu and Coleman, 2001a). Therefore, glutamine transport and signal sensing mechanisms could be important regulatory processes in season N cycling.

The conserved family of PII nutritional signaling proteins occurs in bacteria, archaea and plants (Chellamuthu et al., 2013; Leigh and Dodsworth, 2007; Sant'Anna et al., 2009; Uhrig et al., 2009). Plant PII are conserved ~15 kDa proteins that form a ~45 kDa homotrimeric complex (Chellamuthu et al., 2013; Leigh and Dodsworth, 2007; Sant'Anna et al., 2009; Uhrig et al., 2009). Besides their role in sensing cellular C and N balance, PII signaling proteins are also involved in protein interactions with metabolic enzymes, signal transduction proteins, transcription factors and metabolite transporters (Leigh and Dodsworth, 2007; Osanai and Tanaka, 2007; Uhrig et al., 2009). PII C/N sensing involves ATP and 2-oxoglutarate binding to PII homotrimers to produce distinct PII conformations (Fokina et al., 2010; Forchhammer, 2008; Huergo et al., 2013; Zeth et al., 2014). A protruding T loop for each subunit is involved in ligand binding and receptor interactions (Forchhammer, 2008; Huergo et al., 2013). Structural analysis reveal feedback inhibition by arginine of the trimeric PII sensors is alleviated by interact with hexameric N-acetyl glutamate kinase (NAGK) (Chellamuthu et al., 2014; Llácer et al., 2007, 2008; Mizuno et al., 2007a, 2007b; Ramón-Maiques et al., 2006). While most plant PII proteins possess a C-terminal extension, or Q loop, which is required for glutamine binding, this extension is absent in archaea, bacteria and red algae (Uhrig et al., 2009). Alleviation of feedback inhibition by arginine involves interaction of trimeric P_{II} with hexameric NAGK facilitated by the Q-loop (Chellamuthu et al., 2014). Although most plant PII

proteins possess the C-terminal Q loop extension, it is notable that the *Brassicaceae* P_{II} sensors, including that from *Arabidopsis*, lack part of the plant-specific C-terminal extension that comprises the glutamine binding loop (Chellamuthu et al., 2014), yet the *A. thaliana* PII retains the ability to bind NAGK and regulate enzyme activity.

Arabidopsis AtGLB1 was first plant PII identified and cloned (Hsieh et al., 1998). In *Arabidopsis*, *AtGLB1* expression was induced by light and sucrose and repressed by glutamine and glutamate (D'Apuzzo et al., 2014; Hsieh et al., 1998). A transcription factor WRI1 directly binds the promoter of *AtGLB1* and controls its transcription activity (Baud et al., 2010). PII knock-out mutants did not differ from wild-type plants in growth and developmental phenotypes in non-limiting growth conditions but did show a greater sensitivity to nitrite even though no differences in NiR activity was observed, prompting Ferrario-Méry et al., (2005) to suggest that PII lacks a crucial role in plant growth and development. Furthermore, reduced ornithine, citrulline and arginine levels were also observed in PII knock-out mutants in response to NH_4^+ following N starvation, yet none of the genes in the arginine biosynthetic pathway were differentially expressed suggesting that the loss of PII likely reduced the activation of NAGK (Ferrario-Méry et al., 2006). *Arabidopsis* overexpressing PII also accumulate greater levels of anthocyanins at elevated C/N ratios and alleviation of anthocyanin accumulation by Gln was less effective compared with wild type plants (Hsieh et al., 1998). *Arabidopsis* and rice PII interacts with chloroplast-localized NAGK in the presence of Mg-ATP which catalyzes a regulatory step of arginine biosynthesis (Chen et al., 2006; Feria Bourrellier et al., 2009; Sugiyama et al., 2004). This interaction relieved the inhibition of NAGK, activating downstream

biosynthesis of ornithine and arginine. The PII-NAGK interaction was antagonized by binding of either 2-oxoglutarate (2-OG), arginine, glutamate, citrate and oxaloacetate (Feria Bourrellier et al., 2009). In addition to NAGK, PII was also found to interact with ACCase, a key enzyme of biosynthesis of fatty acids in plastids, and inhibited chloroplastic ACCase activity (Bourrellier et al., 2010). In *Lotus japonicus*, *PII* expression is also regulated by light-dark cycles and plays a role in nitric oxide production, nodule formation, and stomatal closure (D'Apuzzo et al., 2014; Parlati et al., 2017).

Because of the role of glutamine as both a metabolite and signaling molecule during poplar seasonal N cycling, we investigated the possible role of PII as a glutamine sensor in this process. We found that increased bark PII expression coincided with leaf senescence. Using transgenic PII RNAi knockdown poplars we found changes in both the rate of root growth and anthocyanin accumulation. Furthermore, NH_4NO_3 and glutamine- induced *BSP* expression was reduced in PII RNAi knockdown poplars. Further, glutamine-induced *BSP* expression was reduced by the PII-NAGK binding inhibitor 2-OG. We propose that PII functions as a glutamine sensor in poplar and plays a role in glutamine-mediated *BSP* expression.

Materials and methods

Plant materials and growth conditions

Two poplar genotypes, *Populus trichocarpa* (Nisqually) and the *Populus tremula* × *P. alba* hybrid clone INRA 717-1B4 were used in this study. Nisqually was used in all short-day (SD) photoperiod and low temperature (LT) experiments in controlled environmental chambers. For these experiments Nisqually plants were first grown in

long-day (LD) condition (16h light/8h dark) at 20°C for 8 weeks. After 8-weeks growth in LD, SD treatments were conducted by changing the photoperiod to SD (8h light/16h dark) for 6 weeks at 20°C. LT treatments involved reducing the temperature during SD to 10°C day/4°C night for additional 4 weeks following the initial 6 week SD treatment. Bark and leaf samples were harvested at weekly intervals, immediately frozen in liquid N and then stored at -80°C until used for further analysis. The wild type (*Populus tremula* × *P. alba* hybrid clone INRA 717-1B4) and *PII*-RNAi lines PR1-2 and PR1-6 were grown in LD condition (16h light/8h dark) at 20°C at different N level (0.2mM, 2mM or 20mM NH_4NO_3) for 8 weeks. Leaf area by leaf position and plant height was measured.

Generation of PII–knockdown transgenic poplar

A 216 bp poplar *PII* (Potri.002G191300) cDNA fragment was amplified with the forward primer 5'-CACCGTGGCTCAGAGTTTTCCGAAG-3'and reverse primer 5'-ACCCTCCTGTCATCCTTTCAGC-3'. The cDNA fragment was cloned into pENTR D-TOPO entry vector using pENTR™ Directional TOPO Cloning Kits following the manufacturer's instructions (Invitrogen, Life Technologies). Plasmids were transformed into *E. coli* (DH5α) and plated on LB media supplemented with 50 mg/l kanamycin. Colonies were selected and the insert was verified by PCR and the cDNA sequenced then verified by DNA sequencing (Macrogen). Plasmids in the pENTR D-TOPO entry vector containing correct cDNA sequences were mobilized to the Gateway binary vector pH7GWIWG2(II) (Karimi et al., 2002) using Gateway LR Clonase II enzyme mix (Invitrogen by Life Technologies) following the manufacturer's instructions. Following the Clonase reaction, plasmids were

transformed to *E. coli* (DH5α) and grown on LB plates supplemented with 75 mg/l spectinomycin. Colonies were selected and the plasmid DNA purified, the insert size determined by PCR and the DNA sequence verified by DNA sequencing. The correct destination clone was transformed into *Agrobaterium tumefaciens* strain C58/PMP90 using heat-shock method. Agrobacterium transformants were selected on LB media using 20µg/mL gentomycin and 50µg/mL spectinomycin. 25ml of Agrobacteria culture previously transformed with destination clone was grown overnight at 28 °C, 200 rpm for use in transformations.

Populus alba x tremula clone 717-1B4 initially transformed with a *BSPA* promoter::GUS (basta resistant) were used for transformation as described previously (Leple et al., 1992). Transformed shoots were selected by regeneration on media containing 5mg/L Basta and 20mg/L hygromycin. The rooted plants were propagated and used for further analysis. Regenerated lines were verified by qRT-PCR with the forward primer 5'-AGTCTCGCAAGTTTCCTCGG-3' and reverse primer 5'-TGCCTCTCCTTTGAACCACC-3'.

Excised stem feeding

Nisqually stems approximately 50 cm in length were removed from LD grown greenhouse stock plants and immediately placed in water. All but the apical 5 leaves were subsequently trimmed from the shoots and a fresh cut was made at the stem base and the stems were immediately placed in 500ml flasks filled with 400ml H_2O for 24h in a controlled environmental chamber with continuous light at 20°C. After the 24h pre-incubation period cuttings were transferred to a 500ml flask containing 400ml of 25mM glutamine (Sigma, St. Louis MO), 5mM 2-oxoglutarate (Sigma, St.

Louis MO) or 50μM or 500μM sodium nitroprusside (SNP) (Sigma, St. Louis MO) depending on the experiment. After 24h of treatment, bark tissue was collected and immediately frozen in liquid N and then stored at -80 °C until used for RNA purification. The same procedure was used for handling excised stems of the wild type (*Populus tremula* × *P. alba* hybrid clone INRA 717-1B4) and *PII*-RNAi lines for the treatment with 2mM and 20mM NH_4NO_3, 25mM glutamine and 25mM arginine (Sigma, St. Louis MO) for 24h. The bark tissue were collected and immediately frozen in liquid N and then stored at -80 °C until used for RNA purification.

Measurement of anthocyanin content

Approximately 20-25 leaf discs were collected, weighed and placed in a vial containing 5mL of methanol with 1% HCl (v/v) for each sample. They were sealed and incubated in darkness at 4°C for 24 h with shaking (at 100 rpm). After 24 h of extraction, the samples were then centrifuged and the supernatant was measured at 530nm and 657nm as described previously (Kim et al., 2017; Rabino and Mancinelli, 1986). The content of anthocyanin was expressed using A_{530}-0.25*A_{657} per gram of fresh weight.

RNA extraction and qRT-PCR

Total RNA was extracted from bark tissue using Qiagen RNeasy plant mini kit (Qiagen, USA) and a Qiacube with modifications and on-column DNA digestion as described by Pettengill et al. (2012). The purified RNA was used for cDNA synthesis using iScript™ cDNA Synthesis Kit according to manufacturer's instructions (Bio-Rad, Hercules CA). The cDNA was used for determination of relative transcript level

of target genes using qRT-PCR. Amplification reactions consisted of 30 sec at 95 °C followed by 40 cycles of 5 sec at 95 °C and 15 sec at 60 °C. Reference gene and relative expression analysis was performed using qbasePLUS as previously described (Pettengill et al., 2012). All qRT-PCR primers for target genes and reference genes (Table S4-1.) were designed and validated as previously described (Pettengill et al., 2012).

Results

Expression of PII and arginine biosynthesis genes increase in bark during leaf senescence

Since SD triggers leaf senescence and nitrogen remobilization to bark via glutamine transport we first determined if *PII* expression in bark and leaves changed in SD. To determine this we treated *Populus trichocarpa* (Nisqually) with SD photoperiod in 20 °C for 8 weeks followed by an additional 4 weeks at low-temperature (LT) (10°C/4 °C; day/night) to induce leaf senescence and then examined PII expression at weekly intervals in both leaves and bark (Figure 4-1). Leaf transcript levels of *PII* changed little during leaf senescence and tended to decline in abundance (Figure 4-1A). This same pattern was also observed for genes encoding enzymes (NAOD: *N*-acetylornithinedeacetylase; OTC: Ornithine transcarbamoylase; AL: Argininosuccinate lyase) in the arginine biosynthesis pathway (Figure 4-1B-D). As opposed to leaves, bark levels of *PII* transcripts increased steadily during SD and LT accelerated this increase (Figure 4-1A). A pattern similar to *PII* expression was found for bark expression of genes encoding NAOD, OTC and AL (Figure 4-1B-D).

Thus *PII* expression as well as the expression of genes in the arginine pathway are differentially expressed between bark and leaves and bark expression coincides with leaf senescence and bark expression of *PII* and genes in the arginine pathway appear to be coordinated.

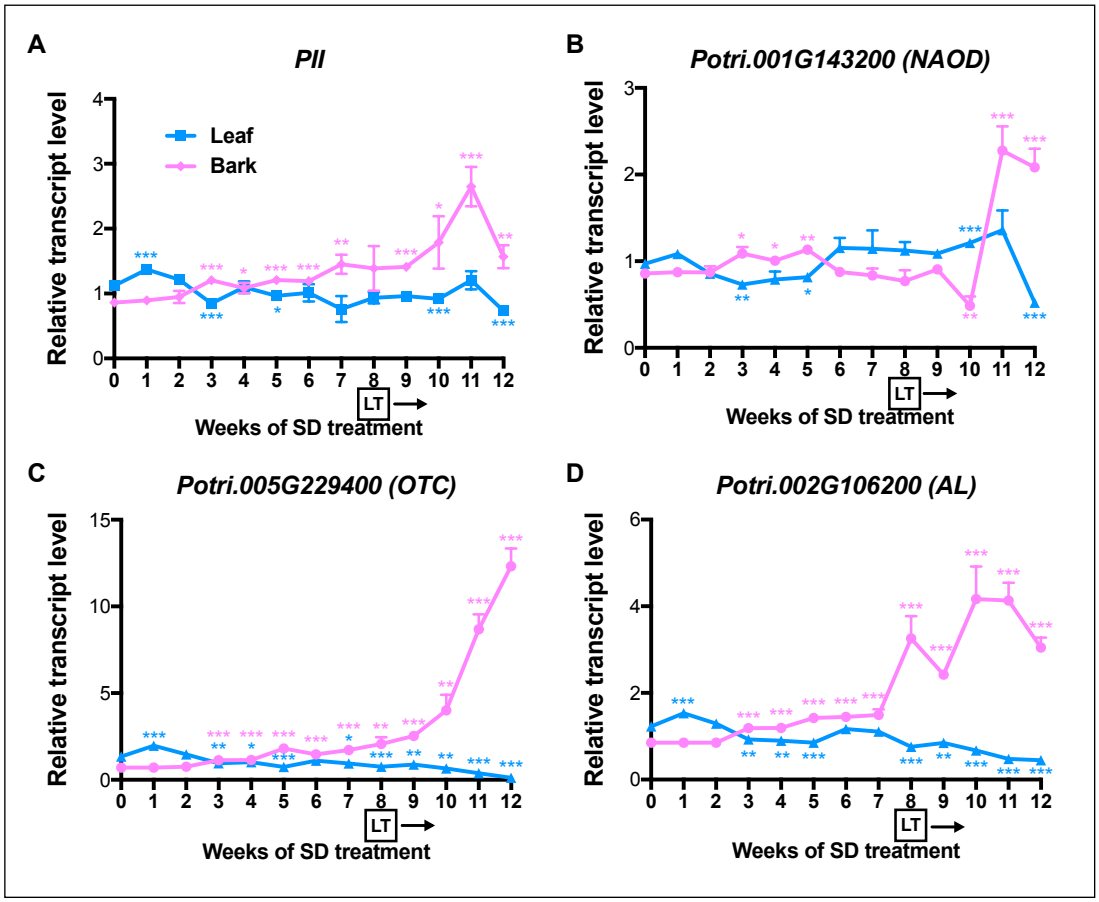

Figure 4-1. Expression of *PII* and arginine synthesis genes in bark and leaves during leaf senescence. Relative transcript levels of (A) *PII*, (B) *NAOD*, (C) *OTC* and (D) *AL* were determined in bark (pink) and leaves (blue) of *Populus trichocarpa* (Nisqually) plants treated with SD photoperiod for 8 weeks at 18 °C followed by an additional 4 weeks at LT (10°C / 4 °C ; day /night). Relative expression was determined at weekly intervals by qRT-PCR. * indicates means significantly different from control at $p<0.05$, ** for $p<0.01$, *** for $p<0.001$.

Root growth and anthocyanin accumulation is altered in PII-RNAi knockdown poplars

In order to further investigate the possible role of PII on bark N storage, PII-RNAi knockdown poplars using *Populus tremula* × *P. alba* hybrid clone INRA 717-1B4 were produced. Screening of the transformation events uncovered two independent transformation events with significantly reduced bark *PII* transcript levels (73% and 83% reduction in line PR1-6 and PR1-2, respectively) compared to control plants (B6) in LD (Figure 4-2A). In addition to the reduced transcript levels of *PII*, the abundance of transcripts for *NAOD*, *OTC* and *AL* were significantly reduced in PR1-6 but not in PR1-2 (Figure 4-2B-D). We next determined if the growth of PII-RNAi poplars differed relative to control plants when grown at different levels of N availability (0.2mM, 2mM and 20mM NH_4NO_3) and found no obvious differences in the appearance of the *PII*-RNAi plants compared to wild-type plants (Figure 4-3A). Since leaf area is strongly influenced by N availability (Cooke et al., 2005) we measured this growth parameter along with plant height and root growth and found no differences between wild-type and *PII*-RNAi plants for mean leaf area (Figure 4-3E), plant height (Figure 4-3F) or leaf area at different leaf positions (Figure 4-3B-D). As expected mean leaf area and plant height was greater for either wild-type or *PII*-RNAi plants treated with 20 mM NH_4NO_3 (Figure 4-2E and F). In contrast to leaf area and plant height, root length was greater for *PII*-RNAi plants compared to wild-type plants of plants grown *in vitro* on ½ strength N-free MS medium with 1mM glutamine as the single N source (Figure 4-3G).

Anthocyanin accumulation is influenced by the C/N ratio of plants with accumulation enhanced at high ratios (Hsieh et al., 1998), thus the leaf anthocyanin content of *in vitro* grown plants on ½ strength N-free MS medium with or without 1mM glutamine was also determined (Figure 4-4). *PII*-RNAi plants accumulated greater levels of anthocyanins on medium lacking N compared to wild-type plants. Although, the addition of 1mM glutamine significantly reduced anthocyanin levels in control plants, no significant differences were detected between N-free medium and glutamine-supplemented medium for the *PII*-RNAi plants (Figure 4-4). These results are consistent with previous studies (Hsieh et al., 1998) that indicate a role for PII in sensing C/N balances in cells and suggest a similar role in poplar

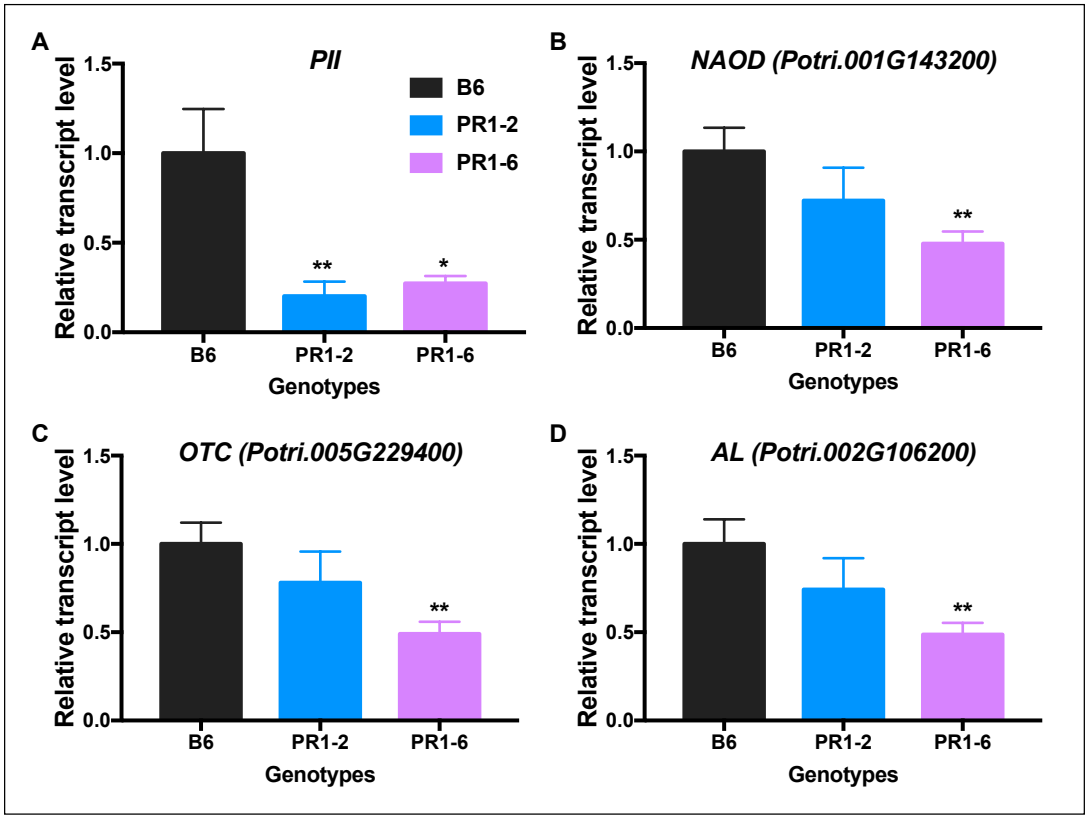

Figure 4-2. *PII* transcript levels in PII-RNAi knockdown poplars. Relative transcript levels of (A) *PII*, (B) *NAOD*, (C) *OTC* and (D) *AL* in bark of *Populus tremula* × *P. alba* hybrid clone INRA 717-1B4 *PII*-RNAi lines PR1-2 and PR1-6 of LD grown plants. Relative expression levels were determined by qRT-PCR and * indicates means significantly different from control at $p<0.05$, ** for $p<0.01$.

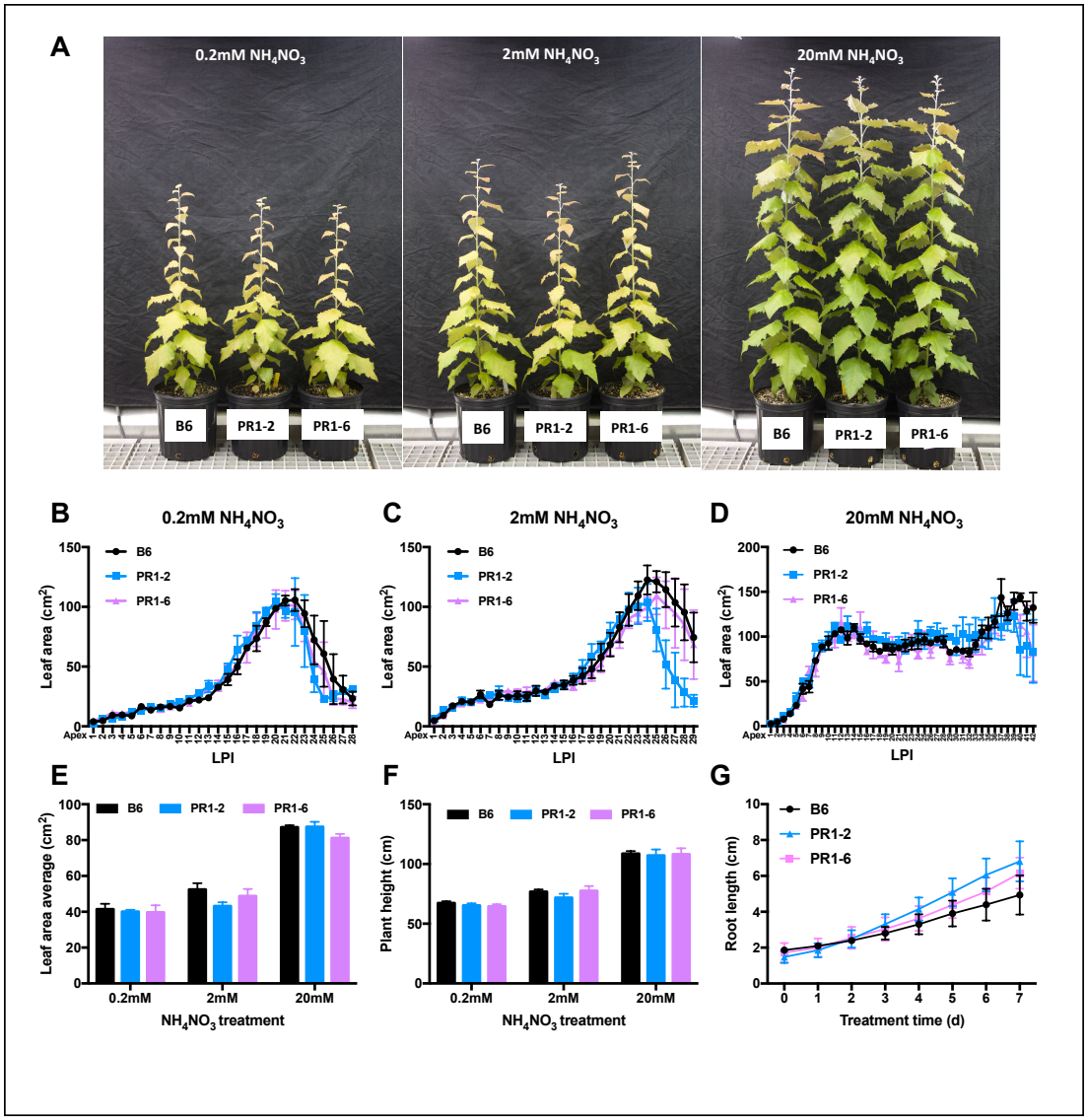

Figure 4-3. Growth of PII RNAi knockdown poplars at different levels of N availability. (A) Photograph of wild type (*Populus tremula* × *P. alba* hybrid clone INRA 717-1B4) and *PII*-RNAi lines PR1-2 and PR1-6 grown at different N levels (0.2mM, 2mM or 20mM NH_4NO_3) in LD. Leaf area by leaf position of wild type and *PII*-RNAi lines of plants treated with either (B) 0.2mM, (C) 2mM or (D) 20mM NH_4NO_3. (E) Mean leaf area (F) and plant height of wild type and PII RNAi lines treated with either 0.2mM, 2mM or 20mM NH_4NO_3. (G) Root length of *in vitro* cultured wild type and *PII*-RNAi lines after 7 days growth on ½ strength N-free MS medium with 1mM glutamine as the sole N source. Root growth was measure daily for up to 7 days.

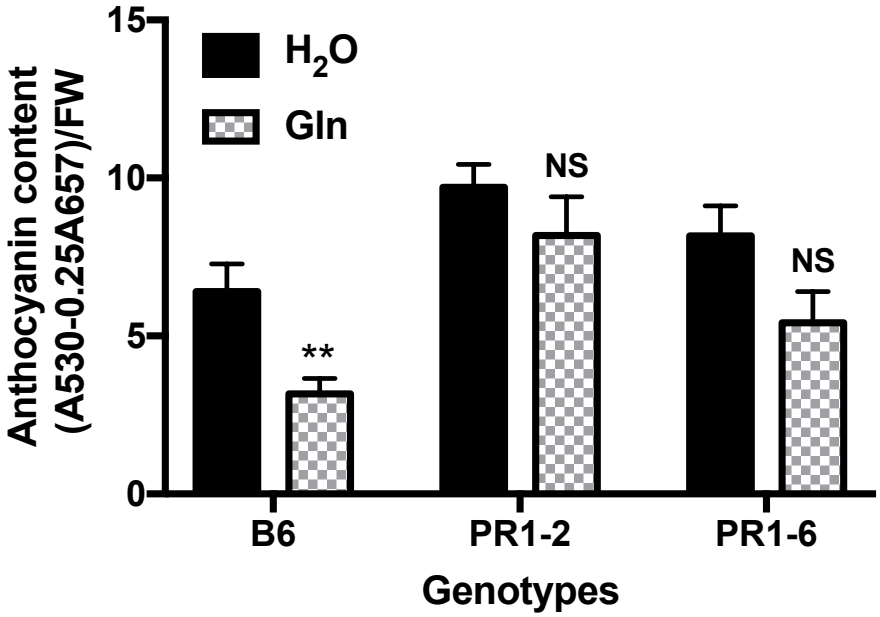

Figure 4-4. Glutamine reduction of anthocyanin accumulation is inhibited in *PII*-RNAi poplars. Wild-type *Populus tremula* × *P. alba* hybrid clone INRA 717-1B4 and *PII*-RNAi lines PR1-2 and PR1-6 grown *in vitro* grown on ½ strength N-free MS medium with 1mM glutamine as the sole N source. After 7 days leaf anthocyanin levels were determined by measuring the absorbance at 530 and 657 nm of leaf disk extracts. ** indicates means significantly different from control at $p<0.01$.

NH4NO3 and glutamine-induced BSP expression is reduced in PII-RNAi but not arginine induction

To determine if PII may play are role in N-induced *BSP* expression, we examined if either NH_4NO_3 or glutamine-induced *BSP* expression differed between wild-type and *PII*-RNAi poplars. Using a stem feeding assay (Zhu and Coleman, 2001a), we found that transcript levels for *BSPA* (Figure 4-5A), *BSPB* (Figure 4-5B), and *BSPC* (Figure 4-5C) were reduced in both PII-RNAi lines when feed 2mM NH_4NO_3. At higher NH_4NO_3 concentrations (20mM) *BSP* expression was also reduced, although differences between wild-type and *PII*-RNA lines was reduced in magnitude. Using the *PII*-RNAi line PR1-2 we also determined if glutamine-induced *BSPs* expression

differed between wild-type and *PII*-RNAi. Similar to previous research (Zhu and Coleman, 2001a) feeding stems 25mM glutamine induced *BSPA* (Figure 4-6A), *BSPB* (Figure 4-6B), and *BSPC* (Figure 4-6C) bark expression within 24 hours of feeding while glutamine-induced expression was absent or reduced in the *PII*-RNAi line PR1-2. Although glutamine-induced *BSP* expression was absent in *PII*-RNAi line PR1-2, feeding stems 25mM arginine induced *BSPA* (Figure 4-6D), *BSPB* (Figure 4-6E) and *BSPC* (Figure 4-6C) expression in both wild-type and *PII*-RNAi line PR1-2. Therefore, it appears that PII-mediated sensing of glutamine plays a role in glutamine-induced *BSP* expression. Since induction by arginine was still observed in the *PII*-RNAi line PR1-2 suggests that the PII-mediated expression of *BSP* may involve regulation of the arginine biosynthesis pathway.

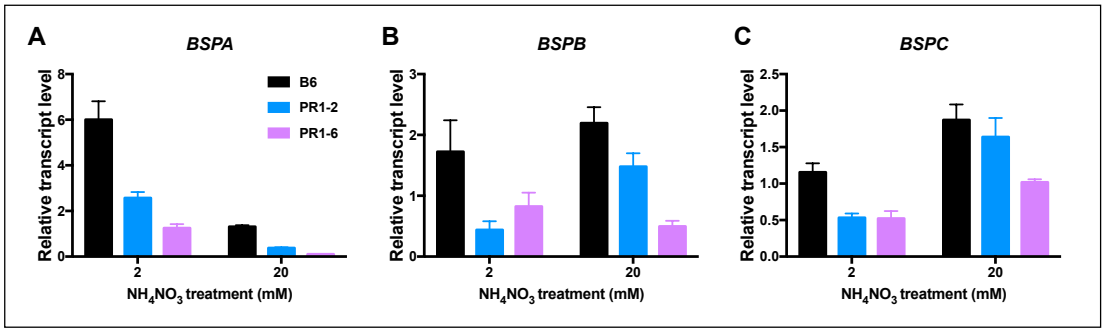

Figure 4-5. NH_4NO_3 induced *BSP* expression is reduced in PII-RNAi poplars. Relative transcript levels of (A) *BPA*, (B) *BSPB* and (C) *BSPC* in bark of wild-type *Populus tremula* × *P. alba* hybrid clone INRA 717-1B4 and *PII*-RNAi lines PR1-2 and PR1-6 stems fed either 2mM or 20mM NH_4NO_3 for 24 hours. Relative transcript levels were determined by qRT-PCR.

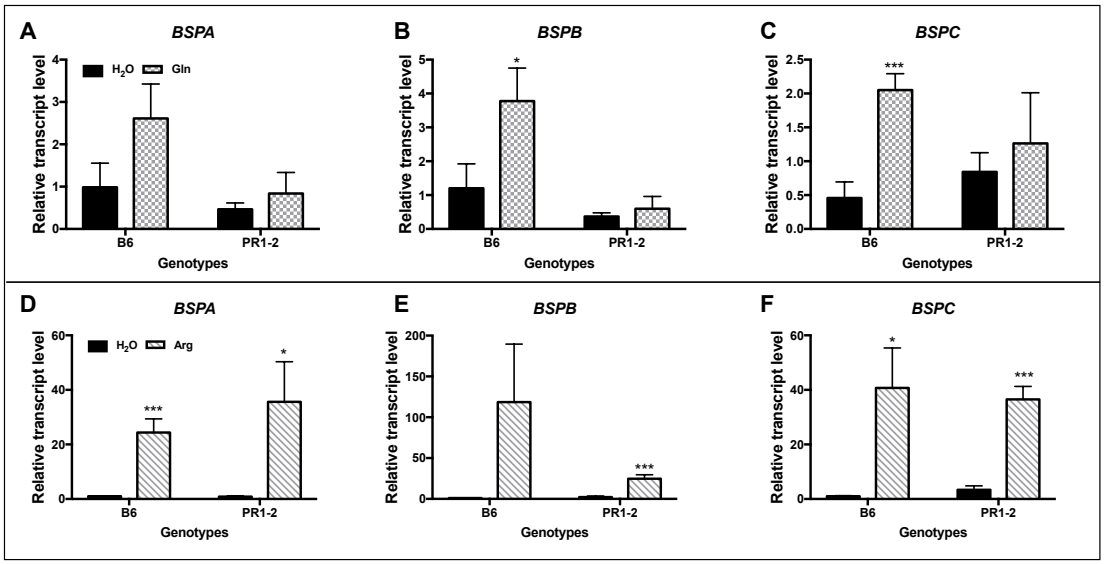

Figure 4-6. Glutamine-induced but not arginine-induced *BSP* expression is reduced in *PII*-RNAi poplars. Relative expression of (A) *BPA*, (B) *BSPB* and (C) *BSPC* in bark of wild-type *Populus tremula* × *P. alba* hybrid clone INRA 717-1B4 and PII-RNAi line PR1-2 stems after 24 hours of feeding 25 mM glutamine or 25 mM arginine (D-E).. Relative transcript levels were determined by qRT-PCR. * indicates means significantly different from control at $p<0.05$, *** for $p<0.001$.

2-oxoglutarate suppresses glutamine-induced BSP expression

The interaction between PII and NAGK is antagonized by 2-OG in *Arabidopsis* (Feria Bourrellier et al., 2009), which in turn negatively regulates downstream arginine synthesis. In order to investigate whether glutamine-induced *BSP*s expression may involve PII-NAGK mediated arginine synthesis, stems of *Populus trichocarpa* (Nisqually) were fed 25mM glutamine, 5mM 2-OG or a combination of glutamine and 2-OG and after 24 hours of feeding bark *BSP* expression was determined. As observed previously, feeding stems glutamine increased expression of all three *BSP* genes (Figure 4-7A-C). Feeding poplar stems 2-OG had little effect on *BSP* expression (Figure 4-7A-C) while feeding 2-OG in combination in glutamine reduced *BSP* expression relative to glutamine alone (Figure 4-7A-C). Arginine induction of *BSP* was also affected when combined with 2-OG but instead of reducing expression as was the case for glutamine, 2-OG combined with arginine produced a synergistic

increase in *BSP* expression (Figure 4-7D-E). These results are consistent with PII sensing glutamine that then activates the arginine biosynthetic pathway. This interaction is antagonized by 2-OG which suppress activation of the arginine pathway leading to reduced *BSP* expression.

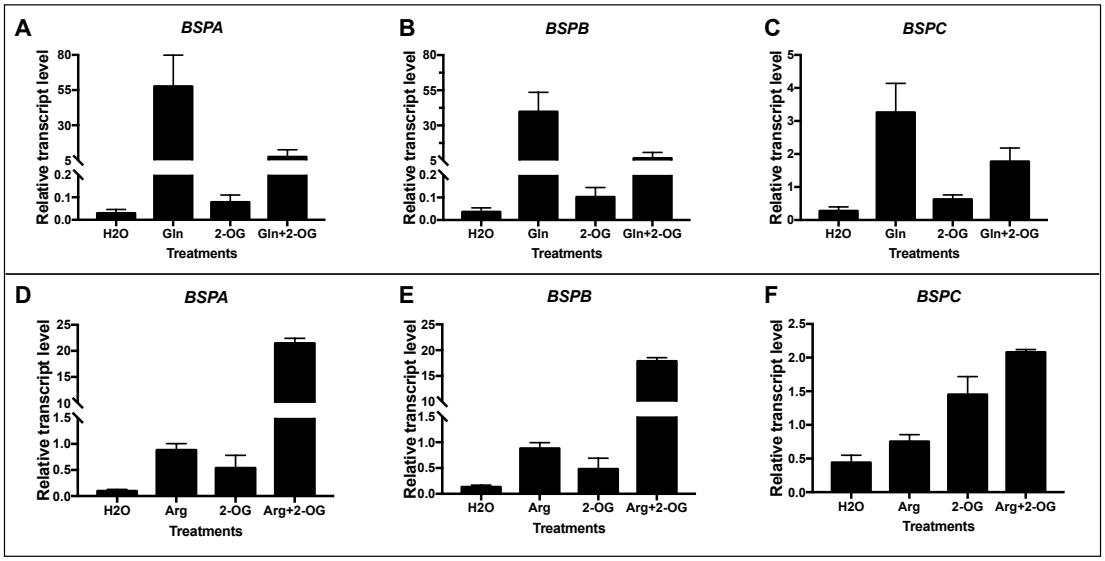

Figure 4-7. 2-OG reduces glutamine-induced *BSP* expression but enhances arginine-induction. Relative expression of (A) *BPA*, (B) *BSPB* and (C) *BSPC* in bark of *Populus trichocarpa* (Nisqually) after 24 hours stems of feeding 25 mM glutamine, 5 mM 2-OG, or a combination of glutamine and 2-OG or 25 mM arginine, 5 mM 2-OG or a combination arginine and 2-OG (D-E). Relative transcript levels were determined by qRT-PCR.

Arginine induction of *BSP* expression does not appear to involve NO

Both a nitrate/nitrite and an arginine dependent pathways have been proposed to be involved in the generation of NO (Besson-Bard et al., 2008). Since our results suggest that glutamine-induced *BSP* expression mediated by PII appears to be related to the activation of the arginine biosynthetic pathway we determined if sodium nitroprusside (SNP), a NO donor, could induce *BSP* expression when fed to poplar stems. We failed to observe any increase in expression of any of the three *BSP* genes when stems were fed 50 or 500 μM SNP (Figure 4-8A-C). Although not conclusive,

this does suggest that glutamine or arginine-induced *BSP* may involve mechanisms independent of NO signaling.

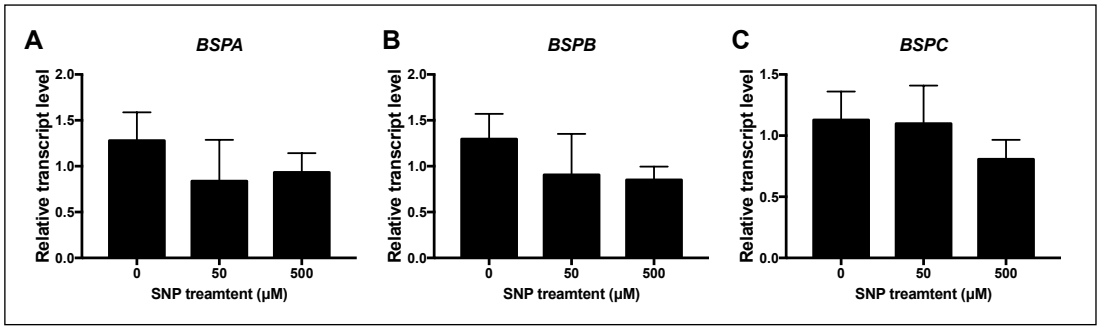

Figure 4-8. Nitric oxide does not induce *BSP* expression. Stems of of *Populus trichocarpa* (Nisqually) were treated with either 50 μM and 500 μM SNP for 24 hours and the relative transcripts level of (A) *BPA*, (B) *BSPB* and (C) *BSPC* were determined by qRT-PCR.

Discussion

Poplar BSPs, encoded by three genes (*BSPA*, *BSPB* and *BSPC*), are the central components of seasonal nitrogen storage and their gene expression is regulated by SD photoperiod, N availability and low temperature (Coleman et al., 1991a; Pettengill et al., 2013; Zhu and Coleman, 2001a). The molecular mechanisms or regulatory components involved in SD-induced *BSP*s induction and N storage are poorly understood. PII is an evolutionary conserved central integrator of cellular status of carbon, nitrogen and energy from cyanobacteria to green algae to higher plants (Chellamuthu et al., 2012; Ermilova and Forchhammer, 2013; Forchhammer, 2008; Forchhammer and Lüddecke, 2016; Moorhead and Smith, 2003; Uhrig et al., 2009). Since seasonal N cycling involves the transport of glutamine from senescing leaves to bark we theorized that PII could play are role in glutamine-induced BSP expression by sensing changes in bark glutamine levels. In this research it was discovered that *PII* is differentially expressed between leaves and bark. This differential expression

appears to be associated with the source-sink status of these organs. As leaf senescence progressed, senescing leaves become an N source where *PII* expression declined while to opposite pattern occurred in bark, which becomes an N sink during N remobilization from senescing leaves.

During autumn N remobilization from leaves glutamine levels initially increase and then decline while arginine levels increase throughout the dormancy period and only decline when growth resumes in the spring (Couturier et al., 2010a; Frak et al., 2002; Wildhagen et al., 2010). In addition to *PII* differential expression between leaves and bark during leaf senescence we also found that genes encoding NAOD, OTC and AL enzymes in the arginine biosynthetic pathway were also differentially expressed between bark and leaves. Glutamine is converted to glutamate by GOGAT which in turn is used by NAOAT (N-acetylornithine aminotransferase) during the synthesis of N-acetylornithine from N-acetylglutamate-5-semialdehyde in the cyclic pathway of arginine biosynthesis (Winter et al., 2015). Glutamine is also involved in the linear pathway where glutamine is converted to carbmoyl-phosphate by CPS (carbamoyl phosphate synthetase) (Winter et al., 2015). Thus the transient increase of glutamine in poplar bark during autumn probably reflects both its use a substrate for amino acid synthesis that are incorporated into BSP but also as a substrate in both the cyclic and linear pathways of arginine synthesis in bark.

To further investigate the possible role of PII in glutamine-mediated *BSP* expression we generated transgenic poplars with *PII* expression knocked down via RNAi expression. Similar to other studies involving knockouts of *PII* which lacked

obvious changes in plant growth and development (Ferrario-Méry et al., 2005) we found that poplar growth and development in *PII*-RNAi was similar to that of wild-type plants. In *Arabidopsis* glutamine relieved anthocyanin accumulation associated with high C/N ratios in wild-type plants but in *PII* overexpressing plants attenuation of anthocyanin levels by glutamine was reduced (Hsieh et al., 1998). In *PII*-RNAi poplars we also found changes in anthocyanin accumulation was altered in response to C/N ratios. When the transgenic plants were place in N starvation conditions (high C/N) the *PII*-RNAi plants accumulated greater levels of anthocyanins and when supplemented with glutamine (lower C/N ratio) the accumulation remained at levels similar to the high C/N ratio. In contrast, glutamine relieved the anthocycanin accumulation in wild-type plants. Thus PII plays are role in the cellular sensing of C/N ratios in poplar. Thus poplar and Arabidopsis PII both seem to be involved in sensing C/N despite the fact that poplar PII possess the glutamine binding Q-loop while Arabidopsis lacks this domain (Chellamuthu et al., 2014).

Since PII serves acts as a glutamine sensor that modulates arginine biosynthesis in plants (Chellamuthu et al., 2014; Chen et al., 2006; Ferrario-Méry et al., 2005, 2006), we wanted to know whether the *PII*-RNAi poplars were altered in glutamine or arginine induction of *BSP* expression. Consistent with this possible role we found that *BSP* expression was attenuated in *PII* knockdown poplars yet these plants retained arginine induction. This supports a role for PII mediated glutamine sensing in the metabolic regulation of *BSP* expression and N storage. Since arginine induction was unaffected it is possible that this regulation is specific to glutamine as opposed to nonspecific metabolic changes. We also found that 2-OG, an antagonist of

PII-NAGK interactions also inhibited glutamine induced *BSP* expression while 2-OG seems to synergistically induce expression with arginine. The reason for these differences is unclear and requires additional research, but arginine exerts feedback inhibition of NAGK activity (Chen et al., 2006; Feria Bourrellier et al., 2009), while 2-OG can relieve the inhibition by arginine. Consequently, 2-OG enhanced arginine-induced *BSP*s expression may occur via alterations in the inhibition of NAGK enzyme activity. This is further supported by the 2-OG inhibition of glutamine-induced *BSP* expression since 2-OG antagonizes PII-NAGK interactions (Feria Bourrellier et al., 2009). Therefore, these results provide evidence for that activation of NAGK mediated by PII-glutamine sensing plays a role in *BSP* expression.

PII regulates the biosynthesis of NO in *Lotus* (Parlati et al., 2017), and an arginine dependent pathway has been proposed to be involved NO production although the molecular mechanism of NO production from arginine remains unclear in higher plants (Corpas et al., 2009; Winter et al., 2015). It is possible that increased arginine results in enhanced NO production that in turn may regulate *BSP* expression. However, treatment of poplar stems with the NO donor SNP failed to induced *BSP* expression. Although this is does not directly prove that NO lacks a role in *BSP* expression, it does suggest the arginine induction is NO-independent.

In conclusion, the role of PII in the N cycling was investigated in poplar for the first time in this study. PII seems to influence root elongation and anthocyanin accumulation in leaves. Moreover, PII-glutamine sensing and PII-NAGK interactions appear to play a role in *BSP* expression. Furthermore, it seems likely that glutamine-induced *BSP* expression is mediated by effects on arginine biosynthesis as opposed to

direct effects of PII-glutamine interactions. How arginine is sensed and regulates BSP expression is unknown and requires further research, of which identification of an arginine receptor or sensor would be critical to uncovering possible mechanisms.

Summary

Seasonal nitrogen (N) cycling is a critical feature of adaptation to N limitation for forest trees. Seasonal N cycling has been more extensively studied in *Populus*, a model forest tree species, than other tree species. Although many studies have suggested an association between seasonal N cycling and physiological processes, such as growth cessation, leaf senescence, plant dormancy and regrowth, a number of questions concerning N source sink establishment and communication during seasonal N cycling, as well as the role of BSP involvement in these processes remain. In the research described in this dissertation, I investigated two aspects of seasonal N cycling to advance our understanding of seasonal nitrogen cycling in poplar. Specifically I wanted to know (1) if BSP accumulation contribute to plant regrowth; (2) what are the regulatory mechanisms controlling BSP catabolism and N remobilization; (3) how is BSP accumulation during short-day photoperiod regulated and (4) what role does glutamine sensing play in regulation *BSP* expression.

In order to query the contribution of N storage to plant regrowth, firstly we tested the shoot regrowth of plants with same level of stored N (source) and different numbers of shoots (sink). Plants with more shoots showed reduced leaf area and shoot length, which indicates that shoot regrowth is hampered by N sink competition and and appears to be source limited. However, it is still unclear about the extent that different N storage pools contribute to plant regrowth. Since N is mainly stored in the form of BSP in poplar, we generated BSP knockdown poplars using RNAi. BSP RNAi lines showed delayed bud break and reduced shoot regrowth (i.e. leaf area,

stem length and shoot biomass), which suggests N remobilized from BSP catabolism serves as a major N source for poplar regrowth before roots can absorb nitrogen from the soil.

Since BSP catabolism an N remobilization contributes to plant regrowth, it is worthwhile to discover the regulatory mechanisms controlling BSP catabolism. Global gene expression in poplar bark during BSP catabolism and regrowth was analyzed using DNA microarrays. Gene ontology (GO) analysis showed hormone response was enriched in differentially expressed genes. More in-depth analysis of this GO category showed genes related to auxin transport and response were enriched, which indicates auxin transport and responses may be associated with bark BSP catabolism. Previous research has shown that expanding buds are required for BSP catabolism, which prompted me to determine the potential role of auxin transport from expanding buds to bark using a series of experiments. First, we found expression of ortholog genes of *AtTAR1* and several *YUCCA* genes increased in expanding buds during BSP catabolism. In addition, auxin transport and response genes were highly induced in bark of intact plants while their expression was reduced in the bark of plants with buds removed, suggesting that auxin in bark is mainly transported from expanding buds. To further verify the importance of polar auxin transport for BSP catabolism, the auxin transport inhibitor NPA was used to block polar auxin transport. Blocking auxin transport by NPA inhibited BSP catabolism and expression of auxin transport and response genes, which further suggests that polar auxin transport is the major auxin route responsible for BSP catabolism. There is also a subset of proteases genes associated with BSP catabolism that were differentially

expressed in both bud-removal and NPA experiments and also inducible by auxin. Taken together, we proposed a model in which auxin, produced in expanding buds (N sink) and transported to bark (N source) appears to regulate BSP catabolism by regulating the expression of specific protease genes. Moreover, from ^{13}N tracer experiment we found that BSP accumulation contributes to N partitioning from senescent leaves to bark, suggesting that BSP accumulation may play a central role of establishment of N sink status in bark.

Previous studies have shown that bark *BSP* expression is induced by short-day (SD) photoperiod, which was originally presumed to be a consequence of N translocation to bark from senescent leaves. To test this hypothesis, timing of SD-induced BSP expression was compared with that of leaf senescence. *BSP* expression increased after 2 weeks of SD treatment while changes of chlorophyll content and expression of senescence-associated genes indicate that leaf senescence occurred after 9 weeks of SD treatment plus 1 week of low temperature treatment. These results suggest that SD-induced *BSP* expression is independent of leaf senescence. To identify the potential regulatory mechanisms of SD-induced *BSP* expression, whole-genome transcript profiling of bark was analyzed using DNA microarrays. GO analysis showed that a group of transcription factors are enriched, among which two ethylene response factors (ERFs, ERF12 and ERF41) are most highly induced transcription factors in bark during SD treatment. More important, the expression of the majority of ERFs were changed according to a pattern where ethylene-induced ERFs showed reduced expression under SD treatment while ethylene-repressed ERFs (e.g. ERF12 and ERF41) showed increased expression under SD treatment.

Consistently, expression of the majority of *ACS* and *ACO* genes and ethylene production in bark were reduced during SD treatment, which indicates that SD treatment repressed ethylene production in bark. To test whether ethylene signaling is the missing link between SD photoperiod and *BSP* expression, effects of ethylene on *BSP* expression were determined with treatment of ethylene precursor ACC, ethephon and ethylene biosynthesis inhibitor AVG. *BSP* expression is repressed by both ACC and ethephon treatment but induced by AVG treatment. Moreover, ethylene insensitive poplars showed reduced repression of *BSP* expression by either ACC and ethephon treatment. Similarly, NH_4NO_3- and glutamine-induced *BSP* expression is repressed by both ACC and ethephon treatment while glutamine-induced BSP expression is enhanced either by AVG treatment or in ethylene insensitive poplar compared with wild type. Furthermore, transient expression both ERF12 and ERF41 into leaves of transgenic tobacco (*BSPA* promoter::uidA) increased GUS activity. Taken together, we proposed that SD photoperiod regulates *BSP* expression through alteration of ethylene production and signaling.

Thus, SD-induced *BSP* expression contributes to establishment of an N sink in bark, which has a positive feedback on N partitioning from senescent leaves (N source) to bark during leaf senescence. Glutamine is the most abundant amino acid in the stem and appears to serve as not only substrate for synthesis of other N components but also a molecular signal involved in N cycling. PII has been identified as a conserved glutamine sensor in plants except *Brassicaceae*. In this study, we found expression of *PII* increased in bark during SD treatment and during leaf senescence in SD and LT condition. Similar changes were also obtained from

expression of three genes involved in arginine biosynthesis. PII-RNAi knockdown poplars showed altered root elongation and anthocyanin accumulation when glutamine is provided as the single N source. Moreover, glutamine-induced *BSP* expression was also reduced in PII-RNAi poplars. 2-OG, an antagonizer of PII-NAGK interaction reduced glutamine-induced *BSP* expression. These results suggest that PII serves as a glutamine sensor and may also regulate *BSP* expression.

This study provides important insights into the contribution of BSP accumulation to plant regrowth and possible mechanism involved in seasonal N partitioning and cycling in poplar. However, there is still substantial knowledge missing in the mechanisms of seasonal N cycling. Due to some limitations, we still don't know which specific auxin transporter and response genes and proteases genes are involved in BSP catabolism and N remobilization. Since CAT10 has shown an association with N remobilization and transport during plant regrowth, it will be worthwhile to verify its role as a transporter of amino acids, especially glutamine. In addition, future work is also needed to determine the interaction between either ERF12 or ERF41 and *BSP* promoter and biological function of these two ERFs in poplar. Since glutamine induced BSP expression possibly through PII-mediated biosynthesis of arginine, it will be interesting to discover whether arginine induces BSP expression via direct sensing system or other signaling pathway.

Appendices

Appendix A

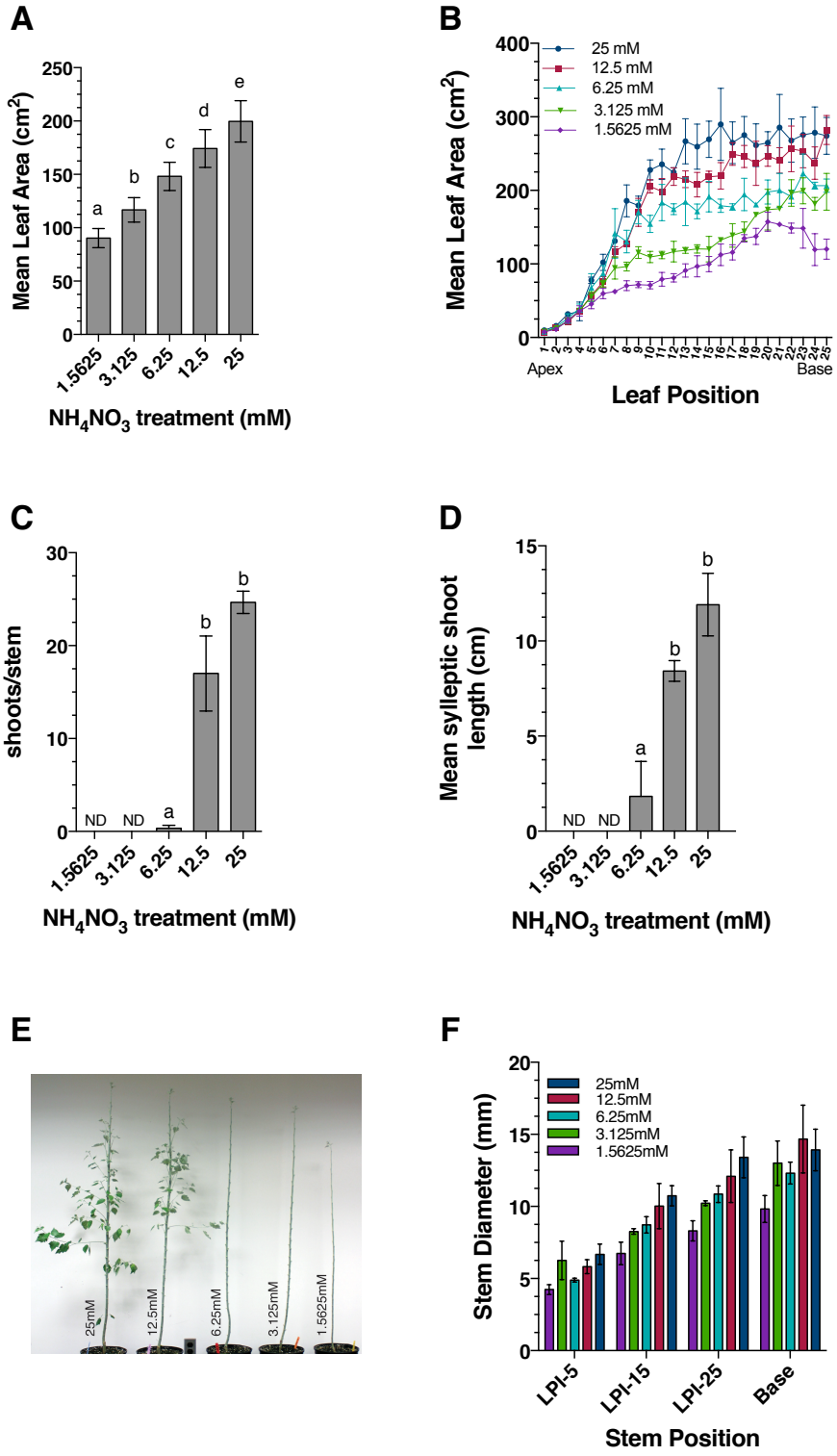
A
Mean Leaf Area (cm2)
250
200
150
100
50
0
a
b
c
d
e
1.5625
3.125
6.25
12.5
25
NH4NO3 treatment (mM)
B
Mean Leaf Area (cm2)
400
300
200
100
0
25 mM
12.5 mM
6.25 mM
3.125 mM
1.5625 mM
Apex
Base
Leaf Position
C
Number sylleptic shoots/stem
30
20
10
0
ND
ND
a
b
b
1.5625
3.125
6.25
12.5
25
NH4NO3 treatment (mM)
D
Mean sylleptic shoot length (cm)
15
10
5
0
ND
ND
a
b
b
1.5625
3.125
6.25
12.5
25
NH4NO3 treatment (mM)
E
25mM
12.5mM
6.25mM
3.125mM
1.5625mM
F
Stem Diameter (mm)
20
15
10
5
0
25mM
12.5mM
6.25mM
3.125mM
1.5625mM
LPI-5
LPI-15
LPI-25
Base
Stem Position

Figure. S2-1 Effects of NH_4NO_3 fertilization on shoot growth of Nisqually. (A) Mean leaf area of whole plant under different NH_4NO_3 concentration. (B) Mean leaf area of each leaf position (Apex-base, 1-25) under different NH_4NO_3 concentration. (C) Number of sylleptic shoots per stem under different NH_4NO_3 concentration. (D) Mean length of sylleptic shoots per stem under different NH_4NO_3 concentration. (E) Photograph of poplar grown under different NH_4NO_3 concentration. (F) Stem diameter at different stem position under different NH_4NO_3 concentration. Error bars indicate mean ± SE and a, b, c and d indicates values significantly different from control at $p<0.05$, ND means no presence.

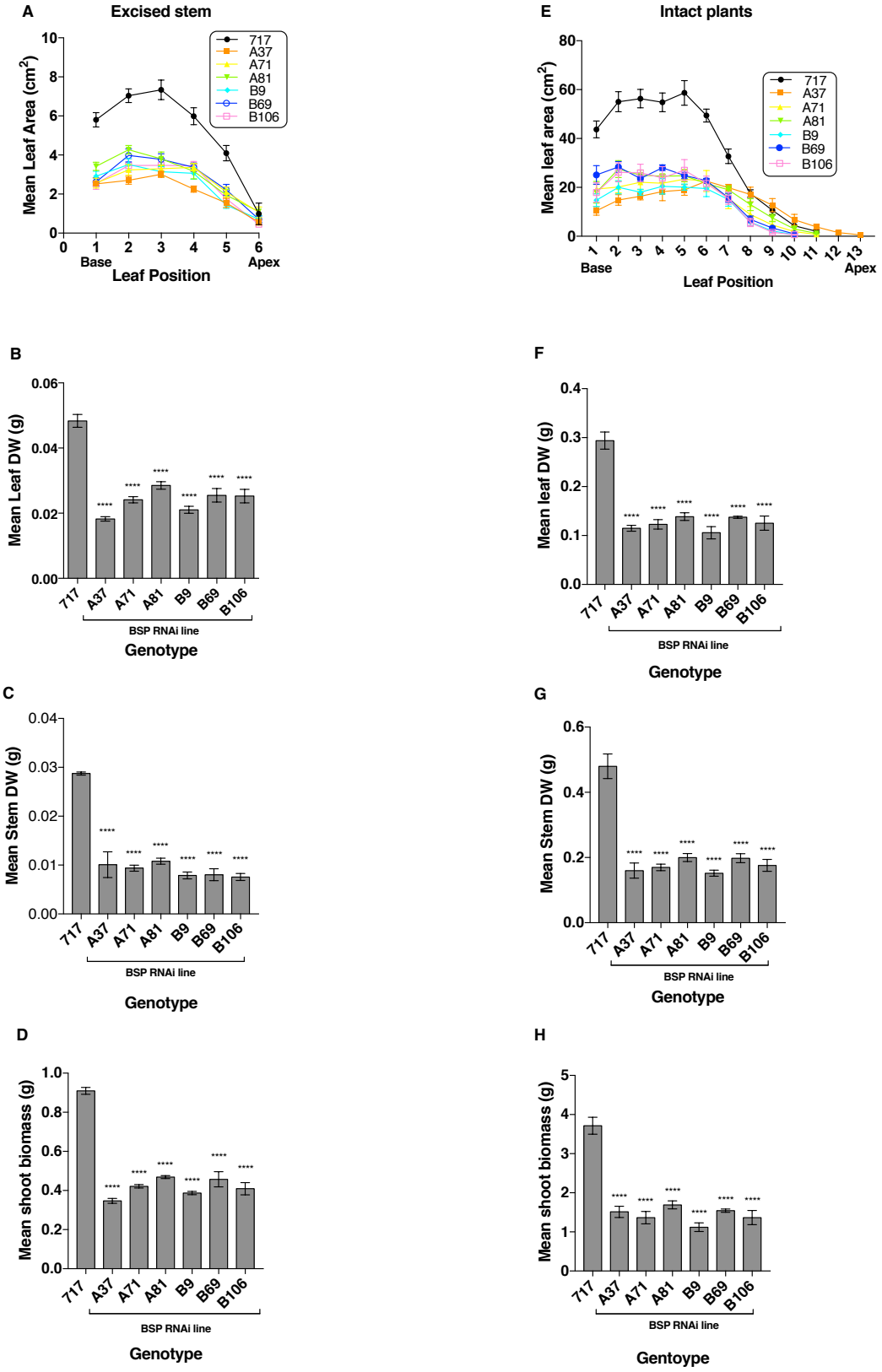
A
Excised stem
Mean Leaf Area (cm2)
Base
Apex
Leaf Position
717
A37
A71
A81
B9
B69
B106
E
Intact plants
Mean leaf area (cm2)
Base
Apex
Leaf Position
B
Mean Leaf DW (g)
BSP RNAi line
Genotype
F
Mean leaf DW (g)
BSP RNAi line
Genotype
C
Mean Stem DW (g)
BSP RNAi line
Genotype
G
Mean Stem DW (g)
BSP RNAi line
Genotype
D
Mean shoot biomass (g)
BSP RNAi line
Genotype
H
Mean shoot biomass (g)
BSP RNAi line
Gentoype

Figure S2-2. Reduced BSP accumulation via RNAi knockdown reduces growth following bud break. (A) Mean leaf area at different leaf positions and (B) mean leaf dry weight (C) mean stem dry weight and (D) mean shoot biomass of new stem growth 6 weeks after bud break of excised stems for control (717) and BSP-RNAi lines (A37, A71, A81, B9, B69, B106). (E) Mean leaf area at different leaf positions and (F) mean leaf dry weight (G) mean stem dry weight and (H) mean shoot biomass of new stem growth 6 weeks after bud break for intact plants. Error bars indicate mean ± SE and **** indicates means significantly different from control at p<0.0001.

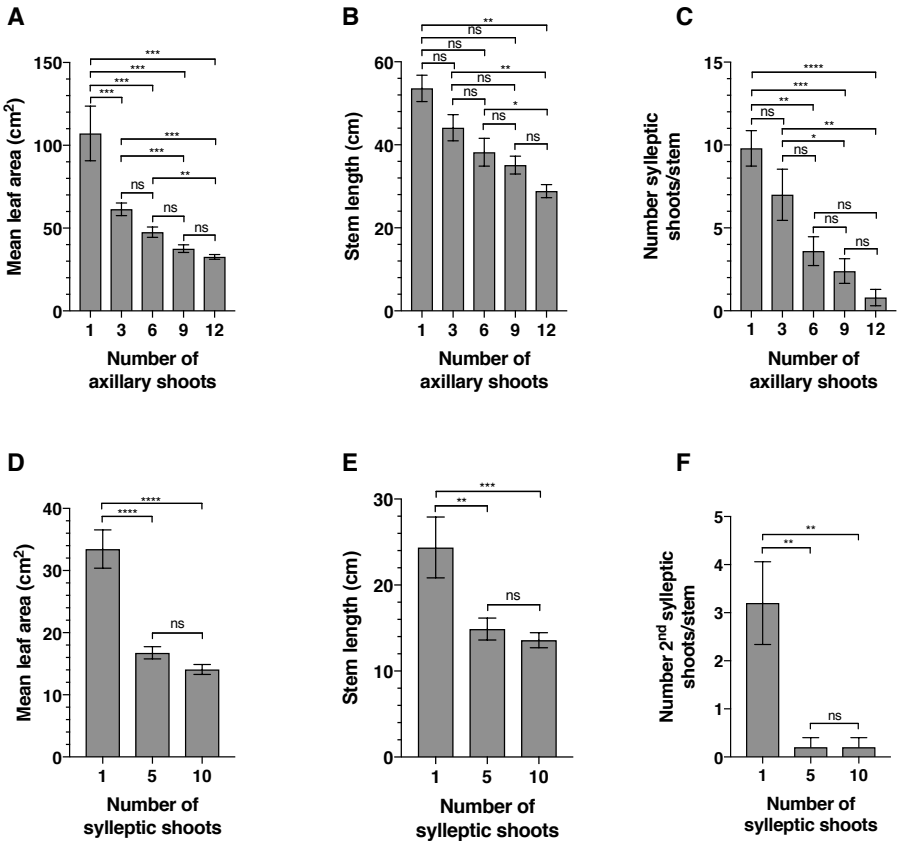

Figure S2-3. Sink competition between axillary shoots or between sylleptic shoots. (A) Mean leaf area, (B) stem length and (C) number of sylleptic shoots per stem of Nisqually plants with different number of axillary shoots grown for 6 weeks after bud break. (D) Mean leaf area, (E) stem length and (F) number of 2nd sylleptic shoots per stem of Nisqually plants with different number of sylleptic shoots grown for 6 weeks after bud break. Error bars indicate mean ± SE and **** indicates means significantly different from control at p<0.0001, *** for p<0.001, ** for p<0.01, * for p<0.05, ns for no significance.

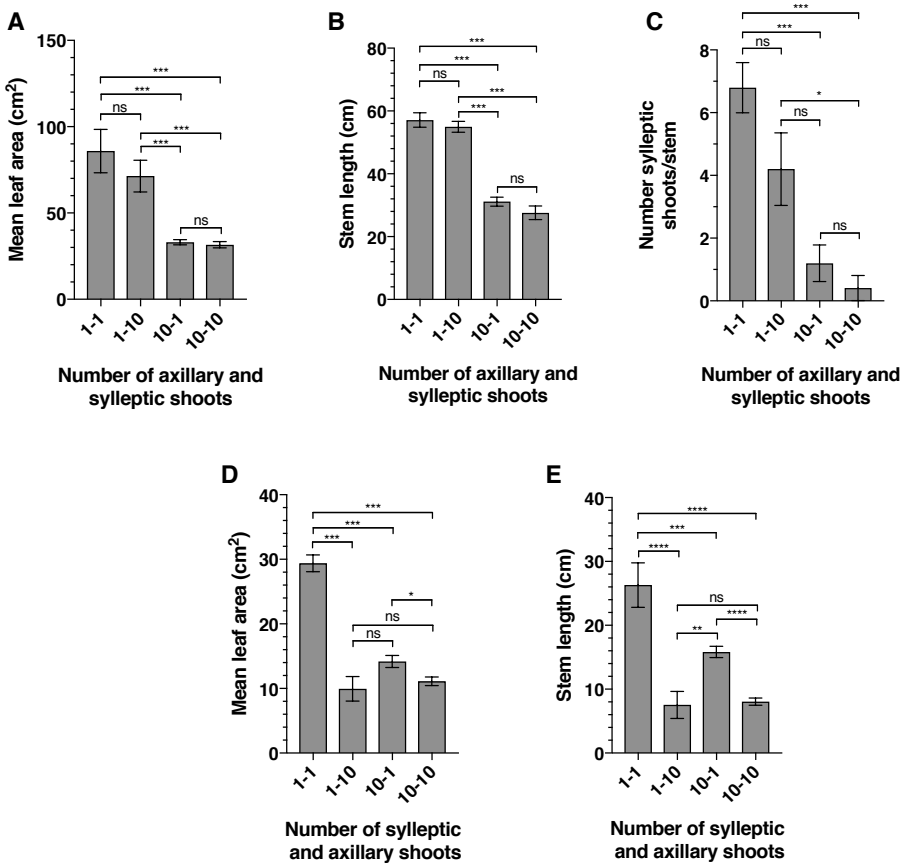

Figure S2-4. Sink competition between axillary and sylleptic shoots. (A) Mean leaf area of axillary shoot, (B) stem length and (C) number of sylleptic shoots per stem of plants with different number of axillary and sylleptic shoots grown for 6 weeks after bun break. (D) Mean leaf area of sylleptic shoot and (E) stem length of plants with different number of sylleptic and axillary shoots grown for 6 weeks after bun break. Error bars indicate mean ± SE and **** indicates means significantly different from control at $p<0.0001$, *** for $p<0.001$, ** for $p<0.01$, * for $p<0.05$, ns for no significance.

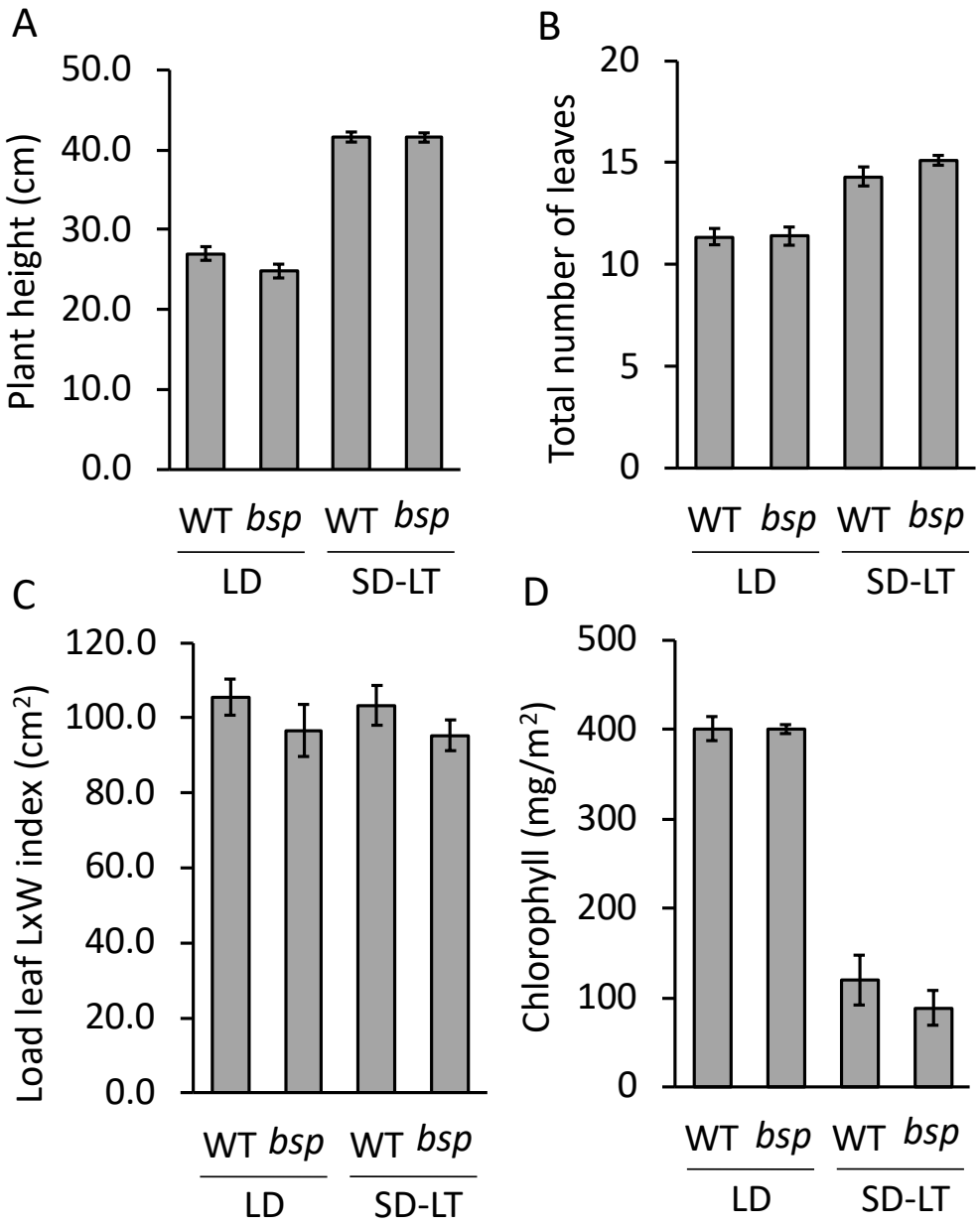

Figure S2-5. Growth and chlorophyll content of wild-type (WT) and BSP RNAi (*bsp*) poplars. Plants were grown in long-day photoperiods (LD), or grown first in LD followed by 6 weeks of short-day (SD) photoperiod plus another 3-5 weeks in SD and low temperature (SD-LT). Measurements were taken before the ^{13}N experiments and the load leaf was the leaf that was fed $^{13}NH_3$. Bars indicate means ± SE.

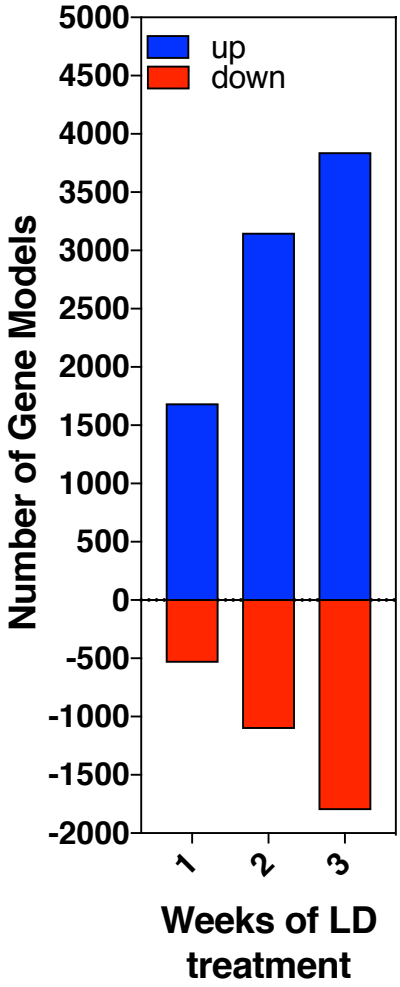

Figure S2-6. Global changes in bark gene expression during growth following dormancy. Number of genes differently expressed (*P*-value ≤ 0.01 and a $\log_2$-fold change ≥ 1.585 or 3-fold change on linear scale), up-regulated (blue) and down-regulated (red) during regrowth for 1, 2 and 3 weeks respectively.

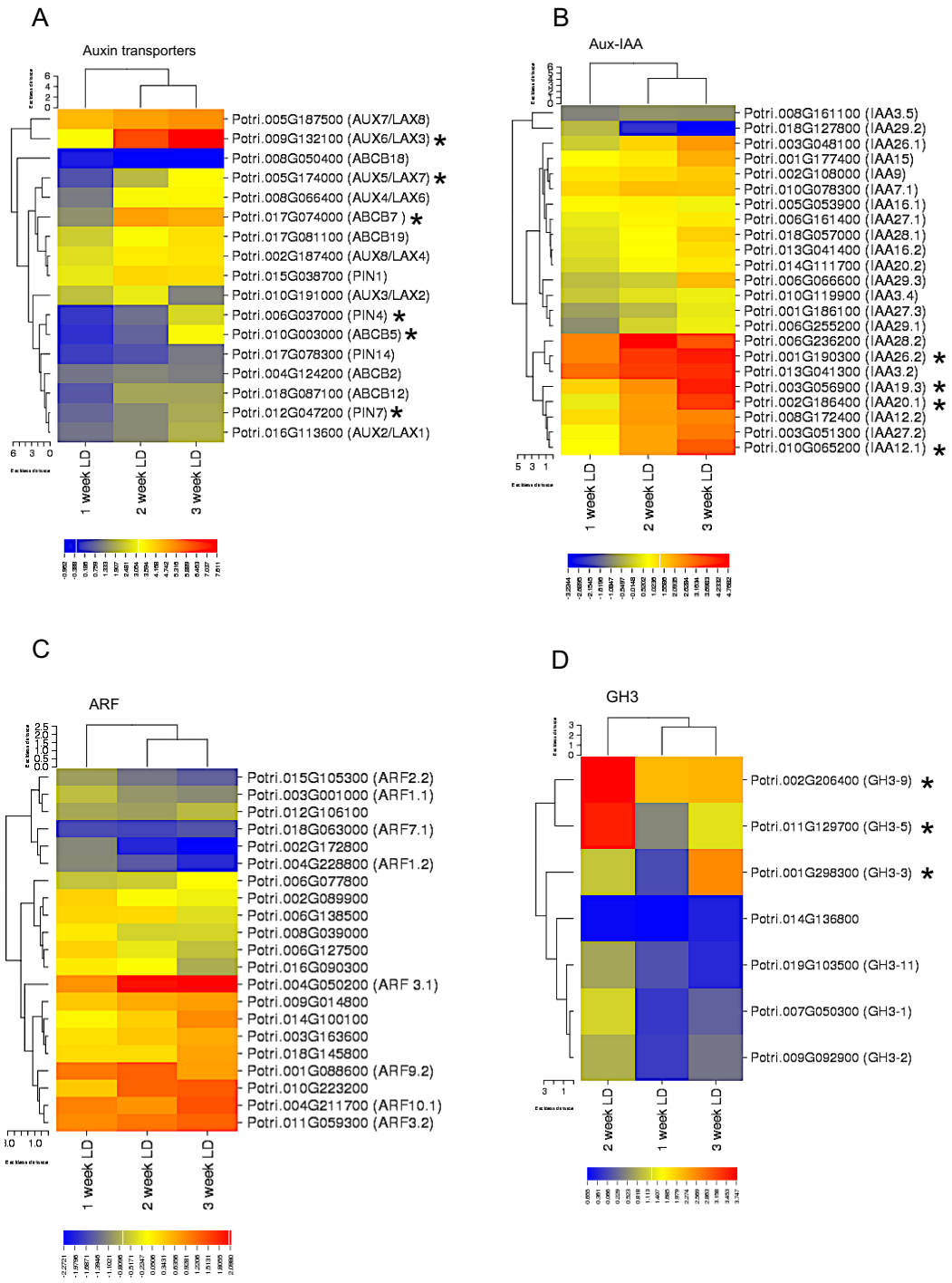

Figure S2-7. Expression profile of auxin transporters and signaling factors in bark during regrowth for 1, 2, 3 weeks following dormancy break. Heatmap was generated using CIMminer (https://discover.nci.nih.gov/cimminer/home.do). Genes with ⋆ indicates genes selected for qRT-PCR verification.

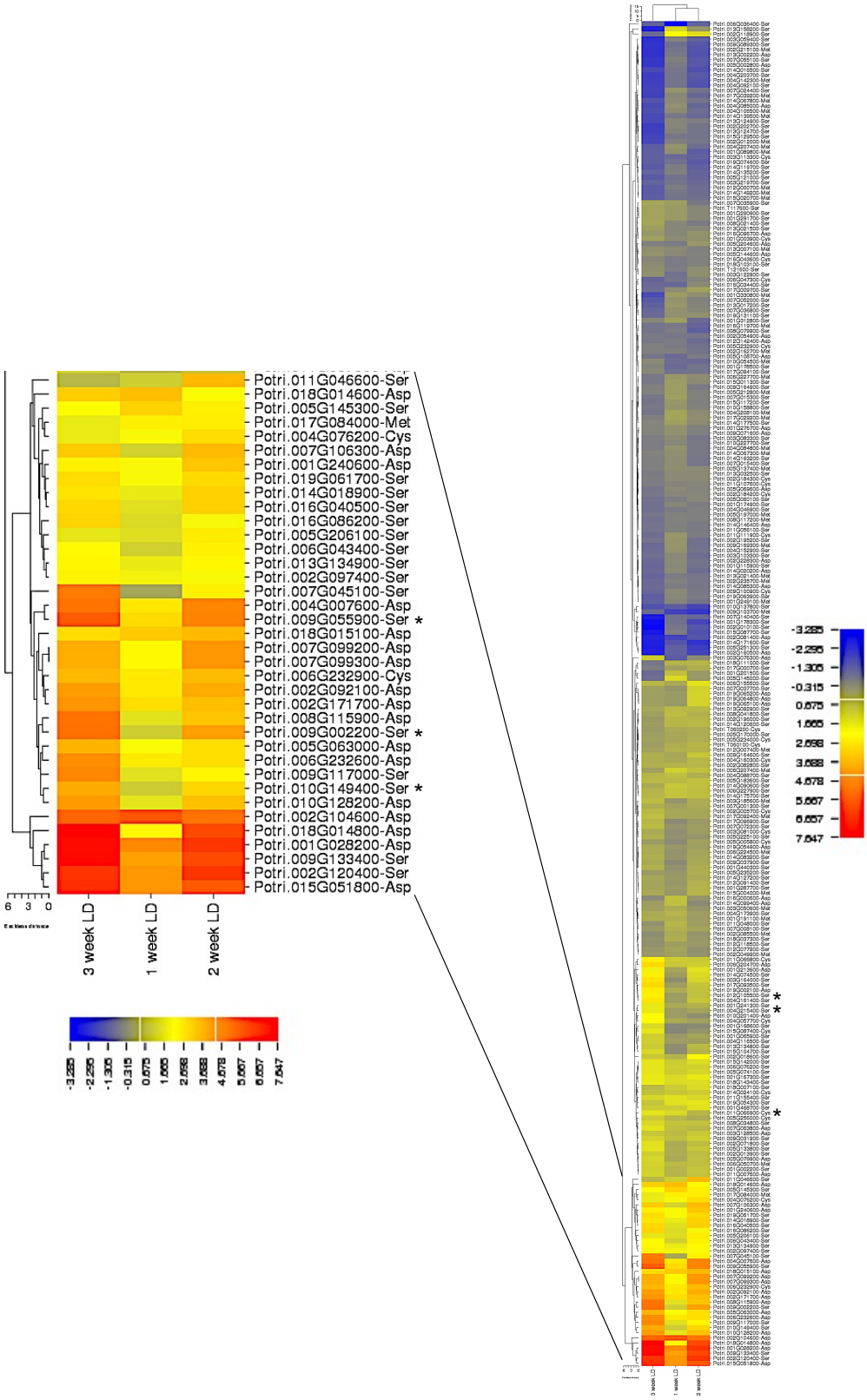
Potri.011G046600-Ser
Potri.018G014600-Asp
Potri.005G145300-Ser
Potri.017G084000-Met
Potri.004G076200-Cys
Potri.007G106300-Asp
Potri.001G240600-Asp
Potri.019G061700-Ser
Potri.014G018900-Ser
Potri.016G040500-Ser
Potri.016G086200-Ser
Potri.005G206100-Ser
Potri.006G043400-Ser
Potri.013G134900-Ser
Potri.002G097400-Ser
Potri.007G045100-Ser
Potri.004G007600-Asp
Potri.009G055900-Ser *
Potri.018G015100-Asp
Potri.007G099200-Asp
Potri.007G099300-Asp
Potri.006G232900-Cys
Potri.002G092100-Asp
Potri.002G171700-Asp
Potri.008G115900-Asp
Potri.009G002200-Ser *
Potri.005G063000-Asp
Potri.006G232600-Asp
Potri.009G117000-Ser
Potri.010G149400-Ser *
Potri.010G128200-Asp
Potri.002G104600-Asp
Potri.018G014800-Asp
Potri.001G028200-Asp
Potri.009G133400-Ser
Potri.002G120400-Ser
Potri.015G051800-Asp
6 3 0
3 week LD
1 week LD
2 week LD
-3.235
-2.295
-1.305
-0.315
0.675
1.665
2.655
3.645
4.635
5.625
6.615
7.605
-3.235
-2.295
-1.305
-0.315
0.675
1.665
2.658
3.648
4.678
5.667
6.657
7.647

Figure S2-8. Expression profile of protease gene in bark during regrowth for 1, 2, 3 weeks following dormancy break. Heatmap was generated using CIMminer. Genes with ⋆ indicates genes selected for qRT-PCR verification.

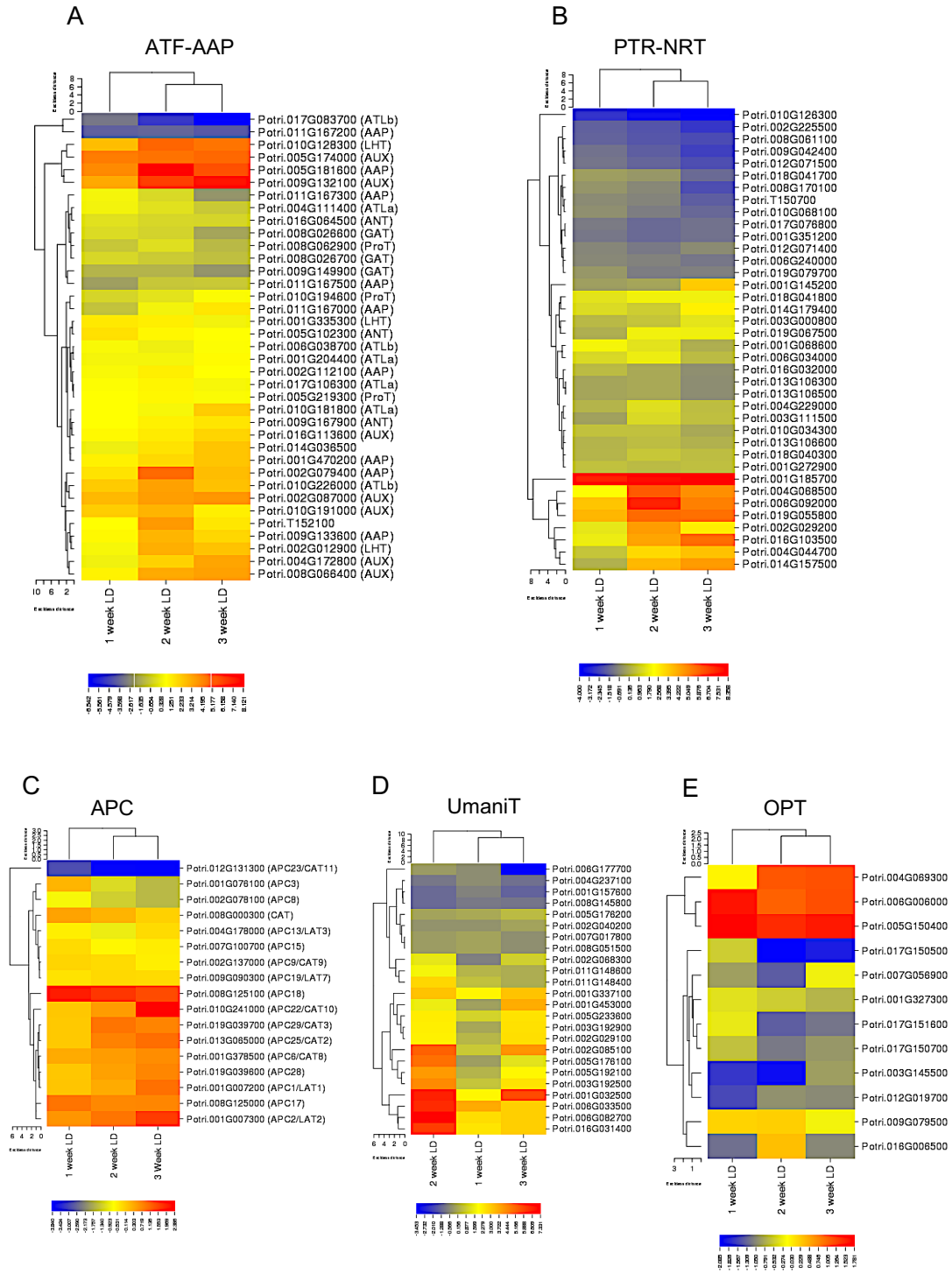

Figure S2-9. Expression profile of amino acid transporter, (A) ATF-AAP family, (B) PTR-NRT family, (C) APC family, (D) UmaniT family and (E) OPT family, in bark

during regrowth for 1, 2, 3 weeks following dormancy break. Heatmap was generated using CIMminer (https://discover.nci.nih.gov/cimminer/home.do).

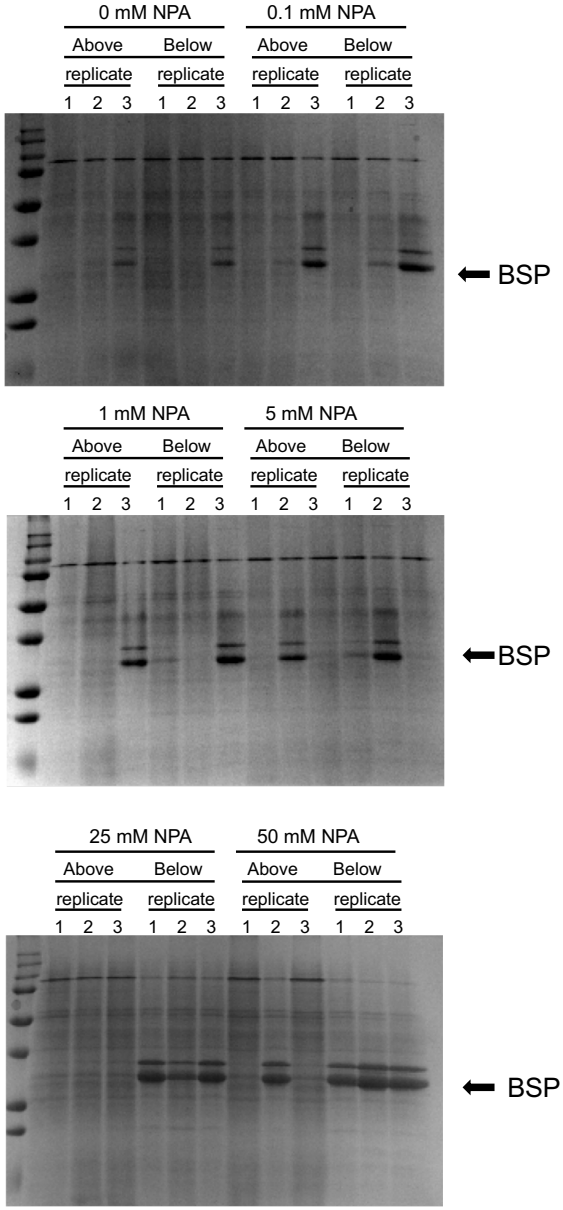

Figure S2-10. BSP abundance in stem with gradient NPA treatment after regrowth for 3 weeks following dormancy break. 0, 0.1, 0.5, 1, 5, 25 and 50 mM NPA mixed with lanolin was applied on poplar stem. Proteins of three replicates from each treatment were analyzed using SDS-PAGE.

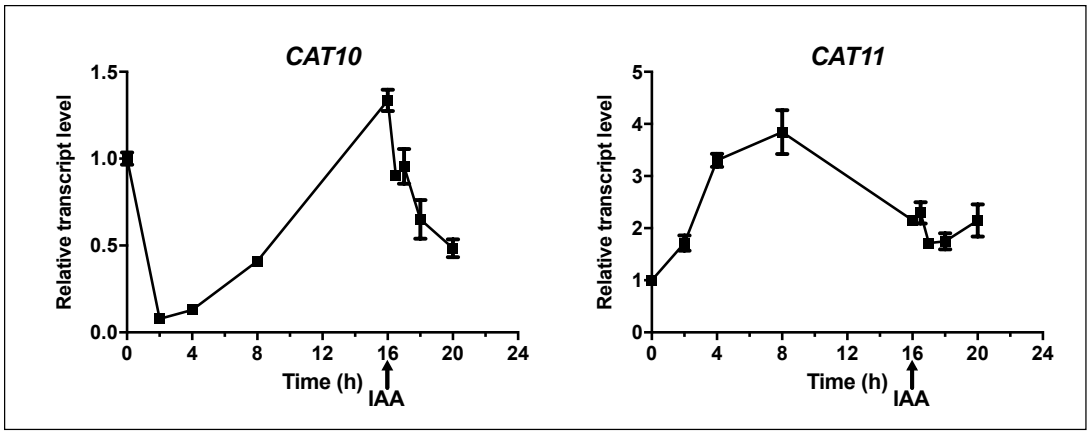

Figure S2-11. Auxin responsiveness of *CAT10* and *CAT11*. *In vitro* grown defoliated stems of poplar (*P. tremula* × *P. alba* hybrid clone INRA 717-1B4) were incubated in growth medium to deplete endogenous auxin. After 16 h of depletion 20 μM IAA was added and incubation was continued for 4 h. Stems were collected at the indicated time points and the relative expression of *CAT10* and *CAT11* was determined by qRT-PCR. At least 3 biological replicates were collected at each time point and error bars indicate mean ± SE.

Appendix B

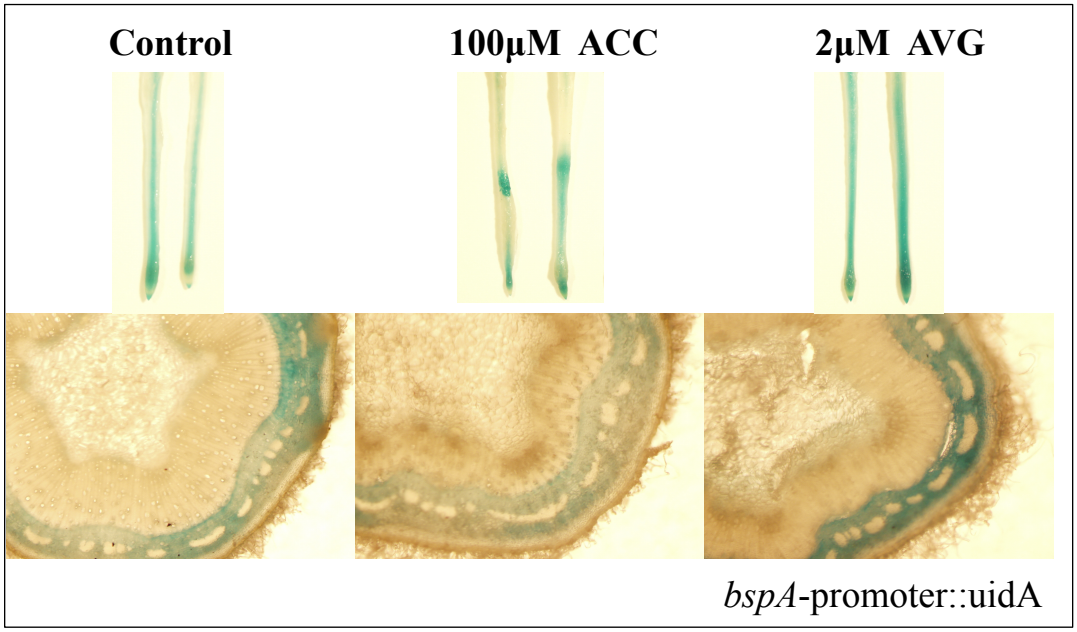

Figure S3-1. . GUS activity of transgenic poplar (*bapA*-promoter::uidA) treated with 100µM ACC or 2µM AVG for 16 h. The cutting stems were hand-sectioned, fixed and stained for GUS activity.

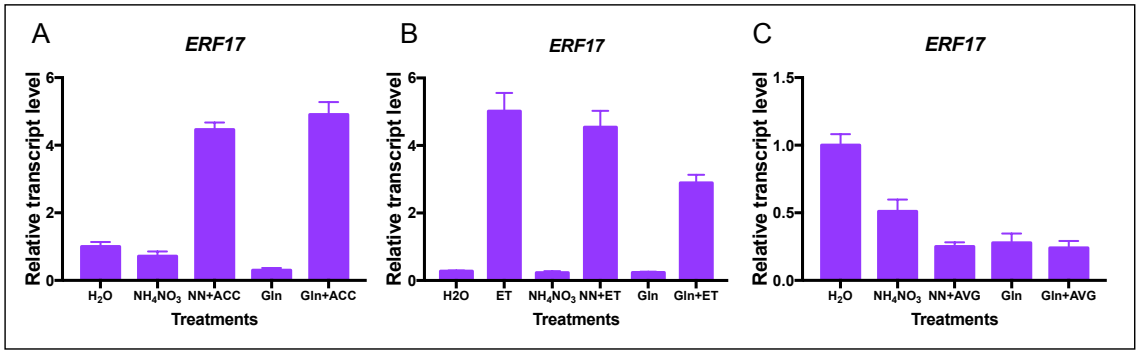

Figure S3-2. Response of *ERF17* to nitrogen plus ethylene manipulation. Relative transcript level of *ERF17* gene in bark treated with 20mM NH_4NO_3 (NN) and 25mM glutamine (Gln) with or without combination of (A) 100µM ACC, (B) 100µM ACC ethephon (ET) and (C) 2µM AVG for 24 h was determined by qRT-PCR.

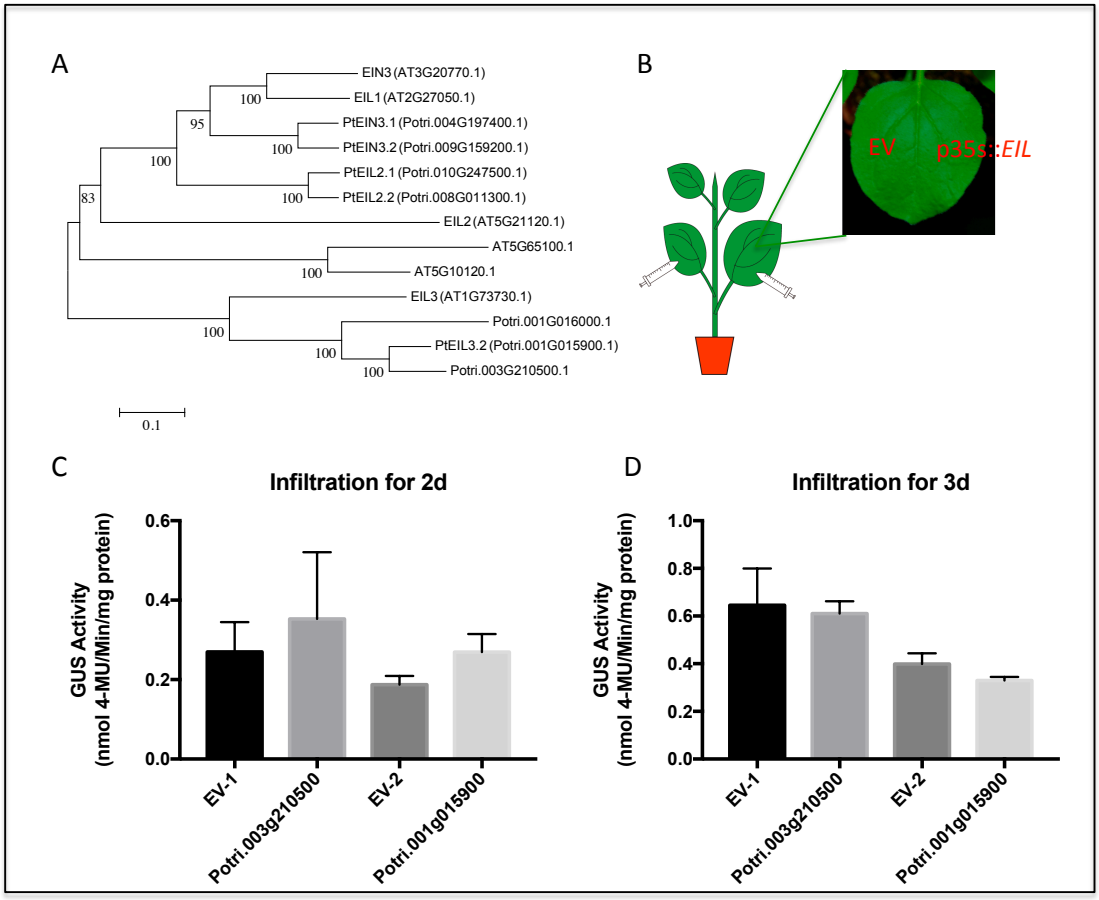

Figure S3-3. Transient expression of two EILs in transgenic tocacco (*bapA*-promoter::uidA). (A) Phylogenetic tree of *Populus* and *Arabidopsis* EIN3/EILs. (B) Scheme of transient expression in tabacco B-6-9-1 (*bspA*-promoter::uidA) leaf. EV, empty vector for negative control. GUS activity was measured after infiltration for (C) 2 days and (D) 3 days.

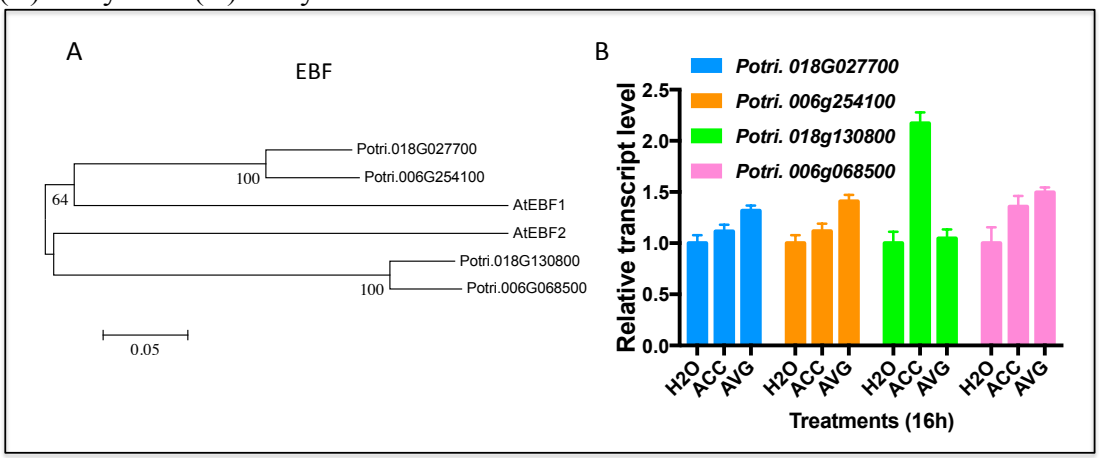

Figure S3-4. Response of *EBF* genes to ACC and AVG treatment. (A) Phylogenetic tree of *Populus* and *Arabidopsis* *EBF* genes. (B) Relative transcript level of *EBF* genes under 100μM ACC and 2μM AVG treatment for 16 h.

Appendix C

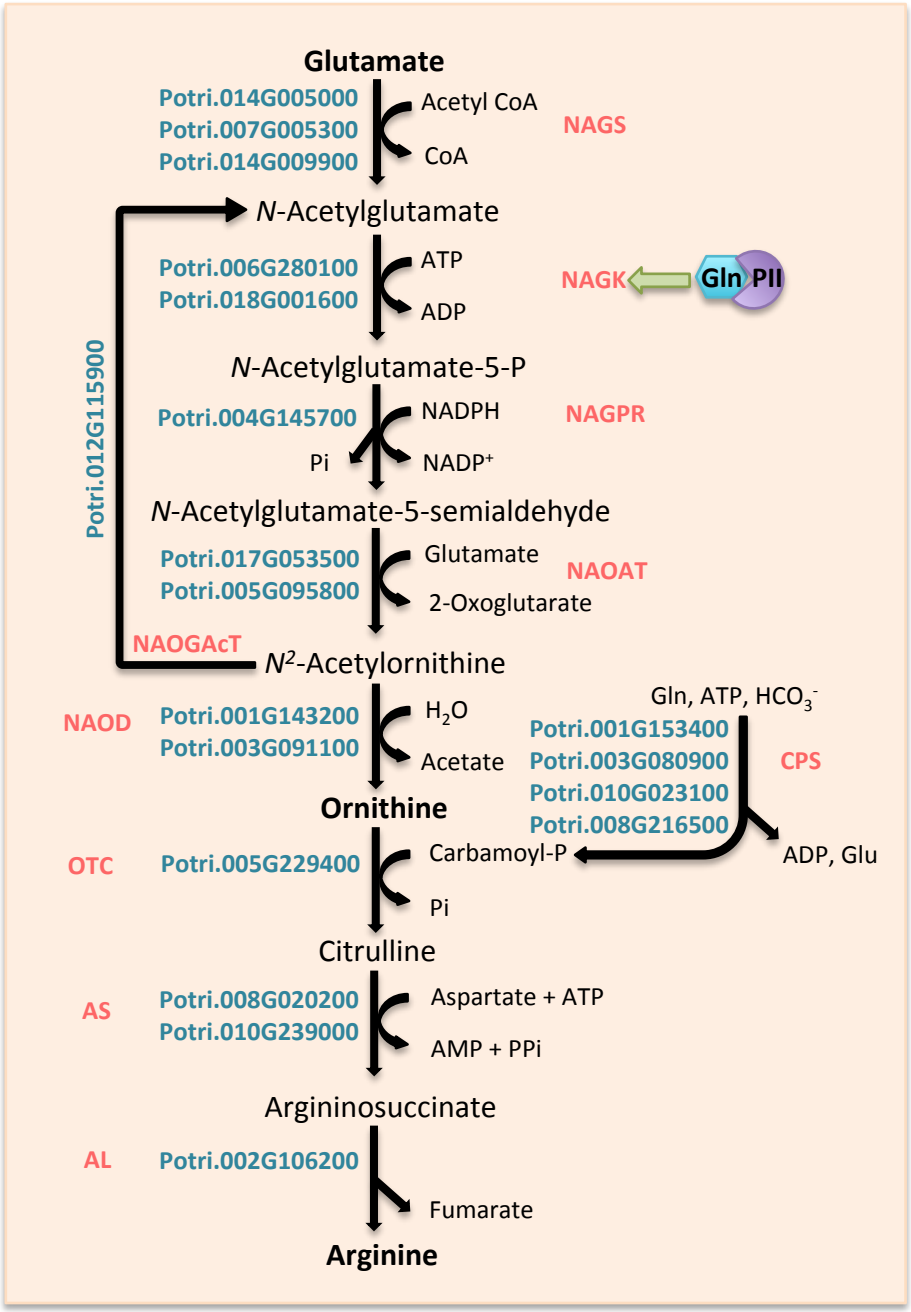

Figure S4-1. Pathway for arginine biosynthesis and genes coding for enzymes in the pathway.

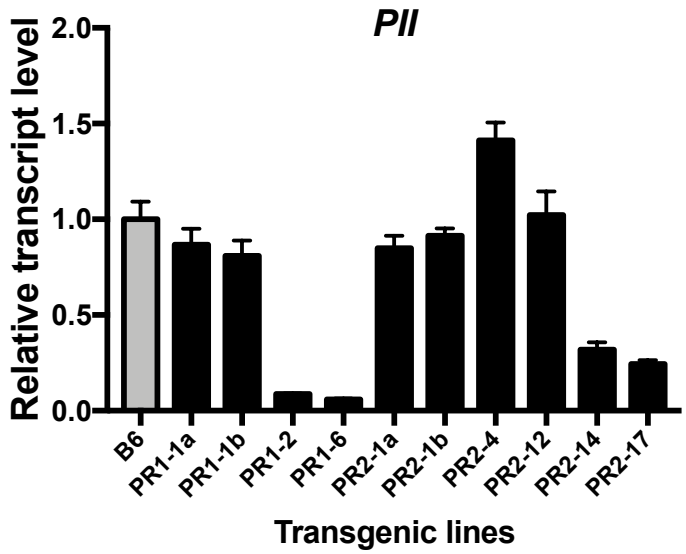

Figure S4-2. Screening of PII RNAi knockdown lines using qRT-PCR.

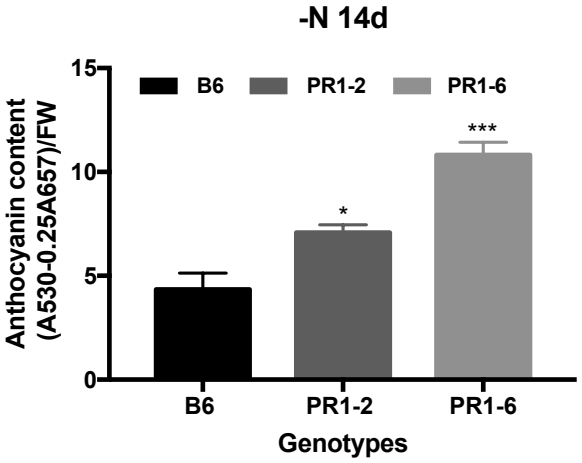

Figure S4-3. Increased anthocyanin accumulation was observed in tissue-cultured PII RNAi poplars under N deficient condition for 14 days.

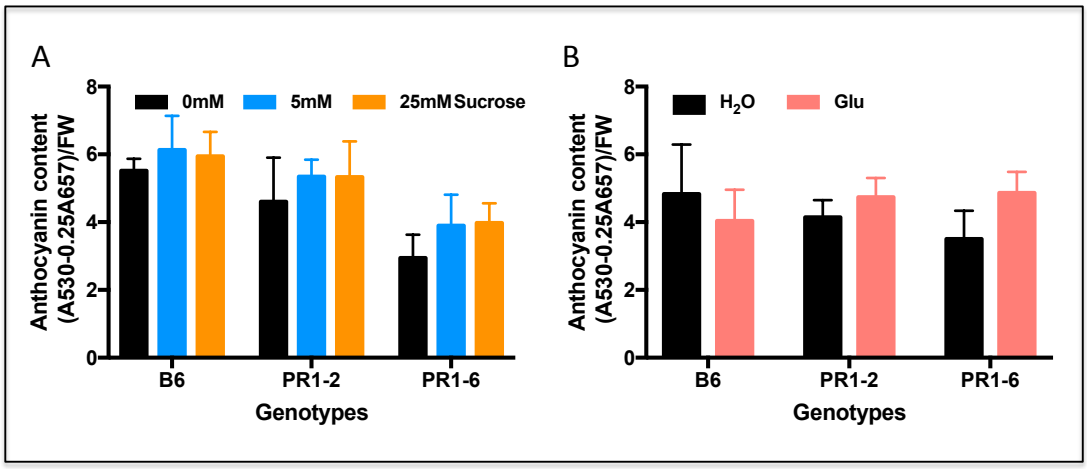

Figure S4-4. The effect of carbon source on anthocyanin accumulation in PII RNAi poplars. Excised stems of PII RNAi poplars PR1-2 and PR1-6 were treated with 5mM and 25mM sucrose or 25mM glucose for 24h and the leaves were collected for anthocyanin measurement.

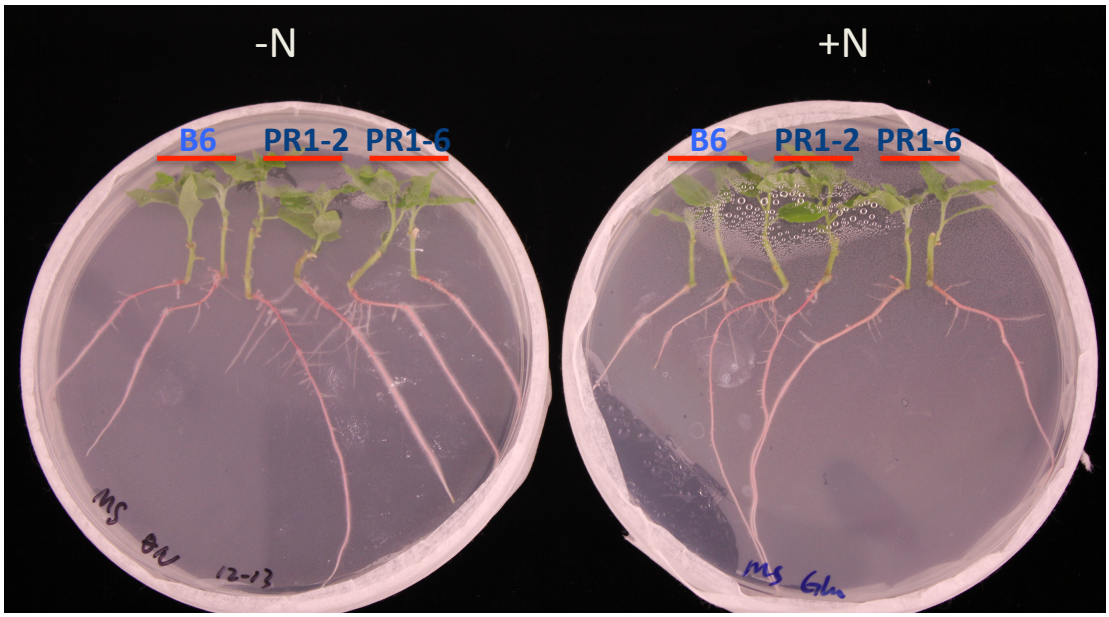

Figure S4-5. Photograph of *in vitro* cultured PII RNAi lines grown on MS with (+N) or without (-N) 1mM glutamine for 7 days.

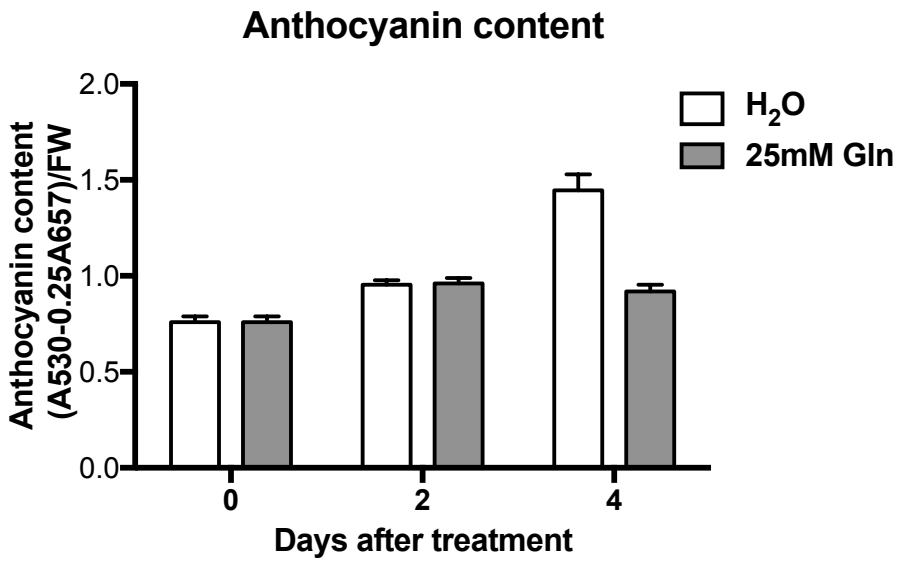

Figure S4-6. Effect of glutamine treatment on anthocyanin accumulation in Nisqually leaves. Excised Nisqually stems were treated with 25mM glutamine for 0, 2 and 4 days and the leaves were used for anthocyanin measurement.

Bibliography

Aerts, R. (1990). Nutrient use efficiency in evergreen and deciduous species from heathlands. Oecologia *84*, 391–397.

Allwright, M.R., and Taylor, G. (2016). Molecular Breeding for Improved Second Generation Bioenergy Crops. Trends Plant Sci. *21*, 43–54.

Alonso, J.M., Hirayama, T., Roman, G., Nourizadeh, S., and Ecker, J.R. (1999). EIN2, a Bifunctional Transducer of Ethylene and Stress Responses in Arabidopsis. Science *284*, 2148–2152.

Al-Sady, B., Ni, W., Kircher, S., Schäfer, E., and Quail, P.H. (2006). Photoactivated Phytochrome Induces Rapid PIF3 Phosphorylation Prior to Proteasome-Mediated Degradation. Mol. Cell *23*, 439–446.

Amon, J., Titgemeyer, F., and Burkovski, A. (2010). Common patterns – unique features: nitrogen metabolism and regulation in Gram-positive bacteria. FEMS Microbiol. Rev. *34*, 588–605.

An, F., Zhao, Q., Ji, Y., Li, W., Jiang, Z., Yu, X., Zhang, C., Han, Y., He, W., Liu, Y., et al. (2010). Ethylene-Induced Stabilization of ETHYLENE INSENSITIVE3 and EIN3-LIKE1 Is Mediated by Proteasomal Degradation of EIN3 Binding F-Box 1 and 2 That Requires EIN2 in Arabidopsis. Plant Cell *22*, 2384–2401.

Anderson, J.M. (1991). Jasmonic acid-dependent increase in vegetative storage protein in soybean tissue cultures. J. Plant Growth Regul. *10*, 5.

Andersson, A., Keskitalo, J., Sjödin, A., Bhalerao, R., Sterky, F., Wissel, K., Tandre, K., Aspeborg, H., Moyle, R., Ohmiya, Y., et al. (2004). A transcriptional timetable of autumn senescence. Genome Biol. *5*, R24.

Andersson-Gunnerås, S., Hellgren, J.M., Björklund, S., Regan, S., Moritz, T., and Sundberg, B. (2003). Asymmetric expression of a poplar ACC oxidase controls ethylene production during gravitational induction of tension wood. Plant J. *34*, 339–349.

Andrews, D.L., Beames, B., Summers, M.D., and Park, W.D. (1988). Characterization of the lipid acyl hydrolase activity of the major potato (Solanum tuberosum) tuber protein, patatin, by cloning and abundant expression in a baculovirus vector. Biochem. J. *252*, 199–206.

Avila-Ospina, L., Moison, M., Yoshimoto, K., and Masclaux-Daubresse, C. (2014). Autophagy, plant senescence, and nutrient recycling. J. Exp. Bot. *65*, 3799–3811.

Babst, B.A., and Coleman, G.D. (2018). Seasonal nitrogen cycling in temperate trees: Transport and regulatory mechanisms are key missing links. Plant Sci. *270*, 268–277.

Babst, B.A., Karve, A.A., and Judt, T. (2013). Radio-Metabolite Analysis of Carbon-11 Biochemical Partitioning to Non-Structural Carbohydrates for Integrated Metabolism and Transport Studies. Plant Cell Physiol. *54*, 1016–1025.

Bannan, M.W. (1955). The vascular cambium and radial growth in Thuja occidentalis L. Can. J. Bot. *33*, 113–138.

Baud, S., Feria Bourrellier, A.B., Azzopardi, M., Berger, A., Dechorgnat, J., Daniel-Vedele, F., Lepiniec, L., Miquel, M., Rochat, C., Hodges, M., et al. (2010). PII is induced by WRINKLED1 and fine-tunes fatty acid composition in seeds of Arabidopsis thaliana. Plant J. *64*, 291–303.

Beardmore, T., Wetzel, S., and Kalous, M. (2000). Interactions of airborne methyl jasmonate with vegetative storage protein gene and protein accumulation and biomass partitioning in Populus plants. Can. J. For. Res. *30*, 1106–1113.

Benjamini, Y., and Hochberg, Y. (1995). Controlling the False Discovery Rate: A Practical and Powerful Approach to Multiple Testing. J. R. Stat. Soc. Ser. B Methodol. *57*, 289–300.

Berger, S., Bell, E., Sadka, A., and Mullet, J.E. (1995). Arabidopsis thaliana Atvsp is homologous to soybean VspA and VspB, genes encoding vegetative storage protein acid phosphatases, and is regulated similarly by methyl jasmonate, wounding, sugars, light and phosphate. Plant Mol. Biol. *27*, 933–942.

Besson-Bard, A., Pugin, A., and Wendehenne, D. (2008). New Insights into Nitric Oxide Signaling in Plants. Annu. Rev. Plant Biol. *59*, 21–39.

Bhalerao, R. (2003). Gene Expression in Autumn Leaves. Plant Physiol. *131*, 430–442.

Binder, B.M., Walker, J.M., Gagne, J.M., Emborg, T.J., Hemmann, G., Bleecker, A.B., and Vierstra, R.D. (2007). The Arabidopsis EIN3 Binding F-Box Proteins EBF1 and EBF2 Have Distinct but Overlapping Roles in Ethylene Signaling. Plant Cell *19*, 509–523.

Black, B.L., Parmentier-Line, C.M., Fuchigami, L.H., and Coleman, G.D. (2001). Ecotypic and genetic variation in poplar bark storage protein gene expression and accumulation. Tree Physiol. *21*, 1289–1297.

Boerner, R. (1984). Foliar Nutrient Dynamics and Nutrient Use Efficiency of Four Deciduous Tree Species in Relation to Site Fertility. J. Appl. Ecol. *21*, 1029–1040.

Bögre, L., Henriques, R., and Magyar, Z. (2013). TOR tour to auxin. EMBO J. *32*, 1069–1071.

Bourrellier, A.B.F., Valot, B., Guillot, A., Ambard-Bretteville, F., Vidal, J., and Hodges, M. (2010). Chloroplast acetyl-CoA carboxylase activity is 2-oxoglutarate–

regulated by interaction of PII with the biotin carboxyl carrier subunit. Proc. Natl. Acad. Sci. *107*, 502–507.

Bravo, K., Marcolini, G., Sorrenti, G., Baldi, E., Quartieri, M., and Toselli, M. (2017). Effect of time of application on nitrogen uptake, partitioning, and remobilization in walnut trees. J. Plant Nutr. *40*, 719–725.

Brown, R., E., Jarvis, K., L., and Hyland, K., J. (1989). Protein measurement using bicinchoninic Acid: elimination of interfering substances. Anal. Biochem. *180*, 136–139.

Brychkova, G., Alikulov, Z., Fluhr, R., and Sagi, M. (2008). A critical role for ureides in dark and senescence-induced purine remobilization is unmasked in the Atxdh1 Arabidopsis mutant. Plant J. *54*, 496–509.

Caldana, C., Li, Y., Leisse, A., Zhang, Y., Bartholomaeus, L., Fernie, A.R., Willmitzer, L., and Giavalisco, P. (2013). Systemic analysis of inducible target of rapamycin mutants reveal a general metabolic switch controlling growth in Arabidopsis thaliana. Plant J. *73*, 897–909.

Carraro, N., Tisdale-Orr, T.E., Clouse, R.M., Knöller, A.S., and Spicer, R. (2012). Diversification and Expression of the PIN, AUX/LAX, and ABCB Families of Putative Auxin Transporters in Populus. Front. Plant Sci. *3*.

Carvalho, R.F., Campos, M.L., and Azevedo, R.A. (2011). The Role of Phytochrome in Stress Tolerance. J. Integr. Plant Biol. *53*, 920–929.

Casal, J.J. (2013). Photoreceptor Signaling Networks in Plant Responses to Shade. Annu. Rev. Plant Biol. *64*, 403–427.

Castro-Rodríguez, V., García-Gutiérrez, A., Canales, J., Avila, C., Kirby, E.G., and Cánovas, F.M. (2011). The glutamine synthetase gene family in Populus. BMC Plant Biol. *11*, 119.

Chaiwanon, J., Wang, W., Zhu, J.-Y., Oh, E., and Wang, Z.-Y. (2016). Information Integration and Communication in Plant Growth Regulation. Cell *164*, 1257–1268.

Chang, C., and Shockey, J.A. (1999). The ethylene-response pathway: signal perception to gene regulation. Curr. Opin. Plant Biol. *2*, 352–358.

Chang, C., Kwok, S.F., Bleecker, A.B., and Meyerowitz, E.M. (1993). Arabidopsis ethylene-response gene ETR1: similarity of product to two-component regulators. Science *262*, 539–544.

Chantranupong, L., Wolfson, R.L., and Sabatini, D.M. (2015). Nutrient-Sensing Mechanisms across Evolution. Cell *161*, 67–83.

Chapin, F.S., and Kedrowski, R.A. (1983). Seasonal changes in nitrogen and phosphorus fractions and autumn retranslocation in evergreen and deciduous taiga trees. Ecology *64*, 376–391.

Chapin, F.S., Schulze, E.D., and Mooney, H.A. (1990). The ecology and economics of storage in plants. Annu. Rev. Ecol. Syst. 423–447.

Chellamuthu, V.R., Alva, V., and Forchhammer, K. (2012). From cyanobacteria to plants: conservation of PII functions during plastid evolution. Planta *237*, 451–462.

Chellamuthu, V.R., Alva, V., and Forchhammer, K. (2013). From cyanobacteria to plants: conservation of PII functions during plastid evolution. Planta *237*, 451–462.

Chellamuthu, V.-R., Ermilova, E., Lapina, T., Lüddecke, J., Minaeva, E., Herrmann, C., Hartmann, M.D., and Forchhammer, K. (2014). A Widespread Glutamine-Sensing Mechanism in the Plant Kingdom. Cell *159*, 1188–1199.

Chen, M., and Chory, J. (2011). Phytochrome signaling mechanisms and the control of plant development. Trends Cell Biol. *21*, 664–671.

Chen, Y.M., Ferrar, T.S., Lohmeir-Vogel, E., Morrice, N., Mizuno, Y., Berenger, B., Ng, K.K.S., Muench, D.G., and Moorhead, G.B.G. (2006). The PII Signal Transduction Protein of Arabidopsis thaliana Forms an Arginine-regulated Complex with Plastid N-Acetyl Glutamate Kinase. J. Biol. Chem. *281*, 5726–5733.

Cheng, L., Ma, F., and Ranwala, D. (2004). Nitrogen storage and its interaction with carbohydrates of young apple trees in response to nitrogen supply. Tree Physiol. *24*, 91–98.

van Cleve, B., and Apel, K. (1993). Induction by nitrogen and low temperature of storage-protein synthesis in poplar trees exposed to long days. Planta *189*, 157–160.

van Cleve, B., Clausen, S., and Sauter, J.J. (1988). Immunochemical Localization of a Storage Protein in Poplar Wood. J. Plant Physiol. *133*, 371–374.

Coleman, G.D., Chen, T.H.H., Ernst, S.G., and Fuchigami, L. (1991). Photoperiod Control of Poplar Bark Storage Protein Accumulation. Plant Physiol. *96*, 686–692.

Coleman, G.D., Chen, T.H.H., and Fuchigami, L.H. (1992). Complementary DNA Cloning of Poplar Bark Storage Protein and Control of Its Expression by Photoperiod. Plant Physiol. *98*, 687–693.

Coleman, G.D., Englert, J.M., Chen, T.H., and Fuchigami, L.H. (1993). Physiological and environmental requirements for poplar (Populus deltoides) bark storage protein degradation. Plant Physiol. *102*, 53–59.

Coleman, G.D., Banados, M.P., and Chen, T.H. (1994). Poplar bark storage protein and a related wound-induced gene are differentially induced by nitrogen. Plant Physiol. *106*, 211–215.

Cooke, J.E.K., and Weih, M. (2005). Nitrogen storage and seasonal nitrogen cycling in Populus: bridging molecular physiology and ecophysiology. New Phytol. *167*, 19–30.

Cooke, J.E.K., Brown, K.A., Wu, R., and Davis, J.M. (2003). Gene expression associated with N-induced shifts in resource allocation in poplar. Plant Cell Environ. *26*, 757–770.

Cooke, J.E.K., Martin, T.A., and Davis, J.M. (2005). Short-term physiological and developmental responses to nitrogen availability in hybrid poplar. New Phytol. *167*, 41–52.

Corpas, F.J., Palma, J.M., Río, L.A.D., and Barroso, J.B. (2009). Evidence supporting the existence of l-arginine-dependent nitric oxide synthase activity in plants. New Phytol. *184*, 9–14.

Côté, B., Vogel, C.S., and Dawson, J.O. (1989). Autumnal changes in tissue nitrogen of autumn olive, black alder and eastern cottonwood. Plant Soil *118*, 23–32.

Côtté, B., and Dawson, J.O. (1986). Autumnal changes in total nitrogen, salt-extractable proteins and amino acids in leaves and adjacent bark of black alder, eastern cottonwood and white basswood. Physiol. Plant. *67*, 102–108.

Couturier, J., Doidy, J., Guinet, F., Wipf, D., Blaudez, D., and Chalot, M. (2010). Glutamine, arginine and the amino acid transporter Pt-CAT11 play important roles during senescence in poplar. Ann. Bot. *105*, 1159–1169.

Crowther, T.W., Glick, H.B., Covey, K.R., Bettigole, C., Maynard, D.S., Thomas, S.M., Smith, J.R., Hintler, G., Duguid, M.C., Amatulli, G., et al. (2015). Mapping tree density at a global scale. Nature *525*, 201–205.

Damme, E.J.M.V., Hao, Q., Barre, A., Rougé, P., Leuven, F.V., and Peumans, W.J. (2000). Major Protein of Resting Rhizomes of Calystegia sepium (Hedge Bindweed) Closely Resembles Plant RNases But Has No Enzymatic Activity. Plant Physiol. *122*, 433–446.

D'Apuzzo, E., Valkov, V.T., Parlati, A., Omrane, S., Barbulova, A., Sainz, M.M., Lentini, M., Esposito, S., Rogato, A., and Chiurazzi, M. (2014). PII Overexpression in Lotus japonicus Affects Nodule Activity in Permissive Low-Nitrogen Conditions and Increases Nodule Numbers in High Nitrogen Treated Plants. Mol. Plant. Microbe Interact. *28*, 432–442.

Davis, J.M., Egelkrout, E.E., Coleman, G.D., Chen, T.H., Haissig, B.E., Riemenschneider, D.E., and Gordon, M.P. (1993). A family of wound-induced genes

in Populus shares common features with genes encoding vegetative storage proteins. Plant Mol. Biol. *23*, 135–143.

DeWald, D.B., Mason, H.S., and Mullet, J.E. (1992). The soybean vegetative storage proteins VSP alpha and VSP beta are acid phosphatases active on polyphosphates. J. Biol. Chem. *267*, 15958–15964.

Dobrenel, T., Marchive, C., Sormani, R., Moreau, M., Mozzo, M., Montané, M., Menand, B., Robaglia, C., and Meyer, C. (2011). Regulation of plant growth and metabolism by the TOR kinase. Biochem. Soc. Trans. *39*, 477–481.

Du, Z., Zhou, X., Ling, Y., Zhang, Z., and Su, Z. (2010). agriGO: a GO analysis toolkit for the agricultural community. Nucleic Acids Res. *38*, W64–W70.

Eckstein, R.L., Karlsson, P.S., and Weih, M. (1999). Leaf life span and nutrient resorption as determinants of plant nutrient conservation in temperate-arctic regions. New Phytol. *143*, 177–189.

Ermilova, E.V., and Forchhammer, K. (2013). PII signaling proteins of cyanobacteria and green algae. New features of conserved proteins. Russ. J. Plant Physiol. *60*, 483–490.

Faus, I., Zabalza, A., Santiago, J., Nebauer, S.G., Royuela, M., Serrano, R., and Gadea, J. (2015). Protein kinase GCN2 mediates responses to glyphosate in Arabidopsis. BMC Plant Biol. *15*, 14.

Felsenstein, J. (1985). Confidence Limits on Phylogenies: An Approach Using the Bootstrap. Evolution *39*, 783–791.

Ferguson, C.W. (1968). Bristlecone Pine: Science and Esthetics: A 7100-year tree-ring chronology aids scientists; old trees draw visitors to California mountains. Science *159*, 839–846.

Feria Bourrellier, A.B., Ferrario-Méry, S., Vidal, J., and Hodges, M. (2009). Metabolite regulation of the interaction between Arabidopsis thaliana PII and N-acetyl-l-glutamate kinase. Biochem. Biophys. Res. Commun. *387*, 700–704.

Ferrario-Méry, S., Bouvet, M., Leleu, O., Savino, G., Hodges, M., and Meyer, C. (2005). Physiological characterisation of Arabidopsis mutants affected in the expression of the putative regulatory protein PII. Planta *223*, 28–39.

Ferrario-Méry, S., Besin, E., Pichon, O., Meyer, C., and Hodges, M. (2006). The regulatory PII protein controls arginine biosynthesis in Arabidopsis. FEBS Lett. *580*, 2015–2020.

Fife, D.N., and Nambiar, E.K.S. (1982). Accumulation and Retranslocation of Mineral Nutrients in Developing Needles in Relation to Seasonal Growth of Young Radiata Pine Trees. Ann. Bot. *50*, 817–829.

Finlayson, S.A., Lee, I.-J., and Morgan, P.W. (1998). Phytochrome B and the Regulation of Circadian Ethylene Production in Sorghum. Plant Physiol. *116*, 17–25.

Finlayson, S.A., Lee, I.-J., Mullet, J.E., and Morgan, P.W. (1999). The Mechanism of Rhythmic Ethylene Production in Sorghum. The Role of Phytochrome B and Simulated Shading. Plant Physiol. *119*, 1083–1090.

Fokina, O., Chellamuthu, V.-R., Forchhammer, K., and Zeth, K. (2010). Mechanism of 2-oxoglutarate signaling by the Synechococcus elongatus PII signal transduction protein. Proc. Natl. Acad. Sci. *107*, 19760–19765.

Forchhammer, K. (2008). PII signal transducers: novel functional and structural insights. Trends Microbiol. *16*, 65–72.

Forchhammer, K., and Lüddecke, J. (2016). Sensory properties of the PII signalling protein family. FEBS J. *283*, 425–437.

Fracheboud, Y., Luquez, V., Bjorken, L., Sjodin, A., Tuominen, H., and Jansson, S. (2009). The Control of Autumn Senescence in European Aspen. Plant Physiol. *149*, 1982–1991.

Frak, E., Millard, P., Roux, X.L., Guillaumie, S., and Wendler, R. (2002). Coupling Sap Flow Velocity and Amino Acid Concentrations as an Alternative Method to 15N Labeling for Quantifying Nitrogen Remobilization by Walnut Trees. Plant Physiol. *130*, 1043–1053.

Frink, C.R., Waggoner, P.E., and Ausubel, J.H. (1999). Nitrogen fertilizer: Retrospect and prospect. Proc. Natl. Acad. Sci. *96*, 1175–1180.

Funk, V., Kositsup, B., Zhao, C., and Beers, E.P. (2002). The Arabidopsis Xylem Peptidase XCP1 Is a Tracheary Element Vacuolar Protein That May Be a Papain Ortholog. Plant Physiol. *128*, 84–94.

Gagne, J.M., Smalle, J., Gingerich, D.J., Walker, J.M., Yoo, S.-D., Yanagisawa, S., and Vierstra, R.D. (2004). Arabidopsis EIN3-binding F-box 1 and 2 form ubiquitin-protein ligases that repress ethylene action and promote growth by directing EIN3 degradation. Proc. Natl. Acad. Sci. U. S. A. *101*, 6803–6808.

Gana, J.A., Kalengamaliro, N.E., Cunningham, S.M., and Volenec, J.J. (1998). Expression of β-Amylase from Alfalfa Taproots. Plant Physiol. *118*, 1495–1506.

García-Lorenzo, M., Sjödin, A., Jansson, S., and Funk, C. (2006). Protease gene families in Populus and Arabidopsis. BMC Plant Biol. *6*, 30.

Gérant, D., Pluchon, M., Mareschal, L., Koutika, L.S., and Epron, D. (2017). Seasonality of nitrogen partitioning (non-structural vs structural) in the leaves and woody tissues of tropical eucalypts experiencing a marked dry season. Tree Physiol. *37*, 790–798.

Godfray, H.C.J., Beddington, J.R., Crute, I.R., Haddad, L., Lawrence, D., Muir, J.F., Pretty, J., Robinson, S., Thomas, S.M., and Toulmin, C. (2010). Food Security: The Challenge of Feeding 9 Billion People. Science *327*, 812–818.

Good, A.G., Shrawat, A.K., and Muench, D.G. (2004). Can less yield more? Is reducing nutrient input into the environment compatible with maintaining crop production? Trends Plant Sci. *9*, 597–605.

Guak, S., Neilsen, D., Millard, P., Wendler, R., and Neilsen, G.H. (2003). Determining the role of N remobilization for growth of apple (Malus domestica Borkh.) trees by measuring xylem-sap N flux. J. Exp. Bot. *54*, 2121–2131.

Guo, H., and Ecker, J.R. (2003). Plant Responses to Ethylene Gas Are Mediated by SCFEBF1/EBF2-Dependent Proteolysis of EIN3 Transcription Factor. Cell *115*, 667–677.

Guranowski, A. (1982). Purine Catabolism in Plants: Purification and Some Properties of Inosine Nucleosidase from Yellow Lupin (Lupinus Luteus L.) Seeds. Plant Physiol. *70*, 344–349.

Harms, U., and Sauter, J.J. (1991). Storage Proteins in the Wood of Taxodiaceae and of Taxus. J. Plant Physiol. *138*, 497–499.

Henriques, R., Bögre, L., Horváth, B., and Magyar, Z. (2014). Balancing act: matching growth with environment by the TOR signalling pathway. J. Exp. Bot. *65*, 2691–2701.

Herman, E.M., and Larkins, B.A. (1999). Protein Storage Bodies and Vacuoles. Plant Cell *11*, 601–613.

Hermans, C., Hammond, J.P., White, P.J., and Verbruggen, N. (2006). How do plants respond to nutrient shortage by biomass allocation? Trends Plant Sci. *11*, 610–617.

Herrero, A., Muro-Pastor, A.M., and Flores, E. (2001). Nitrogen Control in Cyanobacteria. J. Bacteriol. *183*, 411–425.

Hesberg, C., Hänsch, R., Mendel, R.R., and Bittner, F. (2004). Tandem Orientation of Duplicated Xanthine Dehydrogenase Genes from Arabidopsis thaliana DIFFERENTIAL GENE EXPRESSION AND ENZYME ACTIVITIES. J. Biol. Chem. *279*, 13547–13554.

van der Hoorn, R.A.L. (2008). Plant Proteases: From Phenotypes to Molecular Mechanisms. Annu. Rev. Plant Biol. *59*, 191–223.

Hörtensteiner, S., and Feller, U. (2002). Nitrogen metabolism and remobilization during senescence. J. Exp. Bot. *53*, 927–937.

Howe, G.T., Gardner, G., Hackett, W.P., and Furnier, G.R. (1996). Phytochrome control of short-day-induced bud set in black cottonwood. Physiol. Plant. *97*, 95–103.

Hsieh, M.-H., Lam, H.-M., Loo, F.J. van de, and Coruzzi, G. (1998). A PII-like protein in Arabidopsis: Putative role in nitrogen sensing. Proc. Natl. Acad. Sci. *95*, 13965–13970.

Hu, R., Wang, J., Ji, Y., Song, Y., and Yang, S. (2012). Overexpression of poplar wounding-inducible genes in Arabidopsis caused improved resistance against Helicoverpa armigera (Hübner) larvae. Breed. Sci. *62*, 288–291.

Huergo, L.F., Chandra, G., and Merrick, M. (2013). PII signal transduction proteins: nitrogen regulation and beyond. FEMS Microbiol. Rev. *37*, 251–283.

Igamberdiev, A.U., Eprintsev, A.T., Fedorin, D.N., and Popov, V.N. (2014). Phytochrome-mediated regulation of plant respiration and photorespiration. Plant Cell Environ. *37*, 290–299.

Islam, N., Li, G., Garrett, W.M., Lin, R., Sriram, G., Cooper, B., and Coleman, G.D. (2015). Proteomics of Nitrogen Remobilization in Poplar Bark. J. Proteome Res. *14*, 1112–1126.

Jasoni, R.L., Cothren, J.T., Morgan, P.W., and Sohan, D.E. (2000). Circadian ethylene production in cotton. Plant Growth Regul. *36*, 127–133.

Jefferson, R.A. (1987). Assaying chimeric genes in plants: The GUS gene fusion system. Plant Mol. Biol. Report. *5*, 387–405.

Jefferson, R.A., Kavanagh, T.A., and Bevan, M.W. (1987). GUS fusions: beta-glucuronidase as a sensitive and versatile gene fusion marker in higher plants. EMBO J. *6*, 3901–3907.

Jeong, D.-H., Lee, S., Kim, S.L., Hwang, I., and An, G. (2007). Regulation of brassinosteroid responses by Phytochrome B in rice. Plant Cell Environ. *30*, 590–599.

Jung, B., Hoffmann, C., and Möhlmann, T. (2011). Arabidopsis nucleoside hydrolases involved in intracellular and extracellular degradation of purines. Plant J. *65*, 703–711.

Junghans, U., Langenfeld-Heyser, R., Polle, A., and Teichmann, T. (2004). Effect of Auxin Transport Inhibitors and Ethylene on the Wood Anatomy of Poplar. Plant Biol. *6*, 22–29.

Kang, S.-M., and Titus, J.S. (1980). Isolation and Partial Characterization of an Acid Endoprotease Present in Dormant Apple Shoot Bark. Plant Physiol. *66*, 984–989.

Karimi, M., Inzé, D., and Depicker, A. (2002). GATEWAY^{TM} vectors for Agrobacterium-mediated plant transformation. Trends Plant Sci. *7*, 193–195.

Karp, A., and Shield, I. (2008). Bioenergy from plants and the sustainable yield challenge. New Phytol. *179*, 15–32.

Katahira, R., and Ashihara, H. (2006a). Profiles of purine biosynthesis, salvage and degradation in disks of potato (Solanum tuberosum L.) tubers. Planta *225*, 115–126.

Katahira, R., and Ashihara, H. (2006b). Role of adenosine salvage in wound-induced adenylate biosynthesis in potato tuber slices. Plant Physiol. Biochem. *44*, 551–555.

Kato, T., Yamagata, M., and Tsukahara, S. (Shikoku N.A.E.S. (1984). Storage forms and reservoirs of nitrogen used for new shoot development in satsuma mandarin tree. J. Jpn. Soc. Hortic. Sci. Jpn. *52*, 393–398.

Kendrick, M.D., and Chang, C. (2008). Ethylene signaling: new levels of complexity and regulation. Curr. Opin. Plant Biol. *11*, 479–485.

Keskitalo, J., Bergquist, G., Gardeström, P., and Jansson, S. (2005). A Cellular Timetable of Autumn Senescence. Plant Physiol. *139*, 1635–1648.

Khanna, R., Shen, Y., Marion, C.M., Tsuchisaka, A., Theologis, A., Schäfer, E., and Quail, P.H. (2007). The Basic Helix-Loop-Helix Transcription Factor PIF5 Acts on Ethylene Biosynthesis and Phytochrome Signaling by Distinct Mechanisms. Plant Cell *19*, 3915–3929.

Kim, J., Woo, H.R., and Nam, H.G. (2016). Toward Systems Understanding of Leaf Senescence: An Integrated Multi-Omics Perspective on Leaf Senescence Research. Mol. Plant *9*, 813–825.

Kim, S., Hwang, G., Lee, S., Zhu, J.-Y., Paik, I., Nguyen, T.T., Kim, J., and Oh, E. (2017). High ambient temperature represses anthocyanin biosynthesis through degradation of HY5. Front. Plant Sci. *8*.

Kramer, E.M., Lewandowski, M., Beri, S., Bernard, J., Borkowski, M., Borkowski, M.H., Burchfield, L.A., Mathisen, B., and Normanly, J. (2008). Auxin Gradients Are Associated with Polarity Changes in Trees. Science *320*, 1610–1610.

Kumar, S., Stecher, G., and Tamura, K. (2016). MEGA7: Molecular Evolutionary Genetics Analysis Version 7.0 for Bigger Datasets. Mol. Biol. Evol. *33*, 1870–1874.

Lageix, S., Lanet, E., Pouch-Pélissier, M.-N., Espagnol, M.-C., Robaglia, C., Deragon, J.-M., and Pélissier, T. (2008). Arabidopsis eIF2α kinase GCN2 is essential for growth in stress conditions and is activated by wounding. BMC Plant Biol. *8*, 134.

Langheinrich, U., and Tischner, R. (1991). Vegetative storage proteins in poplar induction and characterization of a 32-and a 36-kilodalton polypeptide. Plant Physiol. *97*, 1017–1025.

Lau, O.S., and Deng, X.W. (2010). Plant hormone signaling lightens up: integrators of light and hormones. Curr. Opin. Plant Biol. *13*, 571–577.

Lawrence, S.D., Greenwood, J.S., Korhnak, T.E., and Davis, J.M. (1997). A vegetative storage protein homolog is expressed in the growing shoot apex of hybrid poplar. Planta *203*, 237–244.

Lawrence, S.D., Cooke, J.E.K., Greenwood, J.S., Korhnak, T.E., and Davis, J.M. (2001). Vegetative storage protein expression during terminal bud formation in poplar. Can. J. For. Res. *31*, 1098–1103.

Leiber, R.-M., John, F., Verhertbruggen, Y., Diet, A., Knox, J.P., and Ringli, C. (2010). The TOR Pathway Modulates the Structure of Cell Walls in Arabidopsis. Plant Cell *22*, 1898–1908.

Leigh, J.A., and Dodsworth, J.A. (2007). Nitrogen Regulation in Bacteria and Archaea. Annu. Rev. Microbiol. *61*, 349–377.

Leivar, P., and Quail, P.H. (2011). PIFs: pivotal components in a cellular signaling hub. Trends Plant Sci. *16*, 19–28.

Leple, J.C., Brasileiro, A.C.M., Michel, M.F., Delmotte, F., and Jouanin, L. (1992). Transgenic poplars: expression of chimeric genes using four different constructs. Plant Cell Rep. *11*, 137–141.

Lewkowicz, E.S., and Iribarren, A.M. (2006). Nucleoside phosphorylases. Curr. Org. Chem. *10*, 1197–1215.

Li, G., Wang, B., Tian, Q., Wang, T., and Zhang, W.-H. (2014). Medicago truncatula ecotypes A17 and R108 differed in their response to iron deficiency. J. Plant Physiol. *171*, 639–647.

Liu Mingchun, Chen Yao, Chen Ya, Shin Jun-Hye, Mila Isabelle, Audran Corinne, Zouine Mohamed, Pirrello Julien, and Bouzayen Mondher (2018). The tomato Ethylene Response Factor Sl-ERF.B3 integrates ethylene and auxin signaling via direct regulation of Sl-Aux/IAA27. New Phytol. *0*.

Ljung, K., Bhalerao, R.P., and Sandberg, G. (2001). Sites and homeostatic control of auxin biosynthesis in Arabidopsis during vegetative growth. Plant J. *28*, 465–474.

Llácer, J.L., Contreras, A., Forchhammer, K., Marco-Marín, C., Gil-Ortiz, F., Maldonado, R., Fita, I., and Rubio, V. (2007). The crystal structure of the complex of PII and acetylglutamate kinase reveals how PII controls the storage of nitrogen as arginine. Proc. Natl. Acad. Sci. *104*, 17644–17649.

Llácer, J.L., Fita, I., and Rubio, V. (2008). Arginine and nitrogen storage. Curr. Opin. Struct. Biol. *18*, 673–681.

Lorrain, S., Allen, T., Duek, P.D., Whitelam, G.C., and Fankhauser, C. (2008). Phytochrome-mediated inhibition of shade avoidance involves degradation of growth-promoting bHLH transcription factors. Plant J. *53*, 312–323.

Love, J., Björklund, S., Vahala, J., Hertzberg, M., Kangasjärvi, J., Sundberg, B., and Sederoff, R.R. (2009). Ethylene Is an Endogenous Stimulator of Cell Division in the Cambial Meristem of Populus. Proc. Natl. Acad. Sci. U. S. A. *106*, 5984–5989.

de Lucas, M., and Prat, S. (2014). PIFs get BRright: PHYTOCHROME INTERACTING FACTORs as integrators of light and hormonal signals. New Phytol. *202*, 1126–1141.

Mahfouz, M.M., Kim, S., Delauney, A.J., and Verma, D.P.S. (2006). Arabidopsis TARGET OF RAPAMYCIN Interacts with RAPTOR, Which Regulates the Activity of S6 Kinase in Response to Osmotic Stress Signals. Plant Cell *18*, 477–490.

Malaguti, D., Millard, P., Wendler, R., Hepburn, A., and Tagliavini, M. (2001). Translocation of amino acids in the xylem of apple (Malus domestica Borkh.) trees in spring as a consequence of both N remobilization and root uptake. J. Exp. Bot. *52*, 1665–1671.

Mason, A.C., and Whttfield, A.B. (1960). Seasonal changes in the uptake and distribution of mineral elements in apple trees. J. Hortic. Sci. *35*, 34–55.

Mason, H.S., and Mullet, J.E. (1990). Expression of two soybean vegetative storage protein genes during development and in response to water deficit, wounding, and jasmonic acid. Plant Cell *2*, 569–579.

May, J.D., and Killingbeck, K.T. (1992). Effects of Preventing Nutrient Resorption on Plant Fitness and Foliar Nutrient Dynamics. Ecology *73*, 1868–1878.

McClintick, J., and Edenberg, H. (2006). Effects of filtering by Present call on analysis of microarray experiments. BMC Bioinformatics *7*, 49.

Menand, B., Desnos, T., Nussaume, L., Berger, F., Bouchez, D., Meyer, C., and Robaglia, C. (2002). Expression and disruption of the Arabidopsis TOR (target of rapamycin) gene. Proc. Natl. Acad. Sci. *99*, 6422–6427.

Merchante, C., Alonso, J.M., and Stepanova, A.N. (2013). Ethylene signaling: simple ligand, complex regulation. Curr. Opin. Plant Biol. *16*, 554–560.

Merchante, C., Brumos, J., Yun, J., Hu, Q., Spencer, K.R., Enríquez, P., Binder, B.M., Heber, S., Stepanova, A.N., and Alonso, J.M. (2015). Gene-Specific Translation Regulation Mediated by the Hormone-Signaling Molecule EIN2. Cell *163*, 684–697.

Merrick, M.J., and Edwards, R.A. (1995). Nitrogen control in bacteria. Microbiol. Rev. *59*, 604–622.

Meuriot, F., Noquet, C., Avice, J.-C., Volenec, J.J., Cunningham, S.M., Sors, T.G., Caillot, S., and Ourry, A. (2004). Methyl jasmonate alters N partitioning, N reserves accumulation and induces gene expression of a 32-kDa vegetative storage protein that possesses chitinase activity in Medicago sativa taproots. Physiol. Plant. *120*, 113–123.

Millard, P. (1994). Measurement of the remobilization of nitrogen for spring leaf growth of trees under field conditions. Tree Physiol. *14*, 1049–1054.

Millard, P., and Grelet, G. (2010). Nitrogen storage and remobilization by trees: ecophysiological relevance in a changing world. Tree Physiol. *30*, 1083–1095.

Millard, P., and Proe, M.F. (1991). Leaf demography and the seasonal internal cycling of nitrogen in sycamore (Acer pseudoplatanus L.) seedlings in relation to nitrogen supply. New Phytol. 587–596.

Millard, P., Wendler, R., Hepburn, A., and Smith, A. (1998). Variations in the amino acid composition of xylem sap of Betula pendula Roth. trees due to remobilization of stored N in the spring. Plant Cell Environ. *21*, 715–722.

Millard, P., Wendler, R., Grassi, G., Grelet, G.A., and Tagliavini, M. (2006). Translocation of nitrogen in the xylem of field-grown cherry and poplar trees during remobilization. Tree Physiol. *26*, 527–536.

Mizuno, Y., Berenger, B., Moorhead, G.B.G., and Ng, K.K.-S. (2007a). Crystal Structure of Arabidopsis PII Reveals Novel Structural Elements Unique to Plants. Biochemistry *46*, 1477–1483.

Mizuno, Y., Moorhead, G.B.G., and Ng, K.K.-S. (2007b). Structural Basis for the Regulation of N-Acetylglutamate Kinase by PII in Arabidopsis thaliana. J. Biol. Chem. *282*, 35733–35740.

Moorhead, G.B.G., and Smith, C.S. (2003). Interpreting the Plastid Carbon, Nitrogen, and Energy Status. A Role for PII? Plant Physiol. *133*, 492–498.

Mousdale, D.M. (1982). Endogenous Abscisic Acid and the Regulation of Protein Metabolism in Shoot Bark of Apple (Malus domestics Borkh.). Biochem. Physiol. Pflanz. *177*, 601–610.

Mousdale, D.M. (1983). Endogenous Abscisic Acid and the Regulation of Proteolytic Activities in Shoot Bark of Apple (Malus domestica Borkh.). Biochem. Physiol. Pflanz. *178*, 373–379.

Muñoz, N., Guerri, J., Legaz, F., and Primo-millo, E. (1993). Seasonal uptake of 15N-nitrate and distribution of absorbed nitrogen in peach trees. Plant Soil *150*, 263–269.

Müntz, K. (1998). Deposition of storage proteins. Plant Mol. Biol. *38*, 77–99.

Müntz, K. (2007). Protein dynamics and proteolysis in plant vacuoles. J. Exp. Bot. *58*, 2391–2407.

Müntz, K., Belozersky, M.A., Dunaevsky, Y.E., Schlereth, A., and Tiedemann, J. (2001). Stored proteinases and the initiation of storage protein mobilization in seeds during germination and seedling growth. J. Exp. Bot. *52*, 1741–1752.

Murneek, A.E., and Logan, J.C. (1932). Autumnal migration of nitrogen and carbohydrates in the apple tree (University Of Missouri, Agricultural Experiment Station: Columbia, Missouri).

Nambiar, E.K.S., and Fife, D.N. (1991). Nutrient retranslocation in temperate conifers. Tree Physiol. *9*, 185–207.

Neilsen, D., Millard, P., Neilsen, G.H., and Hogue, E.J. (1997). Sources of N for leaf growth in a high-density apple (Malus domestica) orchard irrigated with ammonium nitrate solution. Tree Physiol. *17*, 733–739.

Nomura, K., Ikegami, A., Koide, A., and Yagi, F. (2008). Japanese chestnut (Castanea crenata) agglutinin may have a role as vegetative storage protein. J. Plant Physiol. *165*, 671–675.

O'Kennedy, B.T., Hennerty, M.J., and Titus, J.S. (1975). The Effects of Autumn Foliar Urea Sprays on Storage Forms of Nitrogen Extracted from Bark and Wood of Apple Shoots. J. Hortic. Sci. *50*, 331–338.

Oland, K. (1959). Nitrogenous Reserves of Apple Trees. Physiol. Plant. *12*, 594–648.

Olsen, J.E., Junttila, O., Nilsen, J., Eriksson, M.E., Martinussen, I., Olsson, O., Sandberg, G., and Moritz, T. (1997). Ectopic expression of oat phytochrome A in hybrid aspen changes critical daylength for growth and prevents cold acclimatization. Plant J. *12*, 1339–1350.

Osanai, T., and Tanaka, K. (2007). Keeping in Touch with PII: PII-Interacting Proteins in Unicellular Cyanobacteria. Plant Cell Physiol. *48*, 908–914.

Parlati, A., Valkov, V.T., D'Apuzzo, E., Alves, L.M., Petrozza, A., Summerer, S., Costa, A., Cellini, F., Vavasseur, A., and Chiurazzi, M. (2017). Ectopic Expression of PII Induces Stomatal Closure in Lotus japonicus. Front. Plant Sci. *8*.

Pettengill, E.A., Parmentier-Line, C., and Coleman, G.D. (2012). Evaluation of qPCR reference genes in two genotypes of Populus for use in photoperiod and low-temperature studies. BMC Res. Notes *5*, 366.

Pettengill, E.A., Pettengill, J.B., and Coleman, G.D. (2013). Elucidating the evolutionary history and expression patterns of nucleoside phosphorylase paralogs (vegetative storage proteins) in Populus and the plant kingdom. BMC Plant Biol. *13*, 118.

Petterle, A., Karlberg, A., and Bhalerao, R.P. (2013). Daylength mediated control of seasonal growth patterns in perennial trees. Curr. Opin. Plant Biol. *16*, 301–306.

Plett, J.M., Khachane, A., Ouassou, M., Sundberg, B., Kohler, A., and Martin, F. (2014). Ethylene and jasmonic acid act as negative modulators during mutualistic symbiosis between Laccaria bicolor and Populus roots. New Phytol. *202*, 270–286.

Potuschak, T., Lechner, E., Parmentier, Y., Yanagisawa, S., Grava, S., Koncz, C., and Genschik, P. (2003). EIN3-Dependent Regulation of Plant Ethylene Hormone Signaling by Two Arabidopsis F Box Proteins: EBF1 and EBF2. Cell *115*, 679–689.

Pugmire, M.J., and Ealick, S.E. (2002). Structural analyses reveal two distinct families of nucleoside phosphorylases. Biochem. J. *361*, 1–25.

Qiao, H., Shen, Z., Huang, S.C., Schmitz, R.J., Urich, M.A., Briggs, S.P., and Ecker, J.R. (2012). Processing and Subcellular Trafficking of ER-Tethered EIN2 Control Response to Ethylene Gas. Science *338*, 390–393.

Quail, P.H. (2002). Phytochrome photosensory signalling networks. Nat. Rev. Mol. Cell Biol. *3*, 85–93.

Quartieri, M., Millard, P., and Tagliavini, M. (2002). Storage and remobilisation of nitrogen by pear (Pyrus communis L.) trees as affected by timing of N supply. Eur. J. Agron. *17*, 105–110.

Rabino, I., and Mancinelli, A.L. (1986). Light, temperature, and anthocyanin production. Plant Physiol. *81*, 922–924.

Ramón-Maiques, S., Fernández-Murga, M.L., Gil-Ortiz, F., Vagin, A., Fita, I., and Rubio, V. (2006). Structural Bases of Feed-back Control of Arginine Biosynthesis, Revealed by the Structures of Two Hexameric N-Acetylglutamate Kinases, from Thermotoga maritima and Pseudomonas aeruginosa. J. Mol. Biol. *356*, 695–713.

Ren, M., Venglat, P., Qiu, S., Feng, L., Cao, Y., Wang, E., Xiang, D., Wang, J., Alexander, D., Chalivendra, S., et al. (2012). Target of Rapamycin Signaling Regulates Metabolism, Growth, and Life Span in Arabidopsis. Plant Cell *24*, 4850–4874.

Rennenberg, H., and Schmidt, S. (2010). Perennial lifestyle—an adaptation to nutrient limitation? Tree Physiol. *30*, 1047–1049.

Rennenberg, H., Wildhagen, H., and Ehlting, B. (2010). Nitrogen nutrition of poplar trees: Nitrogen nutrition of poplar trees. Plant Biol. *12*, 275–291.

Richard-Molard, C., Brugière, N., Moille, M., Carrayol, E., and Limami, A.M. (2004). Molecular characterization of a gene encoding a vegetative storage protein (CiVSP) from Cichorium intybus and its expression in the root and shoot in relation to nitrogen status and pathogen resistance. Physiol. Plant. *121*, 568–577.

Robaglia, C., Thomas, M., and Meyer, C. (2012). Sensing nutrient and energy status by SnRK1 and TOR kinases. Curr. Opin. Plant Biol. *15*, 301–307.

Roberts, R.H. (1921). Nitrogen reserve in apple trees. In Proc. Amer. Soc. Hort. Sci, pp. 143–145.

Robertson, G.P., and Vitousek, P.M. (2009). Nitrogen in agriculture: balancing the cost of an essential resource. Annu. Rev. Environ. Resour. *34*, 97–125.

Ryan, D., and Bormann, F. (1982). Nutrient Resorption in Northern Hardwood Forests. BioScience *32*, 29–32.

Saitou, N., and Nei, M. (1987). The neighbor-joining method: a new method for reconstructing phylogenetic trees. Mol. Biol. Evol. *4*, 406–425.

Sakuraba, Y., Jeong, J., Kang, M.-Y., Kim, J., Paek, N.-C., and Choi, G. (2014). Phytochrome-interacting transcription factors PIF4 and PIF5 induce leaf senescence in Arabidopsis. Nat. Commun. *5*, 4636.

Salzer, M.W., Hughes, M.K., Bunn, A.G., and Kipfmueller, K.F. (2009). Recent unprecedented tree-ring growth in bristlecone pine at the highest elevations and possible causes. Proc. Natl. Acad. Sci. *106*, 20348–20353.

Sant'Anna, F.H., Trentini, D.B., de Souto Weber, S., Cecagno, R., da Silva, S.C., and Schrank, I.S. (2009). The PII Superfamily Revised: A Novel Group and Evolutionary Insights. J. Mol. Evol. *68*, 322–336.

Santiago, J.P., and Tegeder, M. (2016). Connecting source with sink: the role of Arabidopsis AAP8 in phloem loading of amino acids. Plant Physiol. pp.00244.2016.

Sauter, J.J., and Cleve, B. (1992). Seasonal variation of amino acids in the xylem sap of "Populus x canadensis" and its relation to protein body mobilization. Trees-Struct. Funct. *7*, 26–32.

Sauter, J.J., and van Cleve, B. (1992). Seasonal variation of amino acids in the xylem sap of "Populus x canadensis" and its relation to protein body mobilization. Trees *7*, 26–32.

Sauter, J.J., Cleve, B. van, and Apel, K. (1988). Protein bodies in ray cells of Populus x canadensis Moench 'robusta.' Planta *173*, 31–34.

Sauter, J.J., van, C.B., and Wellenkamp, S. (1989). Ultrastructural and Biochemical Results on the Localization and Distribution of Storage Proteins in a Poplar Tree and in Twigs of Other Tree Species. Holzforsch. - Int. J. Biol. Chem. Phys. Technol. Wood *43*, 1–6.

Scarascia-Mugnozza, G.E., Hinckley, T.M., Stettler, R.F., Heilman, P.E., and Isebrands, J.G. (1999). Production physiology and morphology of Populus species

and their hybrids grown under short rotation. III. Seasonal carbon allocation patterns from branches. Can. J. For. Res. *29*, 1419–1432.

Schippers, J.H. (2015). Transcriptional networks in leaf senescence. Curr. Opin. Plant Biol. *27*, 77–83.

Schmidt, S., and Stewart, G.R. (1998). Transport, storage and mobilization of nitrogen by trees and shrubs in the wet/dry tropics of northern Australia. Tree Physiol. *18*, 403–410.

Schneider, A., Kreuzwieser, J., Schupp, R., Sauter, J.J., and Rennenberg, H. (1994). Thiol and amino acid composition of the xylem sap of poplar trees (Populus ×canadensis 'robusta'). Can. J. Bot. *72*, 347–351.

Schrader, J., Baba, K., May, S.T., Palme, K., Bennett, M., Bhalerao, R.P., and Sandberg, G. (2003). Polar auxin transport in the wood-forming tissues of hybrid aspen is under simultaneous control of developmental and environmental signals. Proc. Natl. Acad. Sci. *100*, 10096–10101.

Seo, M., Nambara, E., Choi, G., and Yamaguchi, S. (2009). Interaction of light and hormone signals in germinating seeds. Plant Mol. Biol. *69*, 463.

Seyfferth, C., Wessels, B., Jokipii-Lukkari, S., Sundberg, B., Delhomme, N., Felten, J., and Tuominen, H. (2018). Ethylene-Related Gene Expression Networks in Wood Formation. Front. Plant Sci. *9*.

Shen, Y., Khanna, R., Carle, C.M., and Quail, P.H. (2007). Phytochrome Induces Rapid PIF5 Phosphorylation and Degradation in Response to Red-Light Activation. Plant Physiol. *145*, 1043–1051.

Shi, H., Shen, X., Liu, R., Xue, C., Wei, N., Deng, X.W., and Zhong, S. (2016). The Red Light Receptor Phytochrome B Directly Enhances Substrate-E3 Ligase Interactions to Attenuate Ethylene Responses. Dev. Cell *39*, 597–610.

Shinomura, T., Nagatani, A., Chory, J., and Furuya, M. (1994). The Induction of Seed Germination in Arabidopsis thaliana Is Regulated Principally by Phytochrome B and Secondarily by Phytochrome A. Plant Physiol. *104*, 363–371.

Shinomura, T., Nagatani, A., Hanzawa, H., Kubota, M., Watanabe, M., and Furuya, M. (1996). Action spectra for phytochrome A- and B-specific photoinduction of seed germination in Arabidopsis thaliana. Proc. Natl. Acad. Sci. *93*, 8129–8133.

Shutov, A.D., Bäumlein, H., Blattner, F.R., and Müntz, K. (2003). Storage and mobilization as antagonistic functional constraints on seed storage globulin evolution. J. Exp. Bot. *54*, 1645–1654.

Smith, P.M.C., and Atkins, C.A. (2002). Purine Biosynthesis. Big in Cell Division, Even Bigger in Nitrogen Assimilation. Plant Physiol. *128*, 793–802.

Smith, H., Xu, Y., and Quail, P.H. (1997). Antagonistic but Complementary Actions of Phytochromes A and B Allow Optimum Seedling De-Etiolation. Plant Physiol. *114*, 637–641.

Smith, P.K., Krohn, R.I., Hermanson, G.T., Mallia, A.K., Gartner, F.H., Provenzano, M.D., Fujimoto, E.K., Goeke, N.M., Olson, B.J., and Klenk, D.C. (1985). Measurement of protein using bicinchonic acid. Anal. Biochem. *150*, 76–85.

Smyth, G.K. (2004). Linear Models and Empirical Bayes Methods for Assessing Differential Expression in Microarray Experiments. Stat. Appl. Genet. Mol. Biol. *3*.

Somers, D.E., Devlin, P.F., and Kay, S.A. (1998). Phytochromes and Cryptochromes in the Entrainment of the Arabidopsis Circadian Clock. Science *282*, 1488–1490.

Sonenshein, A.L. (2007). Control of key metabolic intersections in Bacillus subtilis. Nat. Rev. Microbiol. *5*, 917–927.

Song, Y., Yang, C., Gao, S., Zhang, W., Li, L., and Kuai, B. (2014). Age-Triggered and Dark-Induced Leaf Senescence Require the bHLH Transcription Factors PIF3, 4, and 5. Mol. Plant *7*, 1776–1787.

Sparkes, I.A., Runions, J., Kearns, A., and Hawes, C. (2006). Rapid, transient expression of fluorescent fusion proteins in tobacco plants and generation of stably transformed plants. Nat. Protoc. *1*, 2019–2025.

Spicer, R., Tisdale-Orr, T., and Talavera, C. (2013). Auxin-Responsive DR5 Promoter Coupled with Transport Assays Suggest Separate but Linked Routes of Auxin Transport during Woody Stem Development in Populus. PLoS ONE *8*, e72499.

Staswick, P.E. (1994). Storage proteins of vegetative plant tissues. Annu. Rev. Plant Biol. *45*, 303–322.

Stepanova, A.N., and Alonso, J.M. (2009). Ethylene signaling and response: where different regulatory modules meet. Curr. Opin. Plant Biol. *12*, 548–555.

Sugiyama, K., Hayakawa, T., Kudo, T., Ito, T., and Yamaya, T. (2004). Interaction of N-Acetylglutamate Kinase with a PII-Like Protein in Rice. Plant Cell Physiol. *45*, 1768–1778.

Sundberg, B., and Uggla, C. (1998). Origin and dynamics of indoleacetic acid under polar transport in Pinus sylvestris. Physiol. Plant. *104*, 22–29.

Taylor, B.K., and May, L.H. (1967). The Nitrogen Nutrition of the Peach Tree II. Storage And Mobilization of Nitrogen in Young Trees. Aust. J. Biol. Sci. *20*, 389–412.

Taylor, B.K., and Van, den E.B. (1969). The nitrogen nutrition of the peach tree. IV. Storage and mobilization of nitrogen in mature trees. Aust. J. Agric. Res. *20*, 869–881.

Taylor, B.K., and Van, den E.B. (1970). The nitrogen nutrition of the peach tree. VI. Influence of Autumn nitrogen applications on the accumulation of nitrogen, carbohydrate, and macroelements in 1-year-old peach trees. Aust. J. Agric. Res. *21*, 693–698.

Taylor, B.K., Ende, B. van den, and Canterford, R.L. (1975). Effects of rate and timing of nitrogen applications on the performance and chemical composition of young pear trees, cv Williams' Bon Chretien. J. Hortic. Sci. *50*, 29–40.

Tegeder, M., and Masclaux-Daubresse, C. (2018). Source and sink mechanisms of nitrogen transport and use. New Phytol. *217*, 35–53.

Thain, S.C., Vandenbussche, F., Laarhoven, L.J.J., Dowson-Day, M.J., Wang, Z.-Y., Tobin, E.M., Harren, F.J.M., Millar, A.J., and Straeten, D.V.D. (2004). Circadian Rhythms of Ethylene Emission in Arabidopsis. Plant Physiol. *136*, 3751–3761.

Thomas, W. (1927). Nitrogenous Metabolism of Pyrus malus L. III. The Partition of Nitrogen in the Leaves, One and Two Year Branch Growth and Non-Bearing Spurs throughout a Year's Cycle. Plant Physiol. *2*, 109–137.

Tian, W.-M., Peng, S.-Q., Hao, B.-Z., Wu, J.-L., Hu, Z.-H., and Cui, K.-M. (2005). Poplar Trees (Populus canadensis Moench) Initiate Vegetative Storage Protein Accumulation During New Shoot Development in Spring. J. Integr. Plant Biol. *47*, 717–725.

Tian, W.-M., Peng, S.-Q., Wang, X.-C., Shi, M.-J., Chen, Y.-Y., and Hu, Z.-H. (2007). Vegetative Storage Protein in Litchi chinensis, a Subtropical Evergreen Fruit Tree, Possesses Trypsin Inhibitor Activity. Ann. Bot. *100*, 1199–1208.

Tiedemann, J., Schlereth, A., and Müntz, K. (2001). Differential tissue-specific expression of cysteine proteinases forms the basis for the fine-tuned mobilization of storage globulin during and after germination in legume seeds. Planta *212*, 728–738.

Titus, J.S., and Kang, S.-M. (1982). Nitrogen Metabolism, Translocation, and Recycling in Apple Trees. In Horticultural Reviews, J. Janick, ed. (John Wiley & Sons, Inc.), pp. 204–246.

Trupiano, D., Yordanov, Y., Regan, S., Meilan, R., Tschaplinski, T., Scippa, G.S., and Busov, V. (2013). Identification, characterization of an AP2/ERF transcription factor that promotes adventitious, lateral root formation in Populus. Planta *238*, 271–282.

Tuskan, G.A., and et al. (2006). The Genome of Black Cottonwood, *Populus trichocarpa* (Torr. &. Science *313*, 1596–1604.

Uhrig, R.G., Ng, K.K.S., and Moorhead, G.B.G. (2009). PII in higher plants: a modern role for an ancient protein. Trends Plant Sci. *14*, 505–511.

Vahala, J., Felten, J., Love, J., Gorzsás, A., Gerber, L., Lamminmäki, A., Kangasjärvi, J., and Sundberg, B. (2013). A genome-wide screen for ethylene-induced Ethylene Response Factors (ERFs) in hybrid aspen stem identifies ERF genes that modify stem growth and wood properties. New Phytol. *200*, 511–522.

Van Damme, E.J.M., Barre, A., Bemer, V., Rougé, P., Van Leuven, F., and Peumans, W.J. (1995). A lectin and a lectin-related protein are the two most prominent proteins in the bark of yellow wood (Cladrastis lutea). Plant Mol. Biol. *29*, 579–598.

Vitousek, P. (1982). Nutrient Cycling and Nutrient Use Efficiency. Am. Nat. *119*, 553–572.

Weinbaum, S., and Van Kessel, C. (1998). Quantitative estimates of uptake and internal cycling of 14N-labeled fertilizer in mature walnut trees. Tree Physiol. *18*, 795–801.

Weinstein, J.N., Myers, T.G., O'Connor, P.M., Friend, S.H., Fornace, A.J., Kohn, K.W., Fojo, T., Bates, S.E., Rubinstein, L.V., Anderson, N.L., et al. (1997). An Information-Intensive Approach to the Molecular Pharmacology of Cancer. Science *275*, 343–349.

Weller, J.L., Beauchamp, N., Kerckhoffs, L.H.J., Platten, J.D., and Reid, J.B. (2001). Interaction of phytochromes A and B in the control of de-etiolation and flowering in pea. Plant J. *26*, 283–294.

Werner, A.K., and Witte, C.-P. (2011). The biochemistry of nitrogen mobilization: purine ring catabolism. Trends Plant Sci. *16*, 381–387.

Wetzel, S., and Greenwood, J.S. (1989). Proteins as a potential nitrogen storage compound in bark and leaves of several softwoods. Trees *3*, 149–153.

Wetzel, S., and Greenwood, J.S. (1991a). The 32-Kilodalton Vegetative Storage Protein of Salix microstachya Turz Characterization and Immunolocalization. Plant Physiol. *97*, 771–777.

Wetzel, S., and Greenwood, J.S. (1991b). A survey of seasonal bark proteins in eight temperate hardwoods. Trees *5*, 153–157.

Wetzel, S., Demmers, C., and Greenwood, J.S. (1989). Seasonally fluctuating bark proteins are a potential form of nitrogen storage in three temperate hardwoods. Planta *178*, 275–281.

Wildhagen, H., Durr, J., Ehlting, B., and Rennenberg, H. (2010). Seasonal nitrogen cycling in the bark of field-grown Grey poplar is correlated with meteorological factors and gene expression of bark storage proteins. Tree Physiol. *30*, 1096–1110.

Wildhagen, H., Bilela, S., and Rennenberg, H. (2013). Low temperatures counteract short-day induced nitrogen storage, but not accumulation of bark storage protein transcripts in bark of grey poplar (Populus × canescens) trees. Plant Biol. *15*, 44–56.

Winter, G., Todd, C.D., Trovato, M., Forlani, G., and Funck, D. (2015). Physiological implications of arginine metabolism in plants. Front. Plant Sci. *6*.

Wittenbach, V.A. (1982). Effect of Pod Removal on Leaf Senescence in Soybeans. Plant Physiol. *70*, 1544–1548.

Wullschleger, S., Loewith, R., and Hall, M.N. (2006). TOR Signaling in Growth and Metabolism. Cell *124*, 471–484.

Xu, G., Fan, X., and Miller, A.J. (2012). Plant Nitrogen Assimilation and Use Efficiency. Annu. Rev. Plant Biol. *63*, 153–182.

Yao, W., Wang, L., Zhou, B., Wang, S., Li, R., and Jiang, T. (2016). Over-expression of poplar transcription factor ERF76 gene confers salt tolerance in transgenic tobacco. J. Plant Physiol. *198*, 23–31.

Yao, W., Zhang, X., Zhou, B., Zhao, K., Li, R., and Jiang, T. (2017). Expression Pattern of ERF Gene Family under Multiple Abiotic Stresses in Populus simonii × P. nigra. Front. Plant Sci. *8*.

Yoo, S.-D., Cho, Y., and Sheen, J. (2009). Emerging connections in the ethylene signaling network. Trends Plant Sci. *14*, 270–279.

Yordanov, Y.S., Ma, C., Strauss, S.H., and Busov, V.B. (2014). EARLY BUD-BREAK 1 (EBB1) is a regulator of release from seasonal dormancy in poplar trees. Proc. Natl. Acad. Sci. *111*, 10001–10006.

Zdarska, M., Dobisová, T., Gelová, Z., Pernisová, M., Dabravolski, S., and Hejátko, J. (2015). Illuminating light, cytokinin, and ethylene signalling crosstalk in plant development. J. Exp. Bot. *66*, 4913–4931.

Zeth, K., Fokina, O., and Forchhammer, K. (2014). Structural Basis and Target-specific Modulation of ADP Sensing by the Synechococcus elongatus PII Signaling Protein. J. Biol. Chem. *289*, 8960–8972.

Zhang, C., Han, L., Slewinski, T.L., Sun, J., Zhang, J., Wang, Z.-Y., and Turgeon, R. (2014). Symplastic Phloem Loading in Poplar. Plant Physiol. *166*, 306–313.

Zhang, X., Davidson, E.A., Mauzerall, D.L., Searchinger, T.D., Dumas, P., and Shen, Y. (2015). Managing nitrogen for sustainable development. Nature *528*, 51–59.

Zhang, Y., Wang, Y., Kanyuka, K., Parry, M.A.J., Powers, S.J., and Halford, N.G. (2008). GCN2-dependent phosphorylation of eukaryotic translation initiation factor-2α in Arabidopsis. J. Exp. Bot. *59*, 3131–3141.

Zhu, B., and Coleman, G.D. (2001a). Phytochrome-Mediated Photoperiod Perception, Shoot Growth, Glutamine, Calcium, and Protein Phosphorylation Influence the Activity of the Poplar Bark Storage Protein Gene Promoter (bspA). Plant Physiol. *126*, 342–351.

Zhu, B., and Coleman, G.D. (2001b). The poplar bark storage protein gene (Bspa) promoter is responsive to photoperiod and nitrogen in transgenic poplar and active in floral tissues, immature seeds and germinating seeds of transgenic tobacco. Plant Mol. Biol. *46*, 383–394.

Zuckerkandl, E., and Pauling, L. (1965). Evolutionary Divergence and Convergence in Proteins. In Evolving Genes and Proteins, V. Bryson, and H.J. Vogel, eds. (Academic Press), pp. 97–166.